Università degli Studi di Ferrara

Ph.D. course
in
Evolutionary biology and ecology

in cooperation with Università degli studi di Parma

CYCLE XXIX

DIRECTOR Prof. Guido Barbujani

ROLE OF SCAVENGER RECEPTOR B1 IN CUTANEOUS PHYSIOPATHOLOGY

Scientific/Disciplinary Sector (SDS) BIO/07

Candidate
Dott. Muresan Ximena Maria

Supervisor
Prof. Valacchi Giuseppe

Years 2014/2016

Index

CHAPTER 1

Scavenger receptor class B type 1

1.1 General outlook

Scavenger receptor class B type 1 (SR-B1) is a cell surface receptor with multiple binding sites and different ligand binding properties. It is a 509-amino acid-long polypeptide, which belongs to the CD36 membrane proteins superfamily (Krieger 2001) and binds several ligands, such as lipoproteins, maleylated BSA, advanced glycation end product-modified proteins and anionic phospholipids (Rigotti et al. 2003).

Several studies have revealed that SR-B1 is conserved across species, being expressed both in invertebrates and vertebrates. In fact, orthologs of this receptor have been reported to be present in invertebrates like *Drosophila melanogaster* (Philips et al. 2005), *Bombyx mori* (Tanaka et al. 2008) and *Marsupenaeus japonicas* (Bi et al. 2015). Among vertebrates, SR-B1 is expressed in non-mammalian species such as Atlantic salmon (Kleveland et al. 2006), turtle (Duggan et al. 2002), shark, chicken, frog (Shen et al. 2014) and also in mammalians, for example mouse (Acton et al. 1994), rat (Mizutani et al. 1997), cattle (Rajapaksha et al. 1997) and human (Calvo & Vega 1993). All the orthologs of SR-B1 share around 70-80% similarity at the amino acid sequence level (Shen et al. 2014).

The human SR-B1 was first identified by Calvo and Vega (Calvo & Vega 1993) under the name of CLA-1 (CD36 and LIMPII Analougous-1). The gene encoding CLA-1/SR-B1 resides in *locus* 12q24.31 on chromosome 12 and contains 13 exones, all small (< 250 bp) except for exon 13 (~1 kb), and 11 introns (Cao, Garcia, L. Wyne, et al. 1997).

On the cell membrane, SR-B1 is located in caveolae and presents a horseshoe-shaped structure with two trans-membrane domains of 25 and 28 residues, short cytoplasmic amino- and carboxyl-terminal tails and a large extracellular loop of around 403 residues (Krieger 2001). This receptor contains numerous N-linked glycosylation sites (Asn-X-Ser/Thr; 10 in the human form and 11 in the murine form, usually in the following positions: 102, 108, 173, 212, 227, 255, 310, 330 and 383) spread throughout the luminal domain (Calvo & Vega 1993; Viñals et al. 2003). A study on mutant SR-B1 cDNA expression vectors in which each glycosylation site was singularly mutated (Viñals et al. 2003), showed that all N-linked glycosylation sites of the receptor are normally glycosylated. In particular, glycosylation at two positions (173 and 108) appeared to be essential for SR-B1 expression on the cell surface.

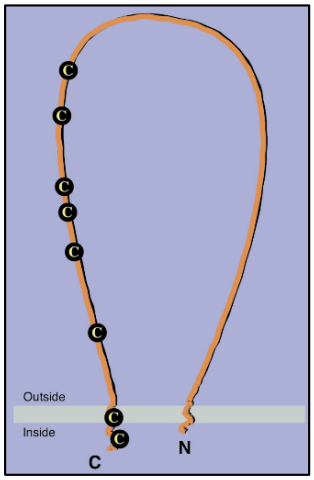

Figure 1.1 – SR-B1 structure; reported from Krieger (Krieger 2001)

SR-B1 amino acidic sequence reveals the presence of several cysteines, located both in the extracellular domain and cytoplasmic carboxyl-terminal region, prolines and glycines, which are conserved among the members of CD36 protein superfamily (Calvo & Vega 1993).

Studies have revealed the existence of alternative forms of SR-B1 as result of alternative splicing of mRNA. Calvo and Vega (Calvo & Vega 1993) identified a product lacking of 300 nucleotides near the amino-terminal region, which encoded for a 409-amino acid-long protein in human. In 1997, Webb and colleagues (Webb et al. 1997) described the presence of another clone of SR-B1, that lacked 129 nucleotides at the extreme 3'-end of the coding sequence. This new clone encoded for a peptide named SR-BI.2 or SR-BII, which contained 44 amino acids in the cytoplasmic tail at the carboxyl-terminal domain instead of the 47 amino acids contained in SR-B1. Further investigations demonstrated that SR-BII isoform represents around 12% of the total immunodetectable level of SR-B1/SR-BII protein in mouse liver and can reach higher expression in other tissues. This isoform has been reported to possess similar functions as SR-B1, but with lower efficacy (Webb et al. 1998). This suggests that the presence of an alternative splicing product might be involved in the regulation of SR-B1, either at a post-transcriptional or functional level (Webb et al. 1997).

SR-B1 can be defined as a multifunctional receptor (Valacchi et al. 2011) since it is involved in several processes such as cholesterol uptake from high density lipoproteins (Gu et al. 1998), vitamins E and A uptake (Mardones et al. 2002; van Bennekum et al. 2005), apoptotic cells identification (Cao et al. 2004), bacteria and viruses recognition and adhesion (Vishnyakova et al. 2006) and vesicles modulation (Angeloni et al. 2016).

1.2 Role of SR-B1 in lipoproteins and cholesterol transport

SR-B1 was first cloned from Chinese hamster ovary (CHO) cells for its ability of binding acetylated LDL (AcLDL) and oxidized LDL (OxLDL), as well as unmodified native LDL (Acton et al. 1994). It has been shown that binding of SR-B1 to OxLDL is followed by lipoprotein internalization, although the intracellular distribution of OxLDL is faster and more specific upon binding to CD36, compared to SR-B1 (Gillotte-Taylor et al. 2001; Sun et al. 2007). Further studies on other cell lines expressing exogenous human SR-B1, incubated with DiI-labeled lipoproteins, revealed the capacity of this receptor to bind not only native and modified LDL, but also VLDL and HDL (Calvo et al. 1997). Moreover, Acton and colleagues (Acton et al. 1996) have demonstrated that SR-B1 is a receptor for

HDL, due to the high affinity binding. In fact, HDL was able to block LDL binding to SR-B1, while LDL appeared to be a poor competitor of HDL binding to the receptor.

Unlike cholesterol uptake mechanism from LDL via LDL receptor, SR-B1 does not induce lipoprotein endocytosis and subsequent degradation. SR-B1-mediated lipids uptake is a selective process, which consists in an initial lipoprotein binding followed by lipids transfer from the lipoprotein particle to the cellular membrane and then to the cytosolic compartment. Since protein components of HDL, ApoA-I and ApoA-II, are not degraded, the lipid-depleted lipoprotein particles are released from the cell surface upon lipids transfer and enter the extracellular fluid (Acton et al. 1996; Krieger 2001). As HDL receptor, SR-B1 is implicated in cholesterol reverse transport (Figure 1.2): HDL particles transport cholesterol from peripheral tissues to the liver and steroidogenic tissues, where cholesteryl esters uptake by cells takes place upon HDL binding to SR-B1 (Rigotti et al. 2003). The receptor binds spherical α-HDL with an affinity, which seems to be proportional to the lipid content of the lipoprotein (Liadaki et al. 2000).

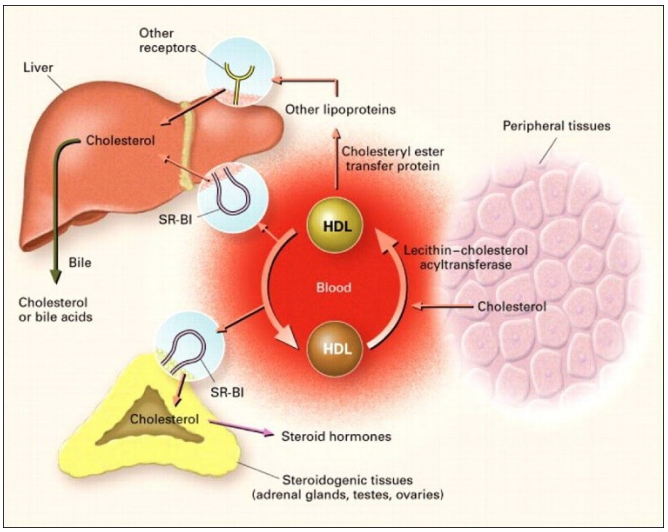

Figure 1.2 – Role of SR-B1 in reverse cholesterol transport; reported from Rigotti et al. (Rigotti et al. 2003)

The role of SR-B1 as receptor for HDL was confirmed in SR-B1$^{-/-}$ mutant mice, that showed increased plasma total cholesterol associated with large HDL particles; ApoA-I levels did not appear significantly changed compared to wild type mice, while decreased amount of ApoA-II and increased levels of ApoE were observed (Rigotti et al. 1997). In parallel, mice overexpressing SR-B1 in the liver showed lower HDL cholesterol in the plasma, due to an increase in HDL clearance and hepatic lipid uptake, which was accompanied by enhanced cholesterol secretion into the bile (Kozarsky et al. 1997). It has been demonstrated that the binding of HDL to SR-B1 depends on ApoA-I expression in lipoprotein structure (Liadaki et al. 2000) and on the amino-terminal domain of SR-B1,

while lipid uptake appears to be directly linked to the extracellular loop of the receptor (Gu et al. 1998). Double arginine mutations in the extracellular domain, on glutamine at positions 402 and 418, reduced lipid uptake and HDL, but not LDL, binding activity (Gu, Lawrence, et al. 2000).

While it promotes cholesteryl esters uptake, SR-B1 has been shown to mediate also the efflux of free cholesterol from cells and its incorporation in lipoproteins; this might depend on the lipid composition of the lipoprotein that binds to SR-B1 (Ji et al. 1997; Gu, Kozarsky, et al. 2000; Yancey et al. 2000). The ability of this receptor in mediating bi-directional lipid flux is essential, for example, in dietary cholesterol uptake by enterocytes and its subsequent transport to the liver via portal vein (Altmann et al. 2002).

1.3 Implication of SR-B1 in vitamins absorption

Liposoluble vitamins such as vitamin E and carotenoids, once absorbed in the intestine, are incorporated in chylomicrons and transferred into the liver, then either secreted into the bile for disposal or distributed to the body tissues via plasma lipoproteins. Both carotenoids and vitamin E are found mainly associated with HDL and LDL and partly with VLDL (Borel et al. 2007). Therefore, it has been speculated a possible role of SR-B1 in the metabolism of these molecules.

Vitamin E represents a group of micronutrients that comprise tocopherols and tocotrienols. Among all, α- and γ-tocopherol are the most abundant in the daily diet, with α-tocopherol being the most active in preventing free radical reactions (Niki 2014). It has been demonstrated that α- and γ-tocopherol are uptaken by SR-B1 at the apical membrane of enterocytes. In fact, the use of anti-SR-B1 antibody or of a specific chemical inhibitor of the receptor's mediated lipid transfer, BLT-1 (Nieland et al. 2002), reduced significantly the absorption of the vitamins. In parallel, plasma levels of γ-tocopherol were substantially higher in mice overexpressing SR-B1 in the intestine compared to wild type mice (Reboul et al. 2006). Mardones and colleagues (Mardones et al. 2002) have shown that SR-B1 also facilitates cellular uptake of plasmatic α-tocopherol in the peripheral tissues *in vivo* (Figure 1.3). SR-B1-deficient mice presented high levels of α-tocopherol in plasma associated with HDL particles, while its levels were significantly reduced in metabolically active tissues, such as ovary, lungs and brain. Moreover, the biliary concentration of tocopherol was low in SR-B1 knockout mice, meaning that this receptor is involved in hepatic uptake of plasmatic α-tocopherol for subsequent biliary secretion and clearance.

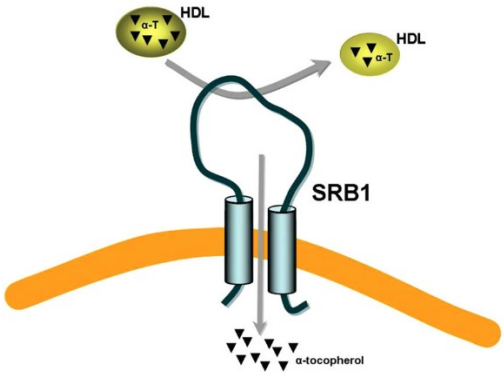

Figure 1.3 – SR-B1-mediated α-tocopherol uptake; reported from Valacchi et al. (Valacchi et al. 2015)

Carotenoids are plant-derived precursors of vitamin A. Several studies on Caco-2 cells have proved that different carotenoids, such as β-carotene, lycopene and lutein, are absorbed across the enterocytes apical membrane through a facilitated transport that involves SR-B1, similarly to vitamin E uptake. The use of anti-SR-B1 antibodies revealed that vitamins uptake depends on their binding to the extracellular domain of the receptor, since antibodies against the carboxyl-terminal tail didn't affect the intestinal absorption (Reboul et al. 2005; During & Harrison 2007; Borel et al. 2013). Furthermore, an *in vivo* study on mice kept on a high fat diet further underlined the importance of SR-B1 for β-carotene absorption, since the absorption of this carotenoid is restricted to the duodenum, where SR-B1 is the predominant receptor (van Bennekum et al. 2005). Little has been reported on the bioavailability of carotenoids related to SR-B1-mediated intestinal uptake. A study on mice overexpressing SR-B1 in the intestine has shown that plasma lycopene levels were significantly increased compared to control mice, indicating once more the role of SR-B1 on carotenoids uptake from diet and their availability in blood circulation (Moussa et al. 2008).

Borel et al. (Borel et al. 2007) have shown that not only SR-B1 regulates tocopherols and carotenoids metabolism, but single nucleotide polymorphisms which interest SR-B1 gene can modulate the plasmatic levels of these vitamins. In particular, SR-B1 exon 1 polymorphism is related to γ-tocopherol, SR-B1 exon 8 to α-tocopherol and SR-B1 intron 5 to α- and β- carotene.

Finally, recent investigations have demonstrated that SR-B1, together with CD36, is involved also in the absorption of vitamin K_1 from food. In fact, experiments on cell lines and mouse intestinal explants have shown that BLT-1 impaired vitamin K_1 uptake, while SR-B1 overexpression increased the vitamin's levels both *in vitro* and *in vivo*. Not only, but vitamin E and cholesterol resulted to be competitors of vitamin K_1 in SR-B1-mediated apical transport (Goncalves et al. 2014).

1.4 Role of SR-B1 in apoptotic cells recognition

As mentioned previously, SR-B1 is able to recognize and bind AcLDL and anionic phospholipids. Such a phospholipid is also phosphatidylserine (PS), which is almost exclusively expressed on the inner layer of the cell membrane in healthy cells and becomes an important marker and physiological signal upon externalization in apoptotic and senescent cells. In fact, cells with exposed PS are marked for phagocytosis and clearance (Vernier et al. 2004), therefore SR-B1 might play a role in the recognition and disposal of damaged cells during disease or tissue remodeling.

Fukasawa and colleagues (Fukasawa et al. 1996) have shown that hamster cells expressing SR-B1 accumulated high amounts of PS-containing liposomes and formed intracellular cholesteryl ester from the liposomal cholesterol. Moreover, these cells had the ability to internalize apoptotic cells. Such event was not perceived in cells not expressing SR-B1 or when cells expressing SR-B1 were incubated with non-apoptotic cells.

Another study demonstrated that also human SR-B1 is a receptor for PS, since the binding of HDL to this receptor was inhibited of 50% by PS-containing unilamellar vesicles, through competition analysis. Since SR-B1 was found to be expressed in monocytes, the authors tested as well its ability to recognize apoptotic cells via the PS-dependent pathway, therefore they incubated SR-B1-transfected cells with apoptotic thymocytes. The binding of apoptotic, but not viable, thymocytes to SR-B1 was high and it was completely prevented by incubation with PS-vesicles, indicating that recognition of apoptotic cells involves SR-B1 and appears to be PS-dependent. Interestingly, despite its implication in apoptotic cells binding, SR-B1 levels decreased when monocytes differentiated into macrophages. A possible explanation, given by the authors, is that the interaction between SR-B1 and apoptotic cells might trigger intracellular signaling leading to expression of components necessary for differentiation and phagocytosis (Murao et al. 1997).

Other studies highlighted the importance of SR-B1 in apoptotic cells recognition and phagocytosis. In the thymus, most immature thymocytes are cleared via apoptosis by negative selection, inside a complex named thymic nurse cell (TNC) where nursing thymic epithelial cells (TEC) exhibit phagocytic activity. Nursing TEC strongly express SR-B1 and engulfing of apoptotic thymocytes resulted decreased for competition upon incubation with PS-rich liposomes. Furthermore, transfection of nursing TEC with antisense oligonucleotides against SR-B1, markedly decreased the binding of apoptotic cells (Imachi et al. 2000; Cao et al. 2004).

Shiratsuchi and colleagues (Shiratsuchi et al. 1999) have shown, by the usage of specific anti-SR-B1 antibodies, that in Sertoli cells this receptor is implicated in binding and engulfing spermatogenic cells. A possible pathway for the SR-B1-induced phagocytosis was described more recently. The receptor appears to be associated at the carboxyl-terminal domain with engulfment adapter protein (GULP), which is activated through the binding of SR-B1 to PS. Such activation induces MAPK phosphorylation, activating downstream proteins with a final rearrangement of the actin cytoskeleton (Osada et al. 2009).

1.5 Pathogens recognition via SR-B1

Among its multiple functions, SR-B1 has been associated with cellular recognition of viruses. In 2002, a study revealed that E2 glycoprotein expressed in Hepatitis C Virus (HCV) envelope binds to human hepatoma cells surface independently of the classical HCV receptor, CD81. Competition assays with anti-E2 antibodies and protein structural characterization have demonstrated that SR-B1 is a receptor of E2 glycoprotein and their binding depends on hypervariable region 1 (HVR1) expression within E2 protein structure. In fact, E2 variants with deleted HVR1 are not able to recognize SR-B1 (Scarselli et al. 2002). Since SR-B1 was demonstrated to mediate the binding and the uptake of HCV from serum of infected patients (Maillard et al. 2006), the question was whether this virus interacts with lipoproteins. It has been shown that HCV associates with lipoproteins, forming lipo-viroparticles which are important for the infectivity (Lavie et al. 2014). Among lipoproteins, it has been reported the interaction of HCV with HDL, that appeared to enhance virus entry into the cells (Bartosch et al. 2005), but also with apoB-containing lipoproteins and VLDL (Maillard et al. 2006). Although these observations suggest that SR-B1-dependent recognition of HCV might be due to the association of the virus with lipoproteins, it has been demonstrated that SR-B1 is able to mediate HCV infection also in the absence of lipoproteins, through a direct molecular interaction between the receptor and the viral particle (Catanese et al. 2007). Still, the mechanism by which SR-B1 modulates HCV uptake in the cells is not fully understood, since HCV infection depends on multiple cellular proteins as well as on mutations within the virus (Catanese et al. 2010; Lavie et al. 2014). Very recently, SR-B1 was reported to be implicated in Newcastle disease virus infection, in fact blockade of SR-B1 function, either by the use of BLT-1 or by transient knockdown, promoted infection. Moreover, SR-B1 seems to have the ability to

enhance interferon-α (IFN-α) bioactivity, via toll-like receptors (TLR) 2 and 4 (Vasques et al. 2016).

Studies *in vitro* have demonstrated that SR-B1, as a macrophage receptor, is also involved in the recognition of bacteria, such as *Mycobacterium tuberculosis* (Schäfer et al. 2009). *Escherichia coli* was reported to bind to SR-B1 as well, leading to increased levels of pro-inflammatory markers; in fact, macrophages isolated from SR-B1-null mice and treated with *E. coli* demonstrated impaired IL-6 secretion (Baranova et al. 2012). Vishnyakova and colleagues (Vishnyakova et al. 2006) have further shown that SR-B1 in implicated in bacteria uptake, since different bacterial strains were detected in the cytoplasm of cells overexpressing SR-B1 upon treatment with such strains. Moreover, SR-B1 is able to recognize negatively charged bacterial phospholipids, like LPS, LTA and Hsp60, and mediates their internalization *in vitro* (Vishnyakova et al. 2003; Bocharov et al. 2004). All these studies might suggest that SR-B1 plays an important role in mediating bacteria infections, but, interestingly, *in vivo* experiments have demonstrated that SR-B1 has a protective function in sepsis via different pathways. It has been reported an increase of tyrosine nitrated proteins and high mortality in LPS-treated SR-B1-null mice, indicating that SR-B1 prevents nitric oxide-induced cytotoxicity upon LPS treatment (Li et al. 2006). Cai et al. (Cai et al. 2008) have shown that SR-B1 mediates glucocorticoid synthesis as protection against LPS-induced death. Such mediation seems to be linked to malfunction of adrenal glands in SR-B1 knockout mice, due to deficient cholesterol delivery. Furthermore, SR-B1 has been demonstrated to modulate inflammation, since SR-B1-null mice present delayed immune response and prolonged cytokines production upon sepsis induction. In fact, SR-B1 suppresses LPS-induced TLR4 activation and subsequent inflammatory responses.

1.6 SR-B1-dependent uptake of vesicles

Very recently, a new role of SR-B1 in exosomes uptake was reported (Figure 1.4). Exosomes are a type of extracellular vesicles secreted by cells under physiological or pathological conditions and they contain material associated with the origin of the cell that are released from, including proteins, lipids, mRNAs and microRNAs, which contribute to intercellular communication (Minciacchi et al. 2015). Once secreted, exosomes are uptaken by target cells through direct fusion with the cellular membrane or via receptor-mediated endocytosis and their uptake takes place mainly in specific plasma membrane

domains rich in cholesterol, called lipid rafts. Depletion of cholesterol in cellular membrane alters lipid raft integrity compromising exosomes uptake (Svensson et al. 2013). It was demonstrated *in vitro* that SR-B1 is localized within lipid rafts on the cellular membrane (Babitt et al. 1997), suggesting a possible relationship between this scavenger receptor and exosomes. Cells incubated with HDL NPs, synthetic HDL-like nanoparticles able to bind to SR-B1, exhibited decreased capacity to uptake exosomes, suggesting that such process depends on the binding of extracellular vesicles to SR-B1. The uptake was further decreased when HDL NPs were associated to BLT-1. Surprisingly, unlike HDL NPs, human HDLs were not able to reduce significantly exosomes uptake, underlying the role of cholesterol homeostasis within lipid rafts, since HDL NPs, but not HDLs, binding to SR-B1 induces cholesterol efflux and subsequent depletion in membrane lipid rafts (Plebanek et al. 2015).

Further studies evinced that SR-B1 not only regulates vesicles uptake through its expression on cell membrane, but it is also expressed in exosomes (Angeloni et al. 2016).

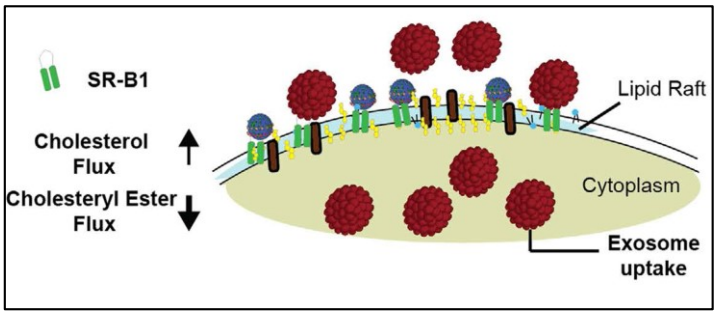

Figure 1.4 – Vesicles cellular uptake facilitated by SR-B1; adapted from Plebanek et al. (Plebanek et al. 2015)

1.7 SR-B1 and pathologies

Due to its multiple functions, SR-B1 has been associated with several pathological conditions.

First, since SR-B1 modulates lipoproteins and lipids metabolism, studies have demonstrated a link between this scavenger receptor and atherosclerosis. It has been reported that normal intimal stroma does not express SR-B1, while SR-B1-positive cells in the intima appear already in the type-I atherosclerotic lesions and increase proportionally to lesions severity. Atherosclerotic lesions are initiated with serum lipids, which permeate into the sub-endothelial space with subsequent infiltration of monocyte-derived macrophages and migration of smooth muscle cells into the intima. In type-IV lesions, SR-B1 was detected also in the foamy cells in the area around the atheroma core (Ishikawa et al. 2009). SR-B1 deficiency in mice led to atherosclerotic lesions represented by fatty

streaks on the arterial wall, together with increased gene expression of markers involved in vascular adhesion and inflammation (Van Eck et al. 2003). A work aimed to study SR-B1 expression in macrophages from ApoE-deficient mice revealed an 86% increase in atherosclerotic lesions in the proximal aorta (Zhang et al. 2003). Moreover, ApoE/SR-B1 double knockout mice kept on standard chow diet developed significant atherosclerotic lesions in the aortic sinus accompanied by extensive lipid-rich coronary artery occlusions and multiple myocardial infarctions and cardiac dysfunction (Braun et al. 2002). Also SR-B1/LDLR double-knockout mice fed with high-fat diet for 2 months showed 6-fold increase in aortic atherosclerosis compared to LDLR-null only, probably due to impaired HDL-cholesterol clearance, which seemed to play a critical role in the development of atherosclerosis in the complete absence of SR-BI expression (Covey et al. 2003). In parallel, it has been shown that over-expression of SR-BI in the liver of LDL receptor knockout mice, kept in high-fat diet, suppressed atherosclerosis by a mechanism that might include either a decrease of atherogenic Apo-B-containing lipoproteins or an induction of reverse cholesterol transport or even the uptake of plasmatic α-tocopherol into vascular endothelium (Trigatti et al. 2003; Trigatti et al. 2004).

The use of SR-B1-null mice in order to understand the physiological implications of this receptor has revealed that female SR-B1 knockout mice are infertile. These mice presented normal ovarian morphology and number of ovulated oocytes. However, the ovulated oocytes appeared dysfunctional, since they died soon after ovulation, suggesting that SR-B1 influences oocyte development (Trigatti et al. 1999). Moreover, recent investigations have shown that SR-B1 knockout mice have a suboptimal luteal steroidogenesis, associated with low plasma progesterone concentration compared to wild type mice, underlining that SR-B1 is essential for maintaining normal ovarian cholesterol homeostasis and luteal steroid synthesis (Jiménez et al. 2010). An *in vitro* study on human granulosa cells confirmed that deficiency of SR-BI significantly reduced progesterone secretion, an effect that was independent of lipoproteins presence in culture media, but significantly associated with down-regulation of key steroidogenic genes (Kolmakova et al. 2010). More recently, an *in vivo* investigation on granulosa cells isolated from women undergoing controlled-ovarian stimulation has demonstrated, by examining the relationship between key SR-B1 single nucleotide polymorphisms and fertility measurements, that several polymorphisms are significantly associated with poor fetal viability, associating SR-B1 with human female reproductive physiology (Yates et al. 2011).

Another pathological condition observed in SR-B1-deficient mice was anemia. Red blood cells appeared irregularly shaped, some with needle-like morphology, compared to wild-type mice. Around 15% of the red blood cells presented cytosolic organelles such as mitochondria and ribosomes, enclosed in autophagolysosomes, characteristic of immature reticulocytes, and this condition was more severe in SR-B1/ApoE double knockout mice. SR-B1 effect on erythrocytes depends on hypercholesterolemia, since SR-B1-null mice kept on high cholesterol diet presented higher anemia, marked macrocytosis and an increase of immature cells number compared to SR-B1-deficient mice kept on normal diet, suggesting an important role of SR-B1 in red blood cells maturation (Holm et al. 2002).

SR-B1 has been also associated with tumors. Imachi et al. (Imachi et al. 1999) have reported that the receptor is over-expressed in adrenal tumors, such as Cushing's adenoma, providing HDL-cholesterol as a substrate to steroidogenesis in the adrenal glands. Furthermore, nasopharyngeal carcinomas have shown high levels of SR-B1 and it has been demonstrated, through transient protein transfection, that this scavenger receptor is implicated in cell motility (Zheng et al. 2013). Recently, an *ex vivo* study has shown that SR-B1 can be associated with malignant behaviors of breast cancer, since it appeared up-regulated in invasive ductal breast cancer (Li et al. 2016).

SR-B1 appeared to be involved in chronic obstructive pulmonary disease (COPD), as well. COPD is a chronic and progressive pathology characterized by lung inflammation, increased apoptosis rate and oxidant/antioxidant imbalance. Since SR-B1 is expressed in the respiratory tract and it is involved in apoptotic cells recognition, uptake of antioxidants, such as α-tocopherol, and regulation of lung surfactant composition, it might be reasonable to associate the receptor to COPD pathogenesis (Valacchi et al. 2015).

Finally, SR-B1 has been linked to neurodegenerative disorders, such as Alzheimer's disease. It has been reported that SR-B1 is expressed in murine brain (Srivastava 2003) and it is involved in C1Q protein complex-mediated amyloid-β uptake by astrocytes. Moreover, this scavenger receptor was found down-regulated in astrocytes of old 5xFAD mice, a model for Alzheimer's disease (Iram et al. 2016), and also in fibroblasts isolated from Rett syndrome patients (Sticozzi et al. 2013).

1.8 SR-B1 regulation and tissue distribution

Several studies demonstrated that SR-B1 expression is controlled through different mechanisms. First, this receptor is regulated by the transcription factor sterol regulatory element-binding protein-1 (SREBP-1) and steroidogenic factor-1 (SF-1) that are able to

bind to the promoter of SR-B1 gene. In fact, SR-B1 promoter contains two putative SREs at positions -1958 (distal SRE) and -238 (proximal SRE) that are known to be SREBP-1 binding sites (Lopez & McLean 1999). Also a motif conforming to the consensus DNA recognition sequence of SF-1, known as Ad4BP, is present 77 bp upstream of the transcription start site (Cao, Garcia, K. Wyne, et al. 1997). Malerod and colleagues have shown that SR-B1 is regulated also by liver X receptor (LXR) together with retinoid X receptor (RXR), receptors involved in cholesterol metabolism (Malerod et al. 2002). A more recent study demonstrated that also other transcription factors are able to bind SR-B1 promoter. In fact, this scavenger receptor's promoter fragment seems to contain PPRE sequence, recognized by peroxisome proliferators-activated receptor-γ (PPAR-γ1 and PPAR-γ2), which have been shown to up-regulate SR-B1 gene expression. Such up-regulation appears to depend on the formation of a dimer between PPAR-γ and RXR (Ahmed et al. 2009). Moreover, Mashurabad et al. (Mashurabad et al. 2016) reported that eicosapentaenoic acid inhibits SR-B1 expression in enterocytes via peroxisome proliferators-activated receptor-α (PPAR-α), suggesting a possible interaction between PPAR-α transcription factor and SR-B1.

SR-B1 expression is regulated also by hormones. An *in vivo* study has demonstrated that intraperitoneal injection of adrenocorticotropic hormone (ACTH) increased adrenal SR-B1 levels, while ACTH release inhibitors markedly decreased SR-B1 expression (Rigotti et al. 1996). Estrogen as well is able to induce SR-B1 expression in the adrenal gland and in the ovary, while it decreases the receptor's expression in the liver, suggesting a tissue-dependent effect (Landschulz et al. 1996). Also administration of human chorionic gonadotropin (HCG) induces a significant increase of SR-B1 in the steroidogenic Leydig cells of rat testes, indicating that increased SR-B1 expression occurs in parallel with increased steroid hormone production (Li et al. 1998). Furthermore, it has been shown that cholesterol is another regulator of SR-B1. In fact, cholesterol depletion by β-cyclodextrin in cultured adrenal cells led to a significant reduction of cellular free cholesterol in association with an increase in SR-B1 mRNA and protein levels (Sun et al. 1999).

Ikemoto and colleagues (Ikemoto et al. 2000) showed that SR-B1 binds at its carboxyl-terminal tail to a cytoplasmic adaptor protein, PDZ domain-containing protein PDZK1. This polypeptide contains four PDZ domains, of which only PDZ4 domain seems responsible for PDZK1 membrane localization and binding to SR-B1 (Tsukamoto et al. 2013). All four domains play a role in controlling abundance, localization and thus function of hepatic SR-B1 (Fenske et al. 2009). Studies have demonstrated that PDZK1 is

able to regulate SR-B1 expression *in vivo*. In fact, inactivation of PDZK1 gene in mice led to a striking decrease of SR-B1 protein expression in hepatocytes and small intestine epithelial cells, while no effect was observed in steroidogenic tissues. Furthermore, these mice showed also plasmatic lipoprotein profile similar to the one observed in SR-B1-null mice (Kocher et al. 2003). The use of SR-B1/PDZK1 double knockout mice with induced hepatic overexpression of wild type SR-B1 presented almost normal levels of functional cell surface SR-B1 levels in the liver, together with restored lipoprotein metabolism. This suggests that PDZK1 is crucial in maintaining adequate steady state expression of hepatic SR-B1, but it appears not essential for its cell surface expression, provided that hepatocytes are able to generate sufficient amount of SR-B1 (Yesilaltay et al. 2006).

Recently, it has been reported the regulation of SR-B1 protein expression by oxidative stress. In fact, it has been demonstrated that cysteine residues contained in SR-B1 protein structure are a target for oxidative stress-induced lipid peroxidation products, such as 4-hydroxynonenal (4-HNE), leading to the formation of covalent bounds between the protein and 4-HNE. In the intracellular compartment, 4-HNE-SR-B1 adducts are recognized by the ubiquitination system, inducing their subsequent degradation by the proteasome (Sticozzi et al. 2012; Valacchi et al. 2014).

SR-B1 was first reported to be expressed mostly in the tissues with critical role in cholesterol transport and metabolism, such as liver and steroidogenic tissues. Following studies have discovered SR-B1 significantly expressed in multiple other body compartments. Therefore, this scavenger receptor can be considered a ubiquitous protein.

Investigations carried out on different organs and cell types reported that SR-B1 is expressed in adrenal tissues, placenta, kidney, ovary and liver (Cao, Garcia, K. Wyne, et al. 1997). In the liver, SR-B1 was found expressed in parenchymal and Kupffer cells (Fluiter et al. 1998), as well as in sinusoidal endothelial cells (Ganesan et al. 2016). SR-B1 is expressed also in steroidogenic tissue (Landschulz et al. 1996), in trophoblastic cells of the maternal side and chorionic cells of the fetal side in placenta (Hatzopoulos et al. 1998), in cortical and tubular kidney cells (Johnson et al. 2003), brain astrocytes (Husemann et al. 2001), pneumocytes (Kolleck et al. 1999), macrophages (Buechler et al. 1999), endothelial cells and vascular smooth muscle cells (Yeh et al. 2002), enterocytes (Werder et al. 2001), melanoma cells (Plebanek et al. 2015) and skin (Sticozzi et al. 2012).

Only recently the presence of SR-B1 in cutaneous tissues has been evidenced although its function in skin is still under investigation.

CHAPTER 2

Cutaneous structure and functions

2.1 Skin structure

The skin represents the largest human organ, which covers the external surface of the body, and it consists of three main layers, hypodermis, dermis and epidermis, as illustrated in Figure 2.1.

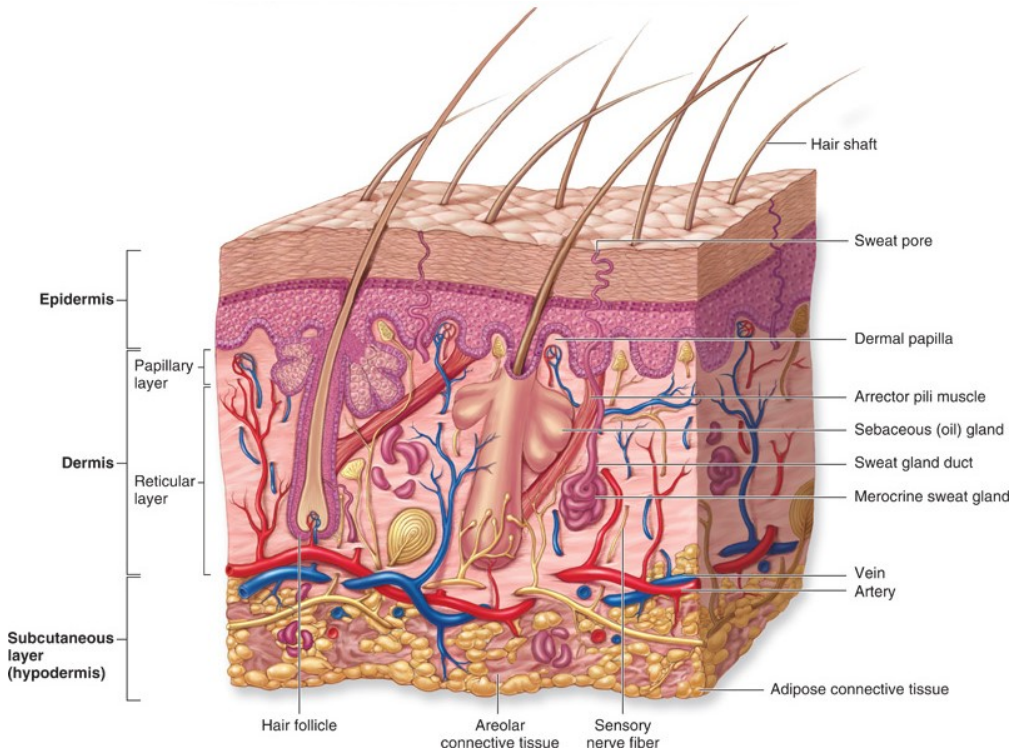

Figure 2.1 – Skin structure and components; Copyright © The McGraw-Hill Companies, Inc.

The innermost skin layer is the hypodermis, a subcutaneous adipose tissue composed by lipocytes. The lipocytes are arranged in structures named lobules, which are separated by fibrous septae made up of collagen and blood vessels. The hypodermis functions as storage of energy and acts as a padding, absorbing physical shocks. Moreover, it is well vascularized and it can be considered an endocrine interface since it allows communication between skin and other organs; furthermore, the lipocytes synthetize leptin, a hormone implicated in body weight regulation. The hypodermis is anchored to the dermis through collagen and elastin fibers originating in the dermis (Holloway & Jones 2005; Kolarsick et al. 2009).

The dermis is the middle cutaneous layer, which confers elasticity and tensile strength to the skin, protecting it from mechanical injury. The dermal structure and composition vary in a depth-dependent manner; in fact, two layers can be distinguished within the dermis: papillary and reticular. The papillary dermis represents the thin upper layer abundantly supplied by blood vessels and sensory nerves, that interdigitates with the epidermal ridges. It contains loose elastic fibers and collagen type III, which form a matrix in which cells are

randomly distributed. The reticular dermis is the main dermal layer, in which cells are spread in a dense matrix made up by coarse elastic fibers and collagen type I. It is located in direct contact with the hypodermis and contains mechanoreceptors such as Pacinian and Ruffini corpuscles. Within the dermis, cells like lymphocytes, dermal dendritic cells, histiocytes and mast cells can be found, although the major cellular population is represented by fibroblasts, that are responsible for the secretion of collagen, elastin fibers and ground substance. The ground substance consists of amorphous mucopolysaccharides and hygroscopic proteoglycan macromolecules in which the cells and fibers reside, in order to offer the dermis the right consistence. The nature of the macromolecules forming the ground substance allows the binding of water that facilitates passage of nutrients, while the high vasculature of the dermis is essential for oxygen and nutrients delivery to cutaneous tissue, as well as for waste products removal (Powell & Soon 2002; Kolarsick et al. 2009; Lai-Cheong & McGrath 2013). Furthermore, the dermis provides nutritional support to the epidermis through the dermal-epidermal junction, called also basal lamina. In fact, it represents a network of macromolecules that create a porous membrane, which allows the exchange of nutrients, cells and molecular signals. Moreover, the basal lamina holds the dermis and the epidermis together; it is formed mainly by collagen type IV, synthetized by basal cells of the epidermis, and it contains also dermal micro-fibrils and anchoring fibrils (Kolarsick et al. 2009). The anchoring fibrils have as principal component collagen type VII and they provide stability to the dermal-epidermal adhesion on the dermal site at papillary dermis level (Chung & Uitto 2010). On the other side, the epidermal basal cells are attached to the basal lamina through hemidesmosomes, cellular junctions that allow the interaction between cytoplasmic keratin fibers and extracellular matrix molecules, maintaining a stable adherence of the epidermis to the dermis (Hopkinson et al. 2014).

The epidermis is the outermost cutaneous layer, a stratified squamous epithelium made up by closely piled cells that form four epidermal layers (Figure 2.2). The epidermis harbors different cell populations, such as melanocytes, Langerhans cells, Merkel cells and keratinocytes, with the last being the most numerous and responsible for the epidermal layout. The deepest layer of the epidermis is the basal layer,

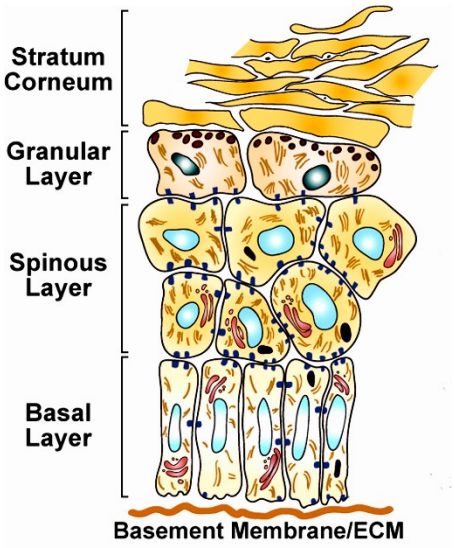

Figure 2.2 – Epidermal layer; adapted from Fuchs (Fuchs 2008)

or *stratum basale*, composed by column-shaped keratinocytes with high mitotic activity. They are tightly attached to the dermal-epidermal junction with hemidesmosomes and to the adjacent cells with desmosomes. Among keratinocytes, the basal layer contains also melanocytes, which produce and secrete melanin, and Merkel cells, mechanoreceptors involved in sensory perception. Keratinocytes of basal layer present a long life span, dividing and generating new cells that move upwards to create the upper epidermal layers. Suprabasally, the next layer is the spinous layer, or *stratum spinosum*, the thickest of all layers of the epidermis. It contains polyhedral-shaped keratinocytes that, in proximity to the *stratum basale*, maintain a slight mitotic activity and become larger and flatter as they move towards the skin surface. Keratinocytes interdigitate with each other forming numerous intercellular junctions. Within this layer Langerhans cells, which are antigen-presenting dendritic cells, can also be identified. Moving upwards, the following layer is the granular layer, called also *stratum granulosum*, which is made up by flattened granulated keratinocytes. These cells present nuclei but lose the limiting membranes. They produce and release keratohyaline granules from their cytoplasm, together with the lipid components, into the extracellular compartment. Finally, the cornified layer, or *stratum corneum*, is the most superficial epidermal layer and it consists of corneocytes, which are keratinocytes that have lost the nuclei and cytosolic organelles. Corneocytes are filled up with fibrils and amorphous proteins and they are surrounded by extracellular lipid matrix. In palmoplantar area, the skin presents a fifth epidermal layer named *stratum lucidum*. It resides between the cornified and the granular layers and it is composed of flat refractive eosinofilic cells, that present thick cellular membranes and almost no nuclei (Greaves 1976; Arda et al. 2014).

The interface between epidermis and dermis is a key zone for the growth of epidermal appendages, which derive as down-growth from the epidermis during development. Cutaneous appendages include eccrine and apocrine sweat glands, hair follicles, sebaceous glands and nails. Such structures are involved in thermal regulation, scent release and protection from the environment (Kolarsick et al. 2009). The sebaceous glands reside in hair-covered areas of human body, connected to hair follicles, and they secrete an oily substance called sebum that contains lipids and debris of dead fat-producing cells. The sebum is produced by cells named sebocytes, which accumulate lipid droplets into the cytoplasm and release them upon burst. Sebum excretion is essential for the functional maintenance of the surface of skin by controlling moisture and waterproofing (Zouboulis 2004).

2.2 Physiological cutaneous processes

In order to maintain its architecture, cutaneous tissue undergoes two main processes that interest the epidermis: proliferation and differentiation. These two processes are tightly linked and need to be balanced so that skin homeostasis and health are preserved. In fact, excessive proliferation can lead to disorders such as psoriasis or skin tumor, while premature differentiation generate a considerably thin epidermis (Fuchs & Raghavan 2002).

Epidermal proliferation occurs into the basal layer, where cells have the ability to divide, continuously providing new cells. Therefore, it is believed that epidermal basal layer harbors stem cells. In 1974, Allen and Potten (Allen & Potten 1974) have defined the presence of the epidermal proliferative unit (EPU), a group of 10-11 tightly packed basal cells that form a hexagonal-shaped area, in which one stem cell is contained and the others are so-called transit-amplifying cells. These last cells are fated to move upwards and differentiate (Figure 2.3). It is assumed that epidermal basal cells divide symmetrically, giving rise to identical daughter cells, and progressively they exit basal layer committing to terminal differentiation (Watt & Hogan 2000). Lately, though, an asymmetric division model has been proposed. With this mechanism, basal cells can either divide perpendicularly to the basement membrane, with the daughter cell being positioned directly into the spinous layer, or divide laterally. In this case, daughter and progenitor cells are not identical, but one inherits a stronger Notch signal and loses contact with basal layer, moving upwards, while the other one remains into the basal layer (Clayton et al. 2007). The fate of the epidermal basal cells is regulated by different stimuli. It has been shown that high expression of β1 integrins on cellular surface increase the life span of cultured keratinocytes, while low levels of such integrins reduce drastically the number of passages (Jones et al. 1995). Also the communication between cells and basal lamina is essential, in fact, the interaction of extracellular laminin 5 with cellular junctions strengthens the anchorage, maintaining the basal cells into mitotic area (Manohar et al. 2004). Other stimuli are the transcription factor p63 (Candi et al. 2015) and EGF receptor (Ehmann et al. 2011), which sustain proliferative capacity of epidermal stem cells, or TGF-β and calcium, which have inhibitory effect on epidermal cell growth and promote differentiation (Yamasaki et al. 2003).

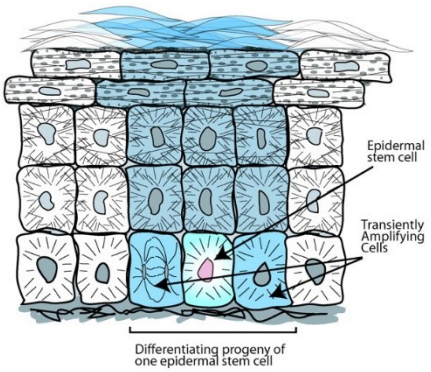

Figure 2.3 – Epidermal proliferative unit; adapted from Alonso & Fuchs (Alonso & Fuchs 2003)

Once an epidermal basal cell commits to terminal differentiation, it down-regulates the expression of basal-specific keratins, K5 and K14, loses the contact with basal lamina and adjacent cells and migrates upwards into the spinous layer. Here the expression of keratins K1 and K10 is induced and cells present larger nuclei due to high activity in synthetizing fibrilar keratins, which aggregate together forming tonofibrils. The tonofibrils go on to form the desmosomes and create strong connections between adjacent keratinocytes. Moving further towards the skin surface, cells reach the granular layer where they start to produce keratohyalin granules containing loricrin and profilaggrin. Cells become more permeable, calcium enters the cytoplasm and induces the processing of profilaggrin into filaggrin. Filaggrin aggregates the keratin filaments into tight bundles, inducing the flattened cellular shape, a characteristic of corneocytes present in the cornified layer. Lipids are also released from the cytoplasm to seal the spaces between cells. Calcium activates epidermal transglutaminases, which catalyze the formation of tight crosslinks between cellular fibrils. Proteolytic enzymes degrade the nuclei and other organelles and cells collapse into flattened squames, which are progressively released from the skin. The entire process of epidermal proliferation and differentiation is cyclic and continuous and each cycle lasts up to 28 days (Fuchs & Byrne 1994; Candi et al. 2005). Several regulators have been reported to be involved in terminal differentiation, among which AP1, NF-kB, PPARs and MAF (Dai & Segre 2004; Klein & Andersen 2015).

Epidermal growth and differentiation are essential not only for cutaneous homeostasis, but also during injury recovery, when it is initialized a process of wound healing involving both dermal and epidermal compartments (Figure 2.4). Wound healing represents a complex biological process involving a cascade of cellular, biochemical and molecular events, which intent to restore the structural and functional integrity of the skin (Reinke & Sorg 2012). The first step of this process is hemostasis induced by aggregation of platelets, followed by three distinctive, overlapping phases: inflammatory, proliferative and remodeling.

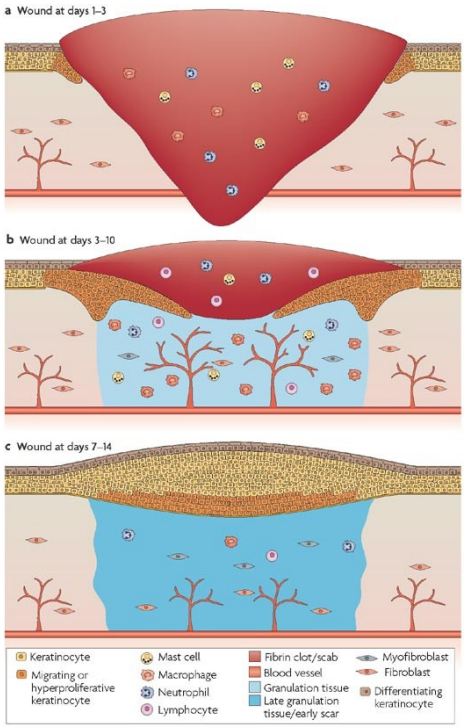

Figure 2.4 – Wound healing stages; reproduced from Schäfer & Werner (Schäfer & Werner 2008)

During these phases, the interaction between various leukocytes-derived inflammatory cytokines, growth factors, cell adhesion molecules and enzymes present in the extracellular matrix, can be observed (Wikramanayake et al. 2014). Upon injury, cutaneous basal lamina is degraded and keratinocytes are stimulated to migrate over a provisional extracellular matrix that is rich in fibronectin and dermal collagen, in order to form a cell monolayer over the denuded dermis. Cell migration is a dynamic process characterized by the organization of cytoskeletal actin to form focal adhesion points, which are mostly regulated by integrins (DiPersio et al. 2016), and involves specific matrix degrading enzymes named matrix metalloproteinases (MMPs), which control keratinocyte attachment and retraction (Michopoulou & Rousselle 2015).

2.3 Functions of skin

The skin is an essential organ for protection against the "outdoor" environment, but also for communication between human body and the external surroundings. In fact, skin contains numerous nervous endings that act as receptors involved in perception of external stimuli. Such receptors detect pressure and vibration (Merkel cells and Pacinian corpuscles), stretch (Ruffini corpuscles), itch (c-fibers), pain (nociceptors) and temperature (thermoreceptors), and transmit the stimuli to the central nervous system through afferent neurons (Laverdet et al. 2015). Cutaneous tissue contributes also to immune protection in order to avoid microorganisms infections. Keratinocytes produce anti-microbial peptides, such as defensins and cathelicinds, which are active against bacteria, fungi and viruses. Moreover, cathelicidins have the ability to act as chemoattractants for inflammatory cells. Langerhans cells function as antigen-presenting cells. Once it binds to an antigen, it leaves the epidermis, enters dermal lymphatic system and reach the lymph nodes where antigen is presented to T-cells that migrate and enter the skin in the site of infection. Another anti-microbial mechanism is given by the cornified layer's dryness and by the continuous desquamation (Venus et al. 2011).

Other functions of the skin comprise protection from ultraviolet (UV) radiation, through the production of melanin, which is transferred from melanocytes to keratinocytes in order to create a hood-like structure on top of cellular nuclei that protects from UV-induced DNA damage (Brenner & Hearing 2008). Skin is also involved in thermoregulation through vasodilatation and vasoconstriction of cutaneous blood vessels, as well as through sweating produced by eccrine sweat glands (Romanovsky 2014). Furthermore, the epidermis is the site where vitamin D is synthetized (Wacker & Holick 2013).

Finally, skin functions as a physical barrier between environment and human body. In fact, the epidermal cornified layer represents a relatively impermeable structure due to the scaffold-like mesh created by the tightly bound fibrous cellular proteins. Cutaneous impermeability is given also by the lipid envelope in which corneocytes are distributed, which protects skin from water and solutes loss (Proksch et al. 2008). The lipid envelope originates from intercellular skin lipids, which are synthesized and stored in granules (Odland bodies) and lamellar bodies in keratinocytes of the granular layer; these lipids are subsequently extruded into the extracellular space during cornification. Most of the cellular lipids in cornified layer are ceramides, cholesterol, fatty acids and cholesterol esters that form lamellae between the corneocytes of the extracellular compartment (Candi et al. 2005). Along with epidermis-derived lipids, skin surface contain also sebaceous lipids such as squalene, poly-unsaturated fatty acids (PUFA), triacylgrlicerol and wax esters (Niki 2015).

Moreover, human skin presents a radical scavenging system (Godic et al. 2014), which allows the protection from environmental agents including UV radiations and chemical mixtures. However, its defensive capacity is not unlimited and excessive exposure to environmental oxidizing stressors may lead to skin disorders. UV-induced photo-oxidation interests the dermis (UVA) and the epidermis (UVB) and it is driven by the formation of singlet oxygen, which can oxidize both lipids (Gruber et al. 2007) and proteins (Pattinson et al. 2012). Also ground-level ozone represents a risk for skin health; its action is superficial, thus leading to oxidation of lipids, such as cholesterol and PUFA, and subsequent barrier perturbation and inflammatory response (Thiele et al. 1997; Wang & Morrison 2010). Cutaneous oxidative and inflammatory damage is given also by other environmental agents, such as cigarette smoke (Armstrong et al. 2011) and airborne particles (Vierkötter et al. 2010). All harmful effects induced by pollutants may lead to skin aging and other pathological alterations, such as erythema, edema, hyperplasia, contact dermatitis, atopic dermatitis, psoriasis, and carcinogenesis (Lanuti & Kirsner 2010; Xu et al. 2011; Valacchi et al. 2012).

CHAPTER 3

Environmental pollutants and oxidative stress

3.1 Environmental pollution

Environmental pollution represents a heterogeneous mixture of compounds, in which chemical composition, size and sources differ in each microenvironment. It is made up by materials in solid, liquid and gaseous phases and it can be caused by both human interventions and/or natural phenomena (Nel 2005). US Environmental Protection Agency has divided pollutants into six major classes, which are able to harm human health and the ecosystem. Three of these classes, that have been extensively associated with diseases, are cigarette smoke, ground-level ozone and particulate matter (web source: www.epa.gov/iaq/pubs/hpguide.html).

3.1.1 Cigarette smoke

Cigarette smoke (CS) is a complex mixture of gas with more than 4000 compounds, steam and solid particles derived from the cigarette combustion and represents one of the principal indoor chemical pollutants. It contains components, such as nicotine, carbon monoxide, tar, oxidants (i.e. hydrogen peroxide) and carcinogenic compounds (i.e. benzene, formaldehyde, metals). It has been estimated that the aerosol inhaled by the active smoker is composed of several billion semi-liquid particles per cm^3 within the mixture of combustion gases (Smith & Fischer 2001).

CS has been associated with several pathological conditions over the years. It has been shown that smoking is implicated in cardiovascular diseases, due to its ability of inducing vascular inflammation, platelet coagulation, vascular dysfunction and impaired serum lipid profile (Siasos et al. 2014). It has been reported also a link between CS-induced oxidative stress and neurodegeneration (Deochand et al. 2016), autoimmune diseases (Perricone et al. 2016) and even corneal injuries (Cejka & Cejkova 2015).

The main two organs which are directly exposed to CS and on which CS exerts its direct detrimental effects are the lungs and the skin (Patel et al. 2008; Ortiz & Grando 2012).

In the respiratory tract, CS has been shown to induce protein carbonylation followed by activation of transcription factors, such as mTOR, leading to inflammation and protein modifications into the respiratory muscle, muscle loss and respiratory dysfunction (Barreiro et al. 2010; Carlos et al. 2014). Moreover, CS activates NF-kB and impairs cellular junctions by oxidative damage in lung epithelial cells (Muresan et al. 2015) and induces excess collagen production and high levels of inflammatory cytokines (Martins-Green et al. 2014). CS also induces pulmonary tumor; in fact, a study has demonstrated that CS leads to aberrant EGF receptor activation and uncontrolled cell growth (Filosto et

al. 2012). In addition smoking has been proven to be the main cause of COPD development (Rahman 2006; Valacchi et al. 2015).

Regarding the skin, CS's most visible effect is the so-called "smoker's face" (Model 1985), characterized by prominent wrinkles, gauntness of facial features with prominence of the underlying bony contours, and gray appearance of the skin. This effect is due to premature skin aging induced by increased reactive oxygen species (ROS), up-regulation of enzymes such as MMPs and collagen degradation (Ortiz & Grando 2012). Along with skin aging, CS was connected also with psoriasis. A case-control study underlined that smokers are more susceptible to pustular lesions and early-stage psoriasis (Naldo et al. 1999). Another interesting process that is disrupted by CS exposure is skin wound healing. This has been demonstrated in a study performed on mice exposed to third hand smoke, namely the accumulation of indirect smoking on surfaces that ages with time, where these mice show many characteristics of poor healing of surgical incisions (Martins-Green et al. 2014).

3.1.2 Ozone

Ground-level ozone (O_3) has been defined by the World Health Organization as "increasing poison" and it is the most widespread health threat. O_3 is formed by three oxygen atoms and in the lower atmosphere it is created by chemical reactions between oxides of nitrogen (NOx) and volatile organic compounds (VOC), coming from sources like motor vehicle exhaust and emissions from industrial facilities, in the presence of sunlight. The photochemistry involved in O_3 generation includes reactions, such as photoactivation, photodecomposition, and free radical chain reaction. In fact, although O_3 is not a radical species, its effects are mediated through free radical reactions (Pryor 1999).

Like in the case of CS, the target tissues of O_3 are the respiratory tract and the skin. O_3 is not able to penetrate the cells, but it reacts with polyunsaturated fatty acids (PUFA) to form H_2O_2 and ROS, and lipid peroxidation products, for example 4-hydroxy-2,3-nonenal (4-HNE) (Hamilton et al. 1998). In the lung, O_3 interacts with respiratory tract lining fluids (RTLFs), which contain radical scavengers, therefore O_3 is removed before it reaches the cells; though, repeated exposures lead to antioxidants depletion and O_3 enters in contact with pulmonary cells, promoting oxidation and inflammation (Cross et al. 2002). In fact, an *in vivo* study reported that mice exposed to O_3 presented decreased α-tocopherol in lung and plasma and increased levels of heme oxygenase 1 (HO-1), cyclooxygenase 2 (COX-2) and proliferating cell nuclear antigen (PCNA), as well as NF-kB activation, in lung and

skin (Valacchi et al. 2004). In the skin, O_3 does not penetrate into the deep layers of the epidermis, but reacts with the lipids of *stratum corneum* leading to lipid peroxidation (4-HNE) and activation of endogenous antioxidant response (Nrf2 pathway), as shown on SKH-1 hairless mice (Valacchi et al. 2002) and later confirmed in an *in vitro* 3D human skin model (Valacchi et al. 2016). In addition, time-lapse analysis conducted in Shanghai, China, revealed a tight association between emergency-room (ER) visits for skin conditions and O_3 exposure. Over 68,000 cases of skin disorders were recorded in two years and, by evaluating the link between the time-period of the day and the concentrations of air pollutants, it was demonstrated that increased O_3 levels corresponded to increased incidence of skin conditions, such as urticaria, eczema, contact dermatitis, rash and infected skin diseases (Xu et al. 2011). Furthermore, recent case-crossover analysis revealed a relationship between ozone exposure and infections by Streptococcus bacteria (Valacchi et al. 2015).

3.1.3 Particulate matter

Airborne particulate matter (PM) consists in a complex mixture of poly-aromatic hydrocarbons, metals, organic toxins and biological materials that potentially trigger oxidative stress and inflammation (Li et al. 2009). PM have both biogenic and anthropogenic origins, such as windborne dust, wild fires, volcanic eruptions, or combustion of fuels, industrial processes and transportation sources (K. Kim et al. 2015). PM is generally classified by the size of the particles: PM_{10}, $PM_{2.5}$ (fine) and $PM_{0.1}$ (ultra-fine). The smaller are the particles the higher is the diameter/surface area rate where molecules could be absorbed. Therefore, fine and ultrafine particles fraction seem to be of major concern from the health perspective, since they can act as carrier for organic and inorganic compounds (Delfino et al. 2005).

It has been reported that PM deleterious effects are caused by oxidative stress, which is involved also in triggering pro-inflammatory pathways by activating NF-kB and inducing the transcription of inflammation-related genes such as IL-1α and COX-1 (Marchini et al. 2014). Moreover, PM accelerates coagulation (Mutlu et al. 2007), promotes neurotoxicity (Liu et al. 2015) and is involved in cardiovascular and respiratory diseases through mitochondria dysfunction and DNA damage (Dominici et al. 2006; Risom et al. 2005).

PM has been also associated with skin pathologies. In fact, PM-induced ROS production (i.e. superoxide and hydroxyl radical) increases MMPs expression including MMP-1, MMP-2 and MMP-9, resulting in the degradation of dermal collagen. This process leads to

skin inflammation and premature aging (Kim et al. 2016). Recently, Magnani and colleagues (Magnani et al. 2016) have demonstrated that PM is able to penetrate the epidermis in a time and dose-dependent manner, leading to lipid peroxidation, NF-kB activation with increased COX-2 and cytochrome P450 levels, as well as apoptosis initiation.

3.2 Oxidative stress: the common denominator of pollution induced tissue damage

Oxidative stress is defined as a disturbance in the prooxidant-antioxidant balance in favor of the oxidants, which leads to potential damage. Oxidants are normally formed during physiological aerobic metabolism and cleaved by antioxidant systems, but they can be produced in elevated quantity during pathological conditions. The antioxidant systems, which play an important role in maintaining the redox balance, consist in intracellular enzymes such as superoxide dismutase (SOD), catalase (CAT), glutathione reductase (GR) and glutathione peroxidase (GPx), but also non-enzymatic molecules, such as glutathione, ubiquinol and vitamins. These non-enzymatic molecules are compounds with chemical structures that give them the ability of radical scavenging, and can be both endogenous and exogenous (Sies 1997).

Free radicals can be divided into two classes: reactive oxygen species (ROS) (Ray et al. 2012) and reactive nitrogen species (RNS) (Bove & van der Vliet 2006). Cell types employed in defense such as granulocytes, eosinophils and macrophages use NADPH oxidase (NOX) and nitric oxide synthase (NOS) as sources of reactive oxygen species. These include hydrogen peroxide, singlet oxygen, superoxide, nitric oxide and peroxynitrite (Sies & de Groot 1992).

Moderate levels of ROS are critical in cellular signaling and pro-survival pathways. They can activate pathways, such as mitogen-activated protein kinase (MAPK) pathway, which is involved in cell proliferation, migration and apoptosis. Also NF-kB can be activated by free radicals, exerting its anti-apoptotic role by inhibition of caspase-dependent cell death. (G. Kim et al. 2015). It has been reported that ROS are able to regulate AP-1 transcription factor, which controls expression of genes such as cytokines, cyclin D and collagenase (Karin & Shaulian 2001).

High levels of free radicals have been demonstrated to harm cellular components, leading to protein oxidation, lipid peroxidation and DNA filaments damage (Davies 1995). Such modified macromolecules together with intracellular oxidants have been associated with

several disorders. For example, atherosclerosis and other cardiovascular diseases involve elements of oxidative stress. Oxidized lipoproteins, such as OxLDLs, appear to play a major role in the formation of fatty lesions and fibrous plaques in the endothelium of blood vessels; these lesions induce monocyte adherence and further LDL oxidation (Di Pietro et al. 2016). It has been demonstrated that free radicals are involved also in mutagenesis, cell transformation and human tumor (Kryston et al. 2011). Oxidative stress in the brain has been shown to be related to neurodegenerative diseases, associated with stimulation of NOS expression together with mitochondria dysfunction (Aliev et al. 2010; Henchcliffe & Beal 2008; Jiang et al. 2016; G. Kim et al. 2015). Other pathological conditions clearly connected to free radicals are the inflammatory diseases. On one hand, reactive oxygen species enhance inflammation; on the other hand, inflammation promotes oxidative stress. When the inflammatory event becomes chronic, oxidative damage becomes a significant contributor to progression of diseases, many of them skin-related, such as rheumatoid arthritis, lupus erythematosus, psoriatic arthritis and dermatitis (Davies 1995).

Since oxidative stress is harmful especially in chronic conditions and leads to multiple disorders in different tissues, it appears crucial to maintain the network of redox steady state in order to maintain health.

CHAPTER 4

Rationale and aims

SR-B1 is a membrane glycoprotein identified as the main physiological receptor for HDL (Acton et al. 1996) and thus it has been studied mostly for its role in cholesterol transport and uptake from HDLs to liver and steroidogenic tissues, influencing cholesterol plasma levels as well as cholesterol distribution into peripheral body compartments (Krieger 2001). Further studies have demonstrated that SR-B1 is implicated also in other processes, such as recognition of viruses and bacteria (Bartosch et al. 2005; Vishnyakova et al. 2006), uptake of liposoluble vitamins (vitamin E and pro-vitamin A) (Borel et al. 2007) and identification of apoptotic cells (Cao et al. 2004). Recently, the involvement of SR-B1 in cellular exosomes trafficking has been also reported (Angeloni et al. 2016). In addition to being a multifunctional receptor (Valacchi, Sticozzi, et al. 2011), SR-B1 is also ubiquitous, being expressed in multiple cells and organs not only related to steroidogenic tissues (Rhainds & Brissette 2004). Indeed, this scavenger receptor was also found in human skin, with high expression in the epidermis (Sticozzi et al. 2012).

Human skin represents the largest organ in human body and it is made up by three main layers. The innermost layer consists of the subcutaneous fat, which functions as a storehouse of energy. The intermediate layer is the dermis, in which the most abundant cell type is represented by fibroblasts, that are integrated in a system of fibrous proteins and nerve and vascular networks. The dermis protects body from mechanical injury and offers elasticity and tensile strength (Powell & Soon 2002; Kolarsick et al. 2009). The outermost layer of the skin is the epidermis, a stratified squamous epithelium where keratinocytes represent the main cell population and form the four layers in which the epidermis is divided. Epidermal cells from the proliferative basal layer migrate upwards, differentiating and forming the spinous and granular layers and finally reaching the horny layer (Fuchs & Raghavan 2002). A correct differentiation process helps to provide proteins and a part of the lipids necessary for the barrier function in the epidermis and for preventing loss of fluids. The other part of lipids contained in the horny layer is provided by the sebum produced in sebaceous glands. Skin surface lipids composition is crucial for the protective role of the cutaneous tissue and alterations of lipid content have been associated with different skin diseases as well as skin aging. (De Luca & Valacchi 2010). Due to the superficial localization, skin and especially epidermal lipids are subjected to oxidative processes, which, when not counteracted by skin antioxidants, lead to generation of bioactive by-products and possible modulation of the deeper cutaneous layers equilibrium (Weber et al. 2001). Such oxidative processes may be induced by environmental stressors, including both ultraviolet (UV) and chemical exposures.

Air pollution is one of the most studied types of chemical exposure, as it represents a heterogeneous mixture of chemicals and solid particles, in which chemical composition, size and source of origin differ in each microenvironment (Nel 2005). Cigarette smoke, ozone and particulate matter represent escalating environmental pollutants and have the ability to induce oxidative stress and inflammation (Sticozzi et al. 2012; Valacchi et al. 2016; Magnani et al. 2016), which target not only the skin lipids but also other cellular molecules.

Since SR-B1 was shown to be expressed in the epidermis, a cutaneous compartment where cells have no direct blood and HDL supply, it was of interest to understand the physiological role that this receptor has in this skin layer. Therefore, our study aimed to investigate the implication of SR-B1 in the main epidermal processes. The first process to be evaluated was proliferation, which involves progeny cells of the basal layer and is of striking importance for the cutaneous turnover (Powell & Soon 2002). The second process taken into consideration was cell migration, which, together with cellular proliferation, is essential upon skin wounding for efficient production of new epidermis and fast wound closure (Werner & Grose 2003). The third process studied was keratinocytes differentiation, which allows the formation of all epidermal layers overlying basal membrane (Fuchs & Raghavan 2002). Since SR-B1 is involved in lipids metabolism, we also investigated the implication of the receptor in lipids content within the epidermis. Moreover, SR-B1 expression was evaluated in sebaceous glands, which provide an important part of the lipids present in the horny layers, and its modulation of sebocytes cholesterol levels.

As mentioned above, environmental stressors target cutaneous tissue, leading to oxidative damage and molecular modifications, which interest lipids, DNA and proteins. For instance, it has been shown in an *in vitro* study that cigarette smoke exposure induced SR-B1 oxidative post-translational modifications (Sticozzi et al. 2012). As a follow up of the above mentioned study, it was of our interest to assess whether such modulation was maintained also in a more complex three-dimensional skin model consisting of all epidermal layers, exposed not only to cigarette smoke but also to ozone and air particles. Furthermore, SR-B1 expression was evaluated in human skin biopsies from subjects exposed to ozone and by the topical application of natural protective compounds we were able to confirm that SR-B1 loss was mediated by oxidative damage.

Understanding SR-B1 function in the skin physiology and the modulation of its expression by environmental pollutants, might underline the importance of SR-B1 as a new target for future studies on cutaneous pathological conditions related to outdoor stressors.

CHAPTER 5

Material and methods

5.1 Two-dimensional study

Cell culture

HaCaT cells (gift from Dr. F. Virgili INRAN, Rome, Italy) were cultured in high glucose Dulbecco's Modified Eagle's Medium (EuroClone, Milan, Italy) supplemented with 10% FBS (EuroClone), 2 mM L-Glutamine (EuroClone), 100 U/ml penicillin and 100 µg/ml streptomycin (EuroClone). SZ95 sebocytes (gift from Dr. C.C. Zouboulis, Dessau, Germany) were grown in Sebomed (Biochrom, Berlin, Germany), supplemented with 10% FBS (EuroClone), 100 U/mL penicillin (EuroClone), 100 µg/mL streptomycin (EuroClone) and 5 µg/L EGF (Biochrom). All cell cultures were performed at 37°C in 5% CO_2 and 95% air.

SR-B1 knockdown

HaCaT or SZ95 cells of 50–60% confluence were transfected using Lipofectamine 2000 (Invitrogen, CA, USA) according to the manufacturer's instructions. 300 µl Opti-MEM medium (Gibco, NY, USA) were mixed with 6 µl of Lipofectamine 2000 and 2 µl of a 100 µM siRNA (Ambion, Cambridgeshire, UK) solution or the scrambled control RNA solution. After incubation at room temperature for 10 min, 250 µl of the solution were added to 2 ml DMEM or Sebomed supplemented with 2 mM L-Glutamine and transferred to the cells. Cells were then incubated at 37°C for 24 h.

Wound healing assay

HaCaT cells were incubated at 37°C, in a humidified 5% CO_2 atmosphere until complete confluence. The adherent cell layer was scratched with a sterile yellow pipette tip and media was removed. Cellular debris were removed by washing off with PBS and fresh media was added. Cells were incubated at 37°C and images of the scratch area were recorded in three different points, using a built-in camera in an inverted Nikon Eclipse microscope (40X magnification) at 0, 2, 4, 6, 8 and 24 h. Data were analyzed with ImageJ software in order to determine the width of the scratch.

Immunocytochemistry

HaCaT cells were grown on coverslips at a density of $1x10^5$ cells/ml. After knockdown and at each post-scratch time point, cells were fixed in 4% paraformaldehyde (PFA) in PBS for 30 min at 4°C. Cells were permeabilized and then blocked in PBS containing 1% BSA, 0.2% Nonidet P-40 and 0.02% sodium azide at room temperature for 1 h. Coverslips were then incubated for 1 h with primary antibody, followed by 1 h with fluorochrome-conjugated secondary antibody. Nuclei were stained with 1 µg/ml DAPI (Molecular Probes, Oregon, USA) for 1 min after removal of secondary antibody. Coverslips were

mounted onto glass slides using anti-fade mounting medium 1,4-diazabicyclooctane in glycerine (DABCO) and examined by the Zeiss Axioplan2 light microscope equipped with epifluorescence. Negative controls were performed by omitting primary antibodies. Images were acquired and analyzed with Axio Vision Release 4.6.3 software.

Viability and Proliferation assay

Cell viability and proliferation were evaluated respectively by Trypan blue exclusion and BrdU incorporation assay. $1x10^5$ cells were seeded and grown for 24 and 48 h. At each time point, cells were trypsinized and resuspended in 1 ml of culture media. 10 µl of Trypan blue solution (Sigma, Milan, Italy) were added on 10 µl of cell suspension and viable cells were counted in a Bürker cell counting chamber. The BrdU procedure was carried out in 96-wells plate according to the original protocol from the manufacturer (Roche, Milan, Italy). Briefly, 20 µL of BrdU labeling solution were added to each well for 4 h. Then cells were blow dried, fixed, and the DNA denatured in order to make the incorporated BrdU more accessible for detection by the antibody. The monoclonal anti-BrdU peroxidase conjugated antibody was added to the cultures and incubated for 90 min at room temperature (RT). After three washing steps the bound peroxidase was detected by subsequent substrate reaction. This reaction was stopped by adding 1 M H_2SO_4 and quantified by measuring the optical density of the yellow reaction product at a wavelength of 450 nm and a reference wavelength of 630 nm using a plate reader (Tecan Infinite M200, Tecan group Ltd., Switzerland).

In vitro cell migration assay

Cell migration assay was performed in 24-wells plate using 8 µm-pore size transwells (QCM™ 24-well Colorimetric Cell Migration Assay kit, Millipore, CA, USA) coated with 0.15 mg/ml bovine collagen IV. The lower chamber was filled with 300 µl of DMEM medium supplemented with 10% FBS, and the cells were seeded at a density of $2x10^5$ in 100 µl of DMEM without FBS in the upper chamber of triplicate wells. Cells were incubated at 37°C for 6 and 24 h. At each time point, transwell inserts were incubated for with 400 µl Cell Stain for 20 min at RT, then rinsed with ddH_2O. Cells in the upper compartment were removed using cotton swabs and pictures of five random fields were recorded by the use of an inverted Nikon Eclipse microscope.

Scanning Electron Microscopy (SEM) Analysis

Cells were grown on coverslips and confluent cell layer was scratched with a sterile pipette tip. 30 min post-scratch, cells were fixed with 2,5% glutaraldehyde in cacodylate buffer (pH 7.0). Afterwards, cells were dehydrated with increasing gradients of ethyl alcohol until

100% concentration. Cell surface was metallized with a 100 À thick layer of gold-platinum, using a sputter coater Reichard 100. Samples were observed with scanning electron microscope (Zeiss EVO 140) source LaB6, at 20 KV accelerating voltage, equipped with computerized microanalysis system (ISIS Link), with the possibility to operate both conventionally in high vacuum and variable pressure (SEM XVP), maximum pressure 6 torr. Images were captured at 4000X and 9000X in variable pressure.

Total proteins extraction

Cell lysates were extracted in ice-cold buffer containing 50 mM Tris (pH 7.5), 150 mM NaCl, 10% glycerol, 1% Nonidet P-40, 1 mM EDTA, 0.1% SDS, 5 mM N-ethylmaleamide (Sigma) and protease and phosphatase inhibitor cocktails (Sigma). Lysates were cleared by centrifugation (13500 rpm) for 15 min at 4°C and protein concentration was measured by Bradford method (BioRad, CA, USA).

Nuclear-cytosolic proteins extraction

Cell pellets were resuspended in hypotonic buffer containing 10 mmol/l HEPES (pH 7.9), 10 mmol/l KCl, 1.5 mmol/l $MgCl_2$, 0.3% Nonidet P-40, 0.5 mmol/l dithithreitiol, 0.5 mmol/l phenyl-methyl-sulphonyl fluoride and protease and phosphatase inhibitor cocktails. The lysates were incubated for 15 min on ice and then centrifuged at 1500 x g for 5 min at 4°C for collection of the supernatant containing cytosolic proteins. Supernatants were further centrifuged for 15 min at 14000 rpm. Pellets containing the nuclei were resuspended in extraction buffer containing 20 mmol/l HEPES (pH 7.9), 1.5 mmol/l $MgCl_2$, 0.6 mol/l KCl, 0.2 mmol/l EDTA, 20% glycerol, 0.5 mmol/l phenyl-methyl-sulphonyl fluoride and protease and phosphatse inhibitor cocktails, and then incubated for 30 min on ice. Samples were centrifuged at 13000 rpm for 15 min to obtain supernatants containing nuclear fractions. Protein concentration was determined by Bradford method (BioRad).

Western blot

Equivalent amounts of proteins were subjected to 10% SDS-PAGE, electro-transferred onto nitrocellulose membrane, which was then blocked in Tris-buffered saline, pH 7.5, containing 0.5% Tween 20 and 5% not-fat milk (BioRad). Membranes were incubated overnight at 4°C with the appropriate primary antibody. The membranes were then incubated with horseradish peroxidase-conjugated secondary antibody (Millipore) for 1 h, and the bound antibodies were detected in a chemiluminescent reaction (ECL, BioRad). Images of the bands were digitized and the densitometry of the bands was performed using ImageJ software.

Oil Red O staining in cells

SZ95 sebocytes were seeded on coverslips and silenced by the used of siRNA. Sebocytes were fixed with 4% PFA for 30 min at RT, then rinsed with distilled H_2O and 60% isopropanol. Fixed cells were stained with freshly prepared Oil Red O solution for 10 min. Extra stain was remove, samples were washed with distilled H_2O and 60% isopropanol and incubated with Hematoxylin. Coverslips were mounted onto glass slides using glycerol-water 9:1 and than images were acquired with a Leica AF CTR6500HS microscope (Microsystems). The quantification was performed using Image-J software.

Total cellular cholesterol determination

Total cholesterol levels in SZ95 sebocytes were determined using a commercially available fluorimetric assay kit (Cell Biolabs, Inc. San Diego, CA, USA), following manufacturer's instructions. Total cholesterol was extracted with chloroform/isopropanol/NP-40. 50 µl of extracted sample, diluted 1:50 in 1X assay diluent, were loaded into a 96-well plate and then treated with a cholesterol reaction reagent that includes cholesterol esterase, cholesterol oxidase, horseradish peroxidase and a fluorescence probe. After an incubation of 45 min at 37ºC, the fluorescence signal was read at 530 nm (excitation) and 590 nm (emission) with a microplate reader (TECAN – infinite M200). Samples' cholesterol concentrations were determined by interpolation from a standard curve. For normalization, the protein concentration was determined by Bradford method (BioRad); data are presented as µg of cholesterol per mg of protein in cell extracts.

Statistical analysis

For each of the variables tested, two-way analysis of variance (ANOVA) was used. Statistical significance was considered at $p<0.05$. Data are expressed as mean ± SD of triplicate determinations obtained in three independent experiments.

5.2 Three-dimensional study

Cell culture

Primary fibroblasts were cultured in high glucose Dulbecco's Modified Eagle's Medium (Lonza, Basel, Switzerland) supplemented with 10% FBS (PAA, Linz, Austria), 100 U/ml penicillin and 100 µg/ml streptomycin (Gibco, NY, USA). Primary keratinocytes were cultured in Keratinocyte Growth Medium-2 (Lonza, Basel, Switzerland). All cell cultures were performed at 37°C in 5% CO_2 and 95% air.

SR-B1 knockdown

Keratinocytes of 50–70% confluence were transfected in T75 flasks by using Lipofectamine 2000 (Invitrogen, CA, USA). Briefly, 2.5 ml OptiMEM medium (Gibco) with 50 µl Lipofectamine 2000 and 2.5 ml OptiMEM medium with 100 µl of a 20 µM Stealth siRNA solution (Invitrogen) were prepared as separate mixes, then pooled and incubated for 10 min at RT. OptiMEM-Lipofectamine-siRNA mix was added into the cells culture containing 20 ml KGM-2 medium and incubated for 24 h at 37°C in 5% CO_2 cell incubator.

Organotypic skin equivalents

A 2.5 ml suspension of collagen type I (Biochrom) containing $2.5x10^5$ fibroblasts, balanced by Hank's buffered salt solution (HBSS) (Gibco) was poured into each cell-culture insert (3 µm pore size; Corning, NY, USA) for 2 h at 37°C in a humidified atmosphere. The gels were then equilibrated with KGM-2 at 37°C in a 5% CO_2 incubator for 2 h, and $1.5x10^6$ keratinocytes were seeded onto each collagen gel and incubated overnight at 37°C. After overnight incubation at 37°C the medium was removed from both the inserts and external wells, and 10 ml serum-free keratinocytes defined medium (SKDM), consisting of KGM-2 without bovine pituitary extract and supplemented with 1.3 mM calcium (Sigma, Vienna, Austria), 10 µg/ml transferrin (Sigma), 50 µg/ml ascorbic acid (Sigma) and 0.1% bovine serum albumin (Sigma) was added to each external well. Organotypic skin cultures and supernatants for the early differentiation time point were harvested after one day for the late differentiation time point after 5 days. Medium was changed every second day.

Hematoxylin/Eosin staining

Skin equivalents were fixed in 10% buffered formalin and embedded in paraffin. For histological observation, the sections (5 µm thickness) were deparafinized in xylene and rehydrated in alcohol gradients and then stained with hematoxylin and eosin (H/E) (Sigma).

Immunohistochemistry

In vitro: Skin equivalents were immersion-fixed in 10% NBF (neutral-buffered formalin) for 24 h, then dehydrated in alcohol gradients and embedded in paraffin. Sections (5 µm) were deparaffinized in xylene and rehydrated in alcohol gradients. After dewaxing, sections were incubated overnight at 4°C with primary antibodies, followed by 1 h with fluorochrome- conjugated secondary antibodies at room temperature. Nuclei were stained with Hoechst 33258 (Molecular Probes) for 30 min after removal of secondary antibodies. Sections were mounted onto glass slides using aqueous mounting medium (FLUOPREP,

BioMerieux) and examined by Olympus (Tokyo, Japan) AX 70 microscope equipped with epifluorescence at different magnifications. Negative controls were performed by omitting primary antibodies.

Human samples: For SR-B1 staining in sebaceous glands, human skin tissues were collected from patients whose informed consent was obtained in writing according to the policies of the Ethics Committee of the European Institute of Oncology and regulations of Italian Ministry of Health. The tissues were fixed in 10% NBF for 24 hrs, then paraffin-embedded. Sections (4 μm) were deparaffinized in xylene and rehydrated in alcohol gradients. After dewaxing, sections were incubated overnight at 4°C with anti-SR-B1 (Novus Biologicals, Inc., Littleton, CO). Slides were washed three times with PBS and endogenous peroxidase was blocked with 3% hydrogen peroxide in absolute methyl alcohol for 30 min at RT. Finally, the slides were incubated with EnVision+System-HRP (DAKO, Glostrup, Denmark) for 45 min. The reaction products were stained with diaminobenzidine (DAB), counterstained with Hematoxylin and mounted with Eukitt mounting medium.

Protein extraction and Western blot

Organotypic epidermis was harvested with lysis buffer (70 mM Tris-HCl, pH6.8, 1,1%SDS, 11,1% (v/v) glycerol, 0,005% bromophenol blue (BioRad)) containing protease inhibitor cocktail (Abcam, Cambridge, UK) and Pierce TM Phophatase Inhibitor Mini Tablets (Thermo Scientific, MA, USA) and immediately sonicated. The protein content was measured using the micro BCA method (Thermo Scientific). Equivalent amounts of proteins were subjected to 4-22% SDS-PAGE, electro-transferred onto nitrocellulose membrane, which was then blocked in PBS containing 0.5% Tween 20 and 5% not-fat milk (BioRad). Membranes were incubated overnight at 4°C with the appropriate primary antibody. The membranes were then incubated with horseradish peroxidase-conjugated secondary antibody for 1 h at RT, and the bound antibodies were detected in a chemiluminescent reaction (ECL, BioRad). Chemiluminescent quantification was performed on ChemiDoc imager (BioRad) and the signal was measured with Image Lab 4.1 analysis software (Bio-Rad).

Oil Red O staining in tissues

10 μm thick skin equivalents cryosections (ALSO IN THE SEBOCYTES) were cut, mounted on glass slides and fixed with 4% paraformaldeheide (PFA) for 1 hour. Right after fixation, cryosections were washed with double-distilled water and incubated for 30 min with ORO solution (Sigma). Subsequently, cryosections were washed in double-

distilled water and mounted in 50% glycerol. Imaging was performed using bright light of Olympus (Tokyo, Japan) AX 70 microscope.

Lipids extraction

Organotypic epidermis was homogenized and total lipids were extracted under argon atmosphere. Samples from two identically manipulated skin equivalents were collected in clean tube glasses containing 2 ml methanol/acetic acid (3%)/BHT (0.01%), then washed with hexane/BHT (0.01). Tubes were vortexed, then hexane layer was removed. After the third wash, 4 ml chloroform/BHT (0.01%) and 1.5 ml HCOOH (0.7 M) was added in the glass tube and followed by vortexing. The lower organic phase was transferred to a glass vial using a glass Pasteur pipette and dried under argon.

Thin layer chromatography

Extracted lipids were solubilized in 20 µl chloroform of which equal volume (5 µl) was transferred to Silica gel 60 TLC plates. Lipid classes were separated using sequentially the following solvent systems: chloroform/methanol/water 40:10:1 (v/v/v) to 10 cm, chloroform/methanol/acetic acid 190:9:1 (v/v/v) to 16 cm and hexane/diethylether/acetic acid 70:30:1 (v/v/v) to 20 cm as described by Mildner and colleagues (Mildner et al. 2010).

RNA extraction and quantitative Real Time PCR

Organotypic epidermis was lysed by TRIzol reagent (Invitrogen) and RNA was isolated using the RNeasy 96 system (Invitrogen). Reverse transcription-PCR was performed using iScript cDNA Synthesis Kit (BioRad) according to the manufacturer's instructions. To investigate the mRNA expression of LDLR, PPAR-α and PPAR-γ genes, quantitative real-time PCR was performed with LightCycler Fast Start DNA Master SYBR Green I (Roche Applied Science, Penzberg, Germany) with a standard protocol according to the manufacturer's protocol. The relative expression of the target genes was calculated by comparing with the housekeeping gene β-2-microglobulin (B2M). The primers used are listed in the table below:

Gene	Forward	Reverse
LDLR	5'-GTGACCGGGAATATGACTGC-3'	5'-TTGATGGGTTCATCTGACCA-3'
PPAR-α	5'-CTGGAAGCTTTGGCTTTACG-3'	5'-CAATGCTCCACTGGGAGACT-3'
PPAR-γ	5'-AGCCCAAGTTTGAGTTTGCT-3'	5'-ATTTTCTGGAGCAGCTTGGC-3'
B2M	5'-GATGAGTATGCCTGCCGTGTG-3'	5'-CAATCCAAATGCGGCATCT-3'

Statistical analysis

For each of the variables tested, two-way analysis of variance (ANOVA) was used. Statistical significance was considered at $p<0.05$. Data are expressed as mean ± SD of duplicate determinations obtained in three independent experiments.

5.3 Exposure to stressors study

Reconstructed Human Epidermis

Reconstructed human epidermis (RHE, EpiDerm™ Tissue) model was purchased from MatTek (MatTek In Vitro Life Science Laboratories, Bratislava, Slovak Republic). RHE were kept at liquid/air interface in a humidified 5% CO_2 atmosphere at 37°C in a maintenance medium provided by manufacturers until exposure to stressors.

CS exposure

CS exposure of RHE was performed in fresh maintenance media for 30 min. CS was generated by burning one research cigarette (12 mg tar, 1.1 mg nicotine) using a vacuum pump to draw air through the burning cigarette and leading the smoke stream over the RHE as described by Valacchi et al (Valacchi, Davis, et al. 2011). Control RHE were exposed to filtered air.

Air particles exposure

Concentrated air particles (CAPs) were used as air particles and were resuspended in PBS. CAPs were collected using a virtual concentrator, the Harvard Ambient Particle Concentrator (HAPC), which concentrates ambient air particles for subsequent exposure in different animal models (Harvard School of Public Health, Boston, Massachusetts), and were generously provided by Dr. T. Marchini. For the exposure, 10 µl of CAPs suspension (25 µg/ml) was topically applied over the RHE in a single dose (0.5 µg/cm^2). Control tissue was exposed to 10 µl of the vehicle (PBS). Tissues were kept at 37°C in a humidified 5% CO_2 atmosphere in maintenance medium. Measurements were made after 24 or 48 h exposure.

O_3 exposure

In vitro: RHE were exposed to 0.8 ppm O_3 for 1 and 4 h. O_3 was generated from O_2 by electrical corona arc discharge (ECO3 model CUV-01, Torino, Italy). The O_2–O_3 mixture (95% O_2, 5% O_3) was combined with ambient air and allowed to flow into a Teflon-lined exposure chamber, with the O_3 concentration in chamber adjusted to the above mentioned ppm output and continuously monitored by an O_3 detector. Control RHE were exposed to filtered air in a similar exposure chamber.

Humans study: A total of 15 healthy volunteer subjects participated to the *in vivo* study. Subjects, aged 18-55 years, included both men and women. Subjects' forearms were randomized (right and left) and exposed to 0.8 ppm O_3 in a suitable Teflon-lined exposure chamber for 3 h/day for 5 consecutive days. 3-mm skin punch biopsies were carried out upon O_3 exposure on the fifth day and control biopsies were obtained from unexposed forearm. The study was performed upon Institutional Review Board approval (Allendale Institutional Review Board; 7015-090-104/106-002; August 10, 2015) and all informed consents were obtained in written form from the subjects previous enrollment in the study.

Treatment with resveratrol

Resveratrol treatment was carried out by topical application on RHE tissues of 5 mg/cm^2 formulation containing 1% resveratrol. Tissues were incubated for 24 h at 37°C, 5% CO^2 previous to O_3 exposure.

Immunohistochemistry

RHE or skin biopsies were immersion-fixed in 10% NBF (neutral-buffered formalin) for 24 h at 4°C, then dehydrated in alcohol gradients and embedded in paraffin. Sections (4 μm) were deparaffinized in xylene and rehydrated in alcohol gradients. After dewaxing, sections were incubated overnight at 4°C with primary antibodies, followed by 1 h with secondary antibodies at RT. Nuclei were stained with 1 μg/ml DAPI for 30 min after removal of secondary antibodies. Sections were mounted onto glass slides using anti-fade mounting medium 1,4-diazabicyclooctane in glycerine (DABCO) and examined by the Zeiss Axioplan2 light microscope equipped with epifluorescence at different magnifications. Negative controls were performed by omitting primary antibodies. Images were acquired and analyzed with Axio Vision Release 4.6.3 software.

Statistical analysis

For each of the variables tested, two-way analysis of variance (ANOVA) was used. Statistical significance was considered at $p<0.05$. Data are expressed as mean ± SD of triplicate determinations obtained in three independent experiments.

CHAPTER 6

Results

6.1 SR-B1 expression in *in vivo* and *in vitro* skin models

The first step was to assess whether SR-B1 was expressed in the skin models used in our study. Therefore, as depicted in Figure 6.1, we performed immuno-staining for SR-B1 in human skin (A), in "home-made" organotypic skin equivalents (B), in commercial reconstructed human epidermis (C), as well as in HaCaT cells (D) and in SZ95 sebocytes (E). They all resulted positive for SR-B1, as shown by the green signal, thus all these models were suitable for our experiments.

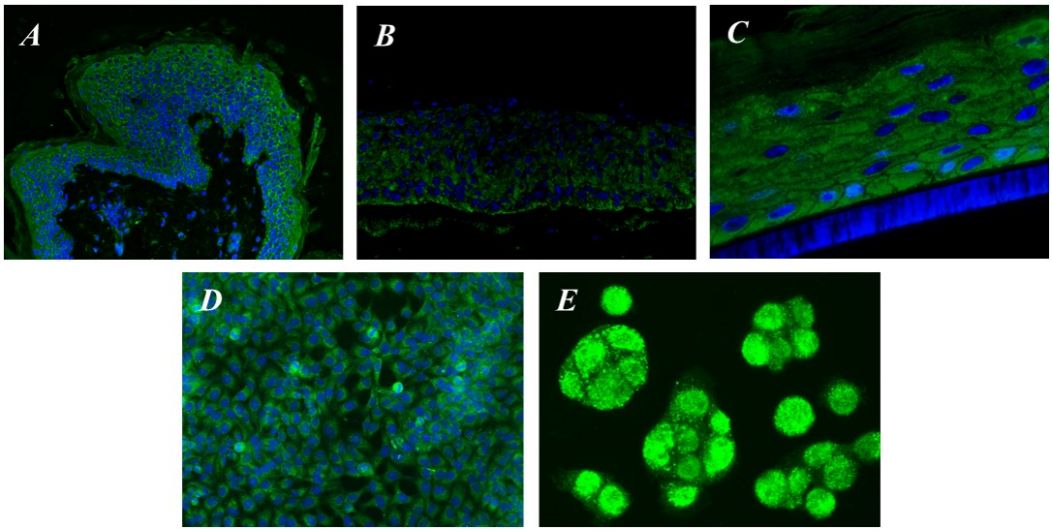

Figure 6.1 - SR-B1 is expressed in human skin and in 2D and 3D in vitro skin models. SR-B1 expression was determined in human skin (A), organotypic SE (B), RHE (C), HaCaT cells (D) and SZ95 cells (E) by IHC/ICC. Green staining represents SR-B1; blue staining (DAPI) represents nuclei; pictures are taken at different magnifications.

6.2 SR-B1 expression increased during wound healing

Human skin acts as a physical barrier against all exogenous harmful elements, therefore its integrity is essential. One common deleterious process, to which cutaneous tissue is subjected, is represented by wounds that activate a series of mechanisms aimed to restore skin cellular layers. Since SR-B1 is involved in cholesterol uptake and cholesterol is essential for new cells membranes formation, we evaluated the receptor's expression during an *in vitro* scratch healing assay. As shown in Figure 6.2, 6 h upon wounding there was a visible increase in SR-B1 protein levels that interested mainly the cells at the edges of the scratch. The increase was maintained up to 12 h after wounding and SR-B1 expression returned to basal levels after 24 h. Such cellular response showed that SR-B1 might be implicated in the healing process.

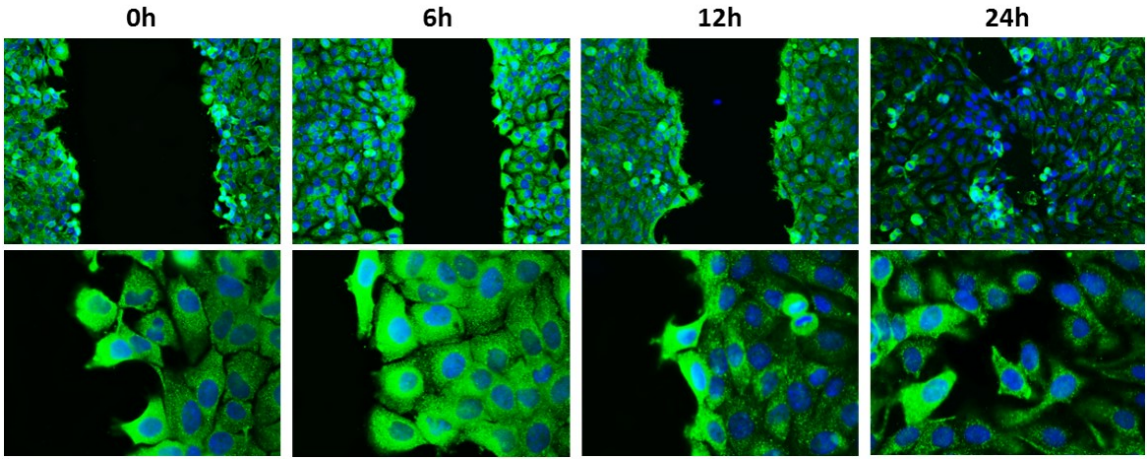

Figure 6.2 - SR-B1 expression during wound closure. Scratch was performed on confluent HaCaT cells monolayer and cells were harvested at different time-points (0-24 h). SR-B1 expression was determined by ICC. Green staining represents SR-B1; blue staining (DAPI) represents nuclei; pictures are taken at different magnifications.

6.3 Keratinocytes lacking SR-B1 presented delayed wound closure ability

In order to understand whether SR-B1 plays an active role in scratch closure, we knocked down SR-B1 in keratinocytes and performed wound healing assay. As depicted in Figure 6.3A-B, in knockdown cells (siRNA SR-B1) the scratch was still 50% open 24 h after wounding, while in control cells it was more than 90% healed. SR-B1 knockdown in not healed wound was also confirmed by immuno-staining (Figure 6.3C). These data show that SR-B1 is essential in part for keratinocytes wound closure.

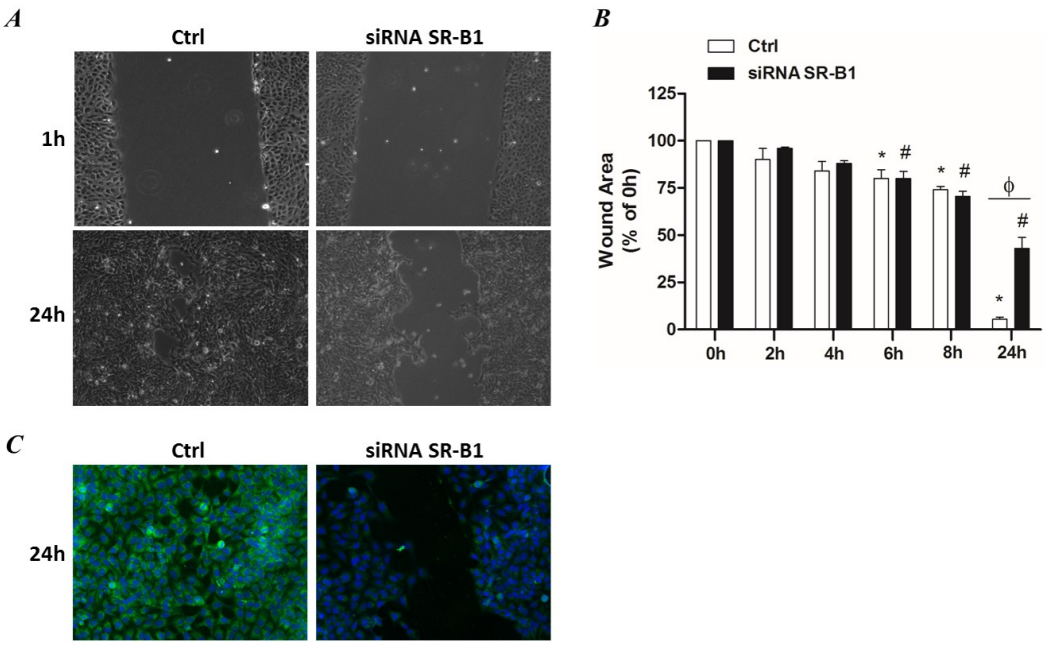

Figure 6.3 - SR-B1 knockdown delayed keratinocytes scratch closure. Scratch was performed on confluent HaCaT cells monolayer and wound area was measured at different time-points (0-24 h). Pictures in the top left show scratch closure after 1 and 24 h (A). Quantification of wound area on the right is representative of three experiments. Data are shown as % of 0 h; $p<0.05$; * vs Ctrl 0h, # vs siRNA SR-B1 0h, φ vs Ctrl 24h (B). SR-B1 expression was determined by ICC on scratched cell monolayer after 24 h. Green staining represents SR-B1; blue staining (DAPI) represents nuclei (C).

6.4 Possible involvement of SR-B1 in cellular proliferation

In vitro scratch healing is characterized mainly by two processes: proliferation and migration. Therefore, our first approach was to determine whether SR-B1 could modulate keratinocytes proliferation. For this purpose, we performed a proliferation assay by the incorporation of BrdU on control and SR-B1-knockdown keratinocytes and, as shown in Figure 6.4A, knockdown cells incorporated 20% lower levels of BrdU, indicating a reduced proliferative ability. Similar results were obtained also by cell counting; control or knockdown cells were seeded at the same density and cells were harvested and counted after 24 and 48 h. As depicted in Figure 6.4B, after 48 h, the number of the knockdown keratinocytes was significantly lower than the controls. A protein involved in cell proliferation is cyclin D1, therefore we evaluated its nuclear level. As shown in Figure 6.4C, cyclin D1 nuclear levels were down-regulated of 40% in knockdown keratinocytes 24 h upon wounding (Figure 6.4C).

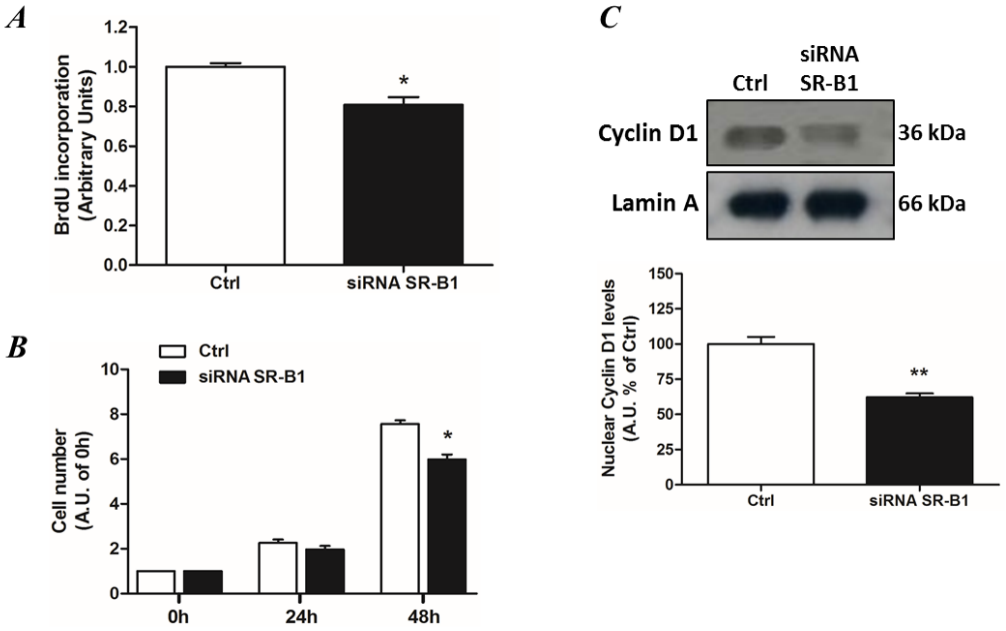

Figure 6.4 - SR-B1 knockdown reduced cell proliferation. Cells were incubated overnight with BrdU, then harvested and processed by the use of anti-BrdU antibody. BrdU incorporation is expressed as arbitrary units (*$p<0.05$) and is representative of three experiments (A). Cells were seeded ($1x10^5$/ml) and harvested after 24 and 48 h. Cell count is representative of three experiments. Data are expressed as arbitrary units (*$p<0.05$) (B). Multiple scratches were performed on confluent HaCaT cells monolayer and cells were harvested after 24 h. Cyclin D1 level was determined on nuclear extract. The WB in the top is representative of three experiments. Lamin A was used as loading control. Quantification of cyclin D1 bands is shown in the bottom panel. Data are expressed as arbitrary units (**$p<0.01$) (C).

6.5 Metalloproteinase 9 expression was modulated by SR-B1

Next, it was of our interest to investigate SR-B1 effect on cell migration. Thus, we evaluated the levels of MMP9, main metalloproteinase involved in keratinocytes migration, both in cellular lysates and in culture media, 1 and 24 h upon scratch assay in control and SR-B1 knockdown cells. As indicated in Figure 6.5A, MMP9 levels in cell

lysate was reduced of 40% in knockdown keratinocytes 1h upon wounding, while after 24h MMP9 resulted significantly increased in cells silenced for SR-B1 compared to control condition. This might indicate a reduced ability of SR-B1 knockdown keratinocytes in releasing the enzyme. In fact, the levels of MMP9 released in culture media at 24h were almost 45% higher in control condition compared to knockdown. No differences were found between the two conditions 1h after wounding. Furthermore, cellular MMP9 expression in not wounded cells showed 75% decreased basal levels of MMP9 in keratinocytes silenced for SR-B1 (Figure 6.5B).

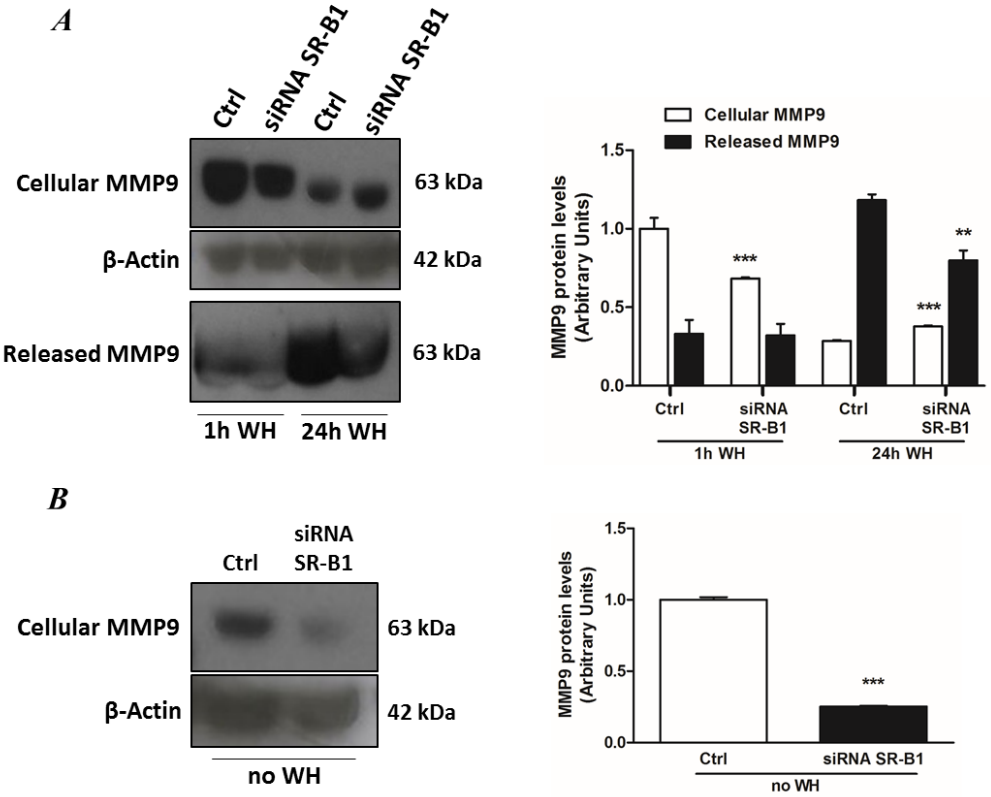

Figure 6.5 - SR-B1 knockdown decreased MMP9 basal expression and secretion upon WH. Scratch was performed on confluent HaCaT cells monolayer and cells were harvested after 1 and 24 h. MMP9 expression was determined on cell lysate and culture medium. WB is representative of three experiments. β-actin was used as loading control. Quantification of MMP9 is shown on the right upper panel; **p<0.01, ***p<0.001, vs Ctrl of each condition (A). MMP9 basal levels were determined on not wounded cells. WB is representative of three experiments. β-actin was used as loading control. Quantification of MMP9 is shown on the right lower panel; ***p<0.01 (B).

6.6 SR-B1 appeared essential in keratinocytes migration

As the levels of MMP9 released in culture media were lower in SR-B1 knockdown keratinocytes, we investigated whether this reduction influenced cell migration. Thus, we performed a migration assay in transwell inserts coated with collagen IV, using FBS as stimulus for cell migration, and we evaluated the rate of migrated cells 6 and 24 h after stimulation. As shown in Figure 6.6A, the ability of SR-B1 knockdown keratinocytes to migrate was 2-fold decreased compared to control. This was visible already at 6h and was

more evident at 24h. In order to better understand the cause of this decrease, we evaluated cell morphology upon wounding by the use of scanning electron microscope (Figure 6.6B) and we observed that, 30 min after scratch formation, control keratinocytes appeared flat which is representative of a migratory phenotype, while SR-B1 knockdown keratinocytes showed a rounded and swollen-like morphology.

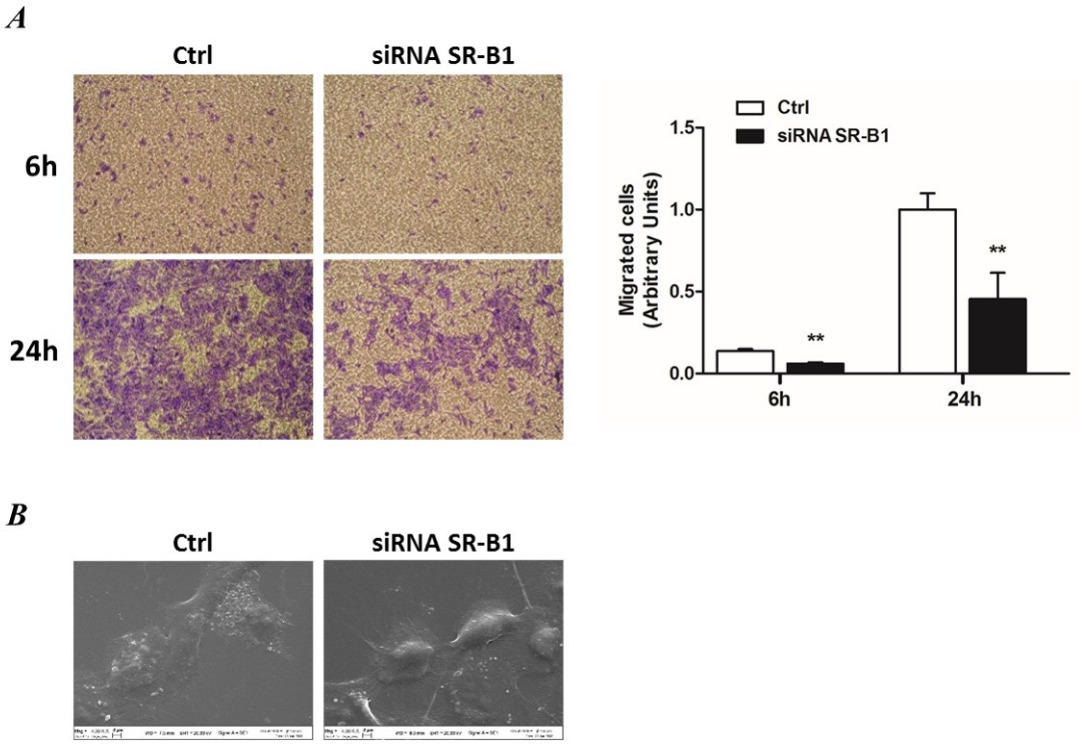

Figure 6.6 - SR-B1 knockdown decreased keratinocytes migration ability. Cells were seeded in collagen IV-coated 8 µm-pore size transwells and incubated for 6 and 24 h in presence of chemotactic stimulus, then fixed and migrated cells were stained. Pictures are representative of three experiments. Quantification of migrated cells is shown on the right; **p<0.01 (A). Scratch was performed on confluent cell monolayer and cells were fixed after 30 min. Cell surface was observed by SEM. Pictures are representative of three experiments; magnification 4000X (B).

6.7 NF-kB activation upon wounding was inhibited by SR-B1 knockdown

Since NF-kB is a transcription factor that regulates the expression of cyclin D1 (Hinz et al. 1999) and it is involved in the inflammatory process of wound healing in which also MMP9 plays an important role (Zhu et al. 2012), we investigated its activation, by the translocation of its p65 subunit into the nucleus, 1h after the scratch was performed. As indicated in Figure 6.7A, the nuclear levels of p65 in wounded SR-B1 knockdown keratinocytes were 1.5-fold lower compared to control. The data were confirmed also by immuno-staining, as shown in Figure 6.7B; p65 nuclear signal in knockdown cells at the edge of the wound was almost absent, while it was present in the nucleus of control cells.

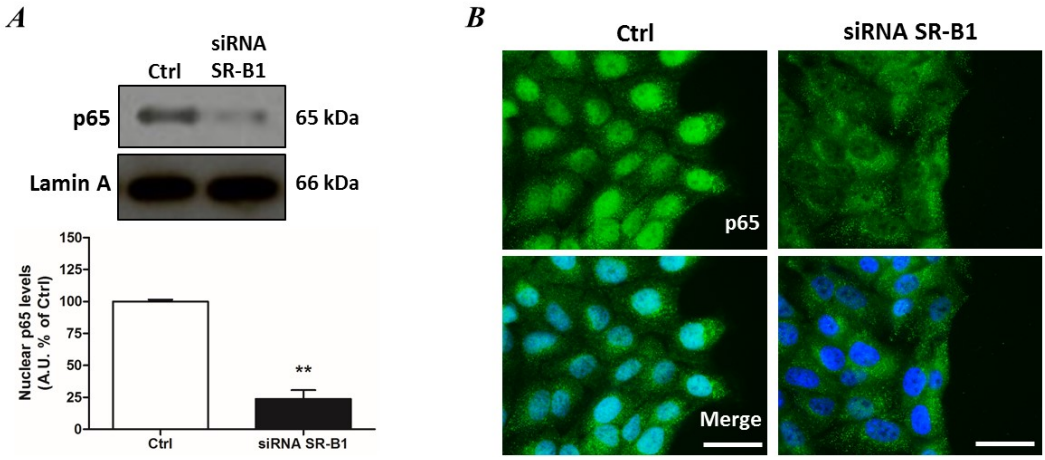

Figure 6.7 - Scratch-induced NF-kB activation was reduced by SR-B1 knockdown. Multiple scratches wer performed on confluent HaCaT cells monolayer and cells were harvested after 1 h. NF-kB activation was determined by p65 subunit translocation into the nuclei. WB shown in the top left is representative of three experiments. Quantification of p65 bands is shown in the bottom panel. Data are expressed as arbitrary units (averages of three different experiments, **p<0.01). Lamin A was used as loading control (A). Data were confirmed by ICC for p65 at wound edge; green staining represents p65 and blue staining (DAPI) represents nuclei; scale bar 50 μm (B).

6.8 Organotypic skin equivalents knockdown for SR-B1

Along with cellular proliferation and migration, another physiological process representative for human skin is cell differentiation, which is crucial for keratinocytes in order to form all epidermal layers. Hence, it was of our interest to evaluate whether SR-B1 could play a role also in keratinocytes differentiation ability and for this purpose we generated "home-made" *in vitro* skin equivalent (SE) with control and SR-B1 knockdown primary keratinocytes. Such model mimics human skin since it is characterized by a dermis, made up by collagen and fibroblasts, and an epidermis, which contains proliferative and differentiated keratinocytes to form the epidermal layers. As shown by H/E staining (Figure 6.8A), the tissues generated with keratinocytes silenced using a siRNA with a nonsense/scrambled sequence (Scrbl) presented similar epidermal organization and thickness to the ones generated with control cells, as expected, while the tissues generated with SR-B1 knockdown keratinocytes presented a slightly thinner epidermis with no clear distinction between the inner layers (basal, spinous). These observations indicate that SR-B1 might modulate in part the epidermal structure. The efficient knockdown of the scavenger receptor was assessed by immuno-staining, as depicted in Figure 6.8B.

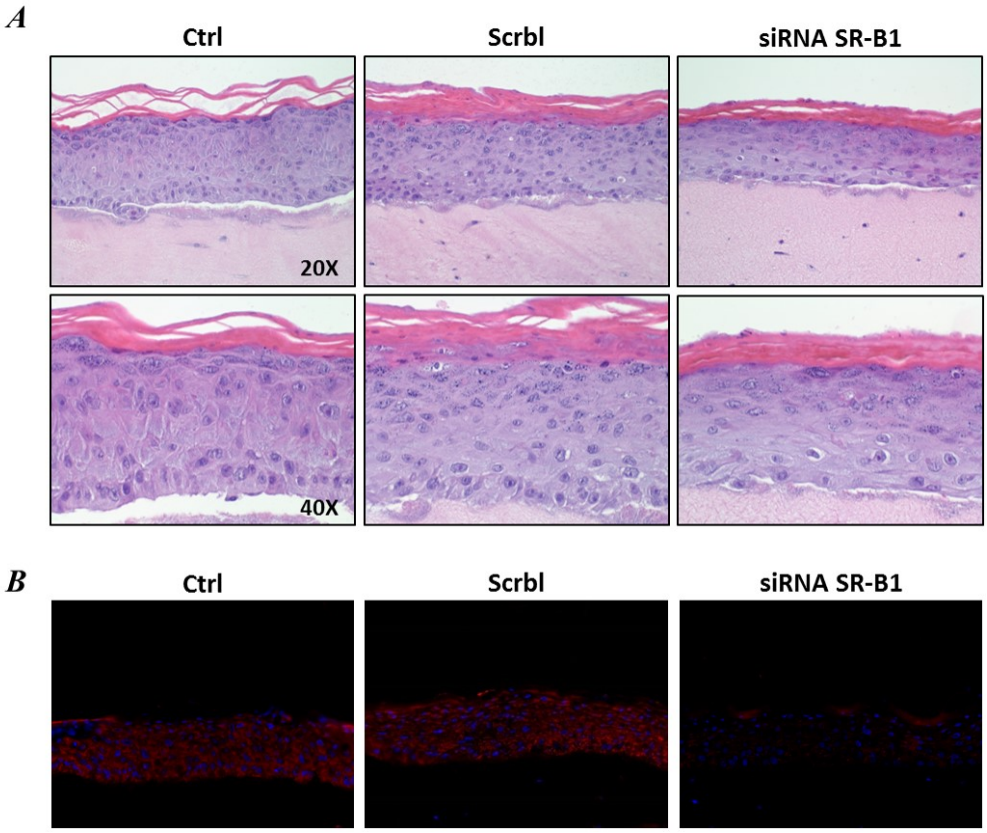

Figure 6.8 - SE generated with SR-B1 knockdown keratinocytes. SE structure was assessed by H/E staining on paraffin-sections; pictures are representative of three experiments (A). SR-B1 knockdown was confirmed by IHC. IHC is representative of three experiments; red staining represents SR-B1 and blue staining (Hoechst) represents nuclei; magnification 20X (B).

6.9 SR-B1 did not modulate K14 expression

To better understand the interconnection between SR-B1 and keratinocytes differentiation, we studied the expression of several differentiation markers. First, we evaluated keratin 14 (K14) levels, a protein produced by basal epidermal cells. As shown by WB in Figure 6.9A, the protein expression of this marker was not significantly modulated by SR-B1. A comparable response was obtained also by immunofluorescence, shown in Figure 6.9B, in fact K14 distribution within the epidermis appeared similar between control, scramble and knockdown tissues. Also the quantification of signal intensity, represented in the plot aside, indicates no change in the expression of K14 in SR-B1 knockdown SE.

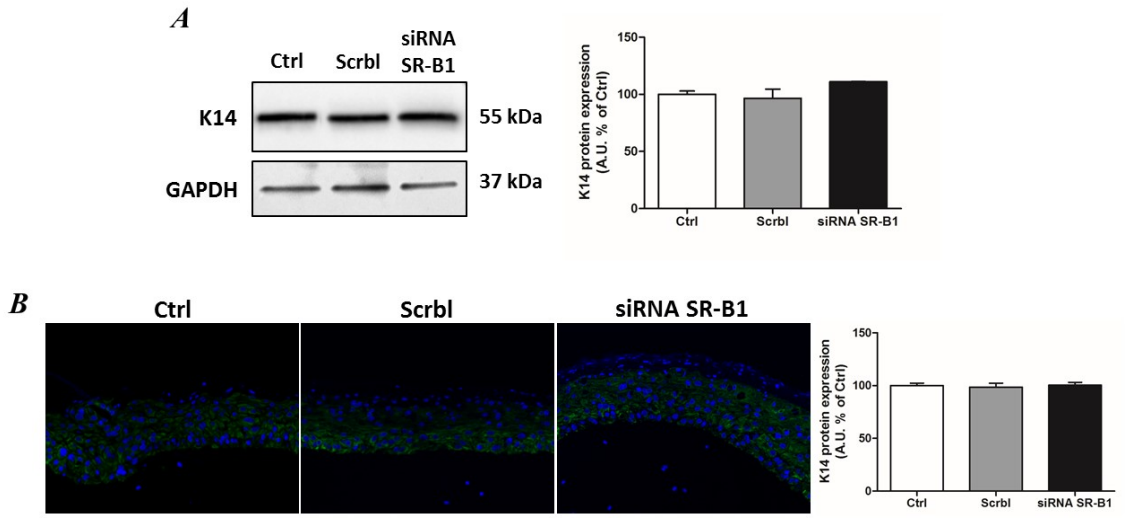

Figure 6.9 - SR-B1 knockdown in keratinocytes did not influence K14 expression. SE were harvested and K14 expression was assessed by WB and IHC. WB shown in the top left is representative of three experiments. Quantification of K14 bands is shown in the panel in the bottom. Data are expressed as arbitrary units (averages of three different experiments, *p<0.05). GAPDH was used as loading control (A). Data were confirmed by IHC for K14; green staining represents K14 and blue staining (Hoechst) represents nuclei; magnification 20X (B).

6.10 K10 protein levels were not influenced by SR-B1

Next, we evaluated Keratin 10 (K10), a keratin expressed in the differentiated suprabasal layers of the cutaneous stratified epithelium. As shown in Figure 6.10, SR-B1 knockdown skin equivalents did not present significantly increased K10 expression, compared to control or scramble.

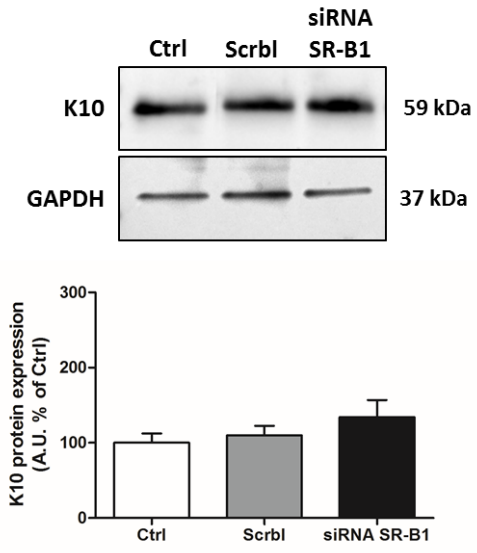

Figure 6.10 - K10 expression in SR-B1 knockdown SE. K10 expression in SE was assessed by WB. WB shown in the top is representative of three experiments. Quantification of K10 bands is shown in the panel in the bottom. Data are expressed as arbitrary units (averages of three different experiments). GAPDH was used as loading control.

6.11 SR-B1 modulated S100A9 expression

S100A9 is a protein expressed exclusively in the differentiated and not proliferative keratinocytes, therefore we assessed its expression as a differentiation marker. As depicted in figure 6.11A, the levels of this protein were reduced of 30% in tissues silenced for SR-B1. Similar pattern was observed also by immunofluorescence (Figure 6.11B). In fact, control and scramble SE expressed comparable S100A9 levels in all epidermal layers overlying *stratum basale*, while SR-B1 knockdown tissues presented a gradual expression of the protein, increasing towards the cornified layer.

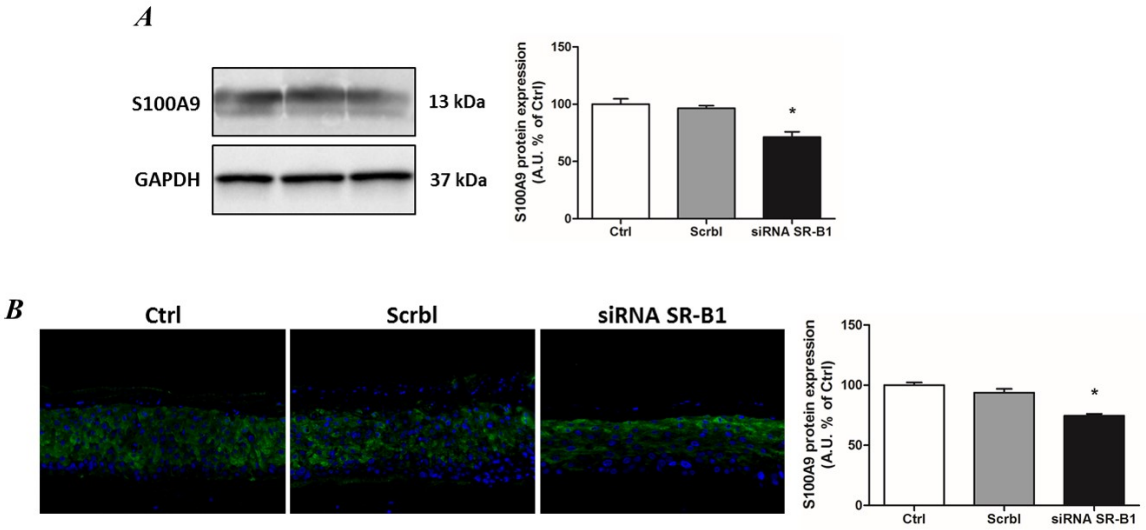

Figure 6.11 - SR-B1 knockdown SE presented reduced S100A9 expression. S100A9 expression in SE was assessed by WB and IHC. WB shown in the top left is representative of three experiments. Quantification of S100A9 bands is shown in the panel in the bottom. Data are expressed as arbitrary units (averages of three different experiments, *$p<0.05$). GAPDH was used as loading control (A). Data were confirmed by IHC for S100A9; green staining represents S100A9 and blue staining (Hoechst) represents nuclei; magnification 20X (B).

6.12 SR-B1 knockdown up-regulated FLG expression

Finally, we investigated the levels of filaggrin (FLG), which fulfils important functions in terminal differentiation in the human epidermis. As represented in Figure 6.12, SR-B1 knockdown SE displayed 20% higher FLG levels and this protein was found also in deeper epidermal layers underlying cornified layer compared to control and scramble conditions.

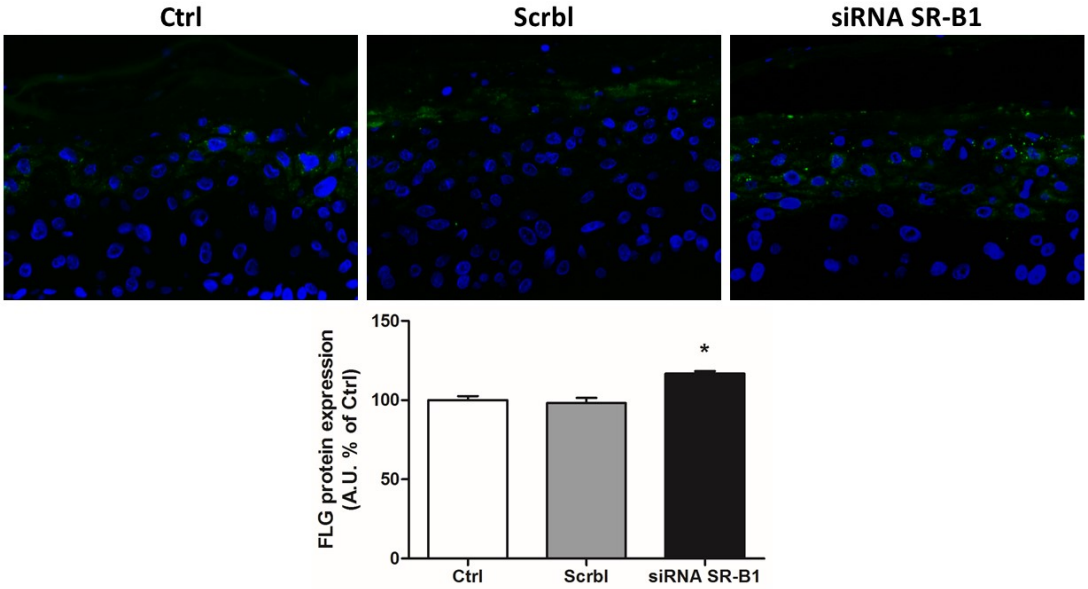

Figure 6.12 - SR-B1 knockdown in SE modulated FLG expression and localization. FLG expression in SE was assessed through IHC; green staining represents FLG and blue staining (Hoechst) represents nuclei; magnification 40X. Quantification of FLG expression is shown in the bottom. Data are expressed in arbitrary units (average of three independent experiments; *$p<0.05$).

6.13 SR-B1 appeared essential in epidermal lipids distribution

Since SR-B1 plays a role in lipids uptake and metabolism, it was of our interest to investigate whether it is able to influence the composition of epidermal lipids. Therefore, we performed Oil Red O staining in SE and we observed that tissues in which SR-B1 was silenced presented lower lipids staining and deficient distribution within the epidermis compared to control and scramble (Figure 6.13A). In fact, control and scramble SE showed a regular lipid distribution through all epidermal layers, while lipids in SR-B1 knockdown SE were present mostly in the cornified layers and less in the underlying layers. In order to assess if SR-B1 promoted changed also in the nature of the lipids, we extracted the lipids from SE and separated the different classes through thin layer chromatography method. As shown in Figure 6.13B, no differences in lipids classes were observed in SR-B1 knockdown SE compared to control and scramble, meaning that SR-B1 under our experimental conditions influences mainly the epidermal lipids levels.

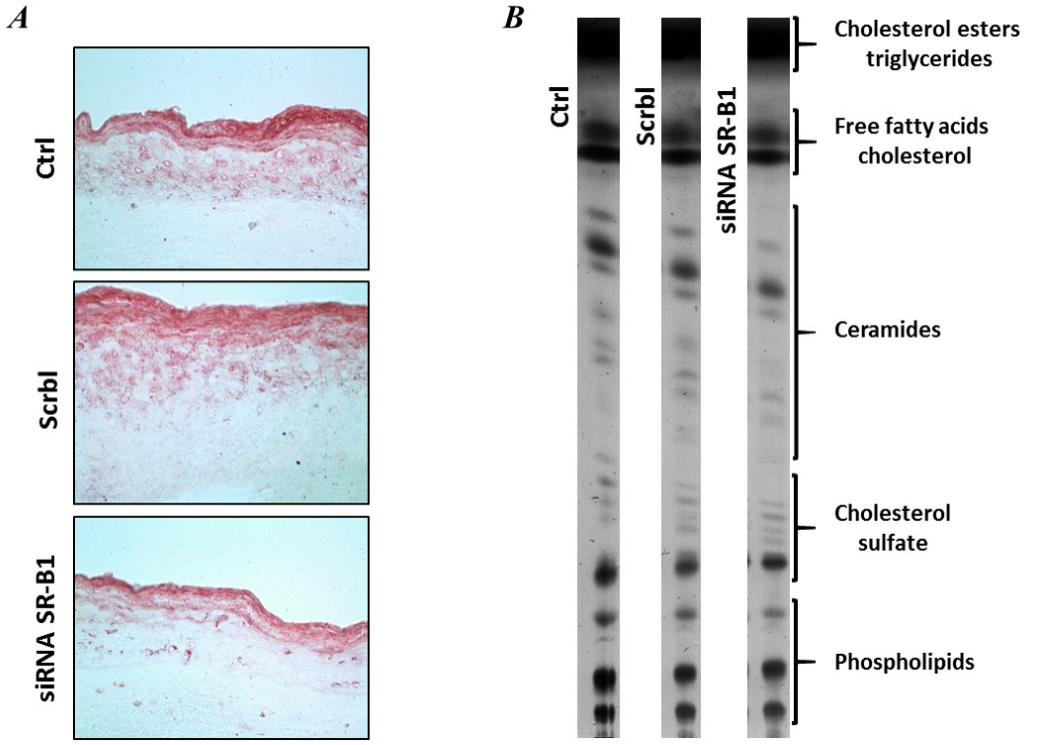

Figure 6.13 - SR-B1 influenced lipids organization within the epidermis. ORO staining on the left is representative of three experiments; magnification 20X (A). Thin layer chromatography of total lipids extracted from epidermis of SE is representative of three experiments (B).

6.14 SR-B1 modulated markers involved in lipid metabolism

Given the effect that SR-B1 had on lipids distribution in the epidermis, we evaluated the gene expression of molecules involved in lipid metabolism in SE. As shown in Figure 6.14, the levels of LDL receptor (LDLR) and peroxisome proliferator-activated receptors alpha and gamma (PPAR-α and -γ) were reduced of 80%, 70% and 75%, respectively, in SR-B1 knockdown SE compared to control and scramble tissues.

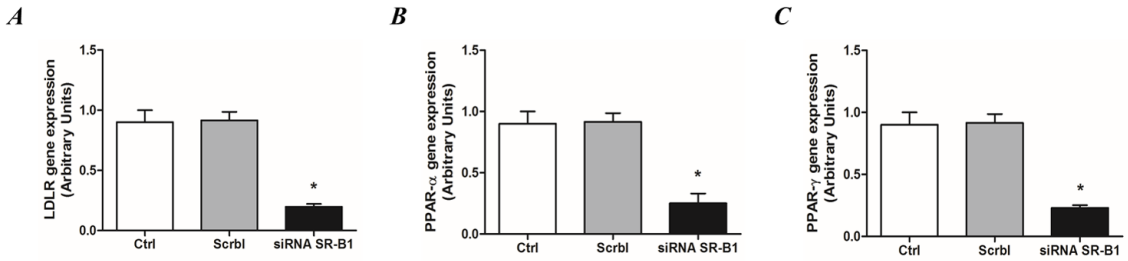

Figure 6.14 - SR-B1 influenced genes related to lipid metabolism. RNA was extracted from epidermis of SE and gene expression of LDLR (A), PPAR-α (B) and PPAR-γ (C) was assessed by RT-PCR. Data are expressed in arbitrary units (average of three independent experiments; *$p<0.05$).

6.15 SR-B1 affected lipid content in human sebocytes

Lipids contained in the horny layer are provided in part by the sebum produced in sebaceous glands, so it was of interest to investigate the implication of SR-B1 in sebocytes

lipids levels. Thus, we first assessed whether SR-B1 was expressed in sebaceous glands of human skin and, as shown in Figure 6.15A, sebaceous glands appeared positive for SR-B1 staining. Next, we evaluated the intracellular lipids content in human sebocytes and, as depicted in Figure 6.15B, we observed that SR-B1 knockdown induced a 95% reduction of lipid droplets as well as 3-fold lower cellular cholesterol levels in sebocytes (Figure 6.15C).

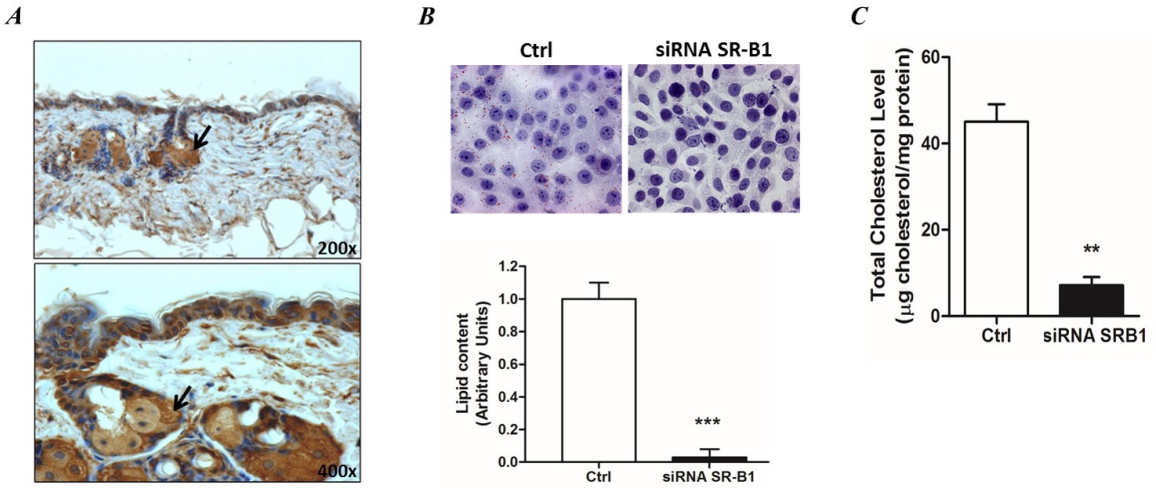

Figure 6.15 -SR-B1 is expressed in sebaceous glands and modulates cholesterol level. IHC images represent anti-SR-B1 stained cytoplasm of the cells of sebaceous glands in normal human skin (black arrows). DAB, original magnifications 200x and 400x (A). ORO staining of SZ95 cells upon knockdown for SR-B1; blue signal represents hematoxylin staining, red staining represents lipid droplets. Quantification of lipid droplets is shown in the panel below. Values are presented as arbitrary units (average of three independent experiments); ***p<0.001 (B). Total cholesterol levels were measured into control and SR-B1 knockdown sebocytes. Data are normalized with protein concentration and expressed in µg cholesterol per mg of protein in cell extracts, as average of three independent experiments; **p<0.01 (C).

6.16 CS exposure reduced SR-B1 protein expression in epidermis

SR-B1 demonstrated to be susceptible to CS in human keratinocytes, thus we investigated whether such modulation was detected also in a three-dimensional skin model. For this purpose, we exposed reconstructed human epidermis (RHE) to CS and evaluated the levels of SR-B1. As illustrated by WB in Figure 6.16A, SR-B1 protein expression decreased of 30% upon CS exposure already after 30 min and the decrease was maintained up to 24h. The result was further confirmed by immuno-staining (Figure 6.16B), where SR-B1 (green signal) appeared less intense in RHE exposed to CS compared to control.

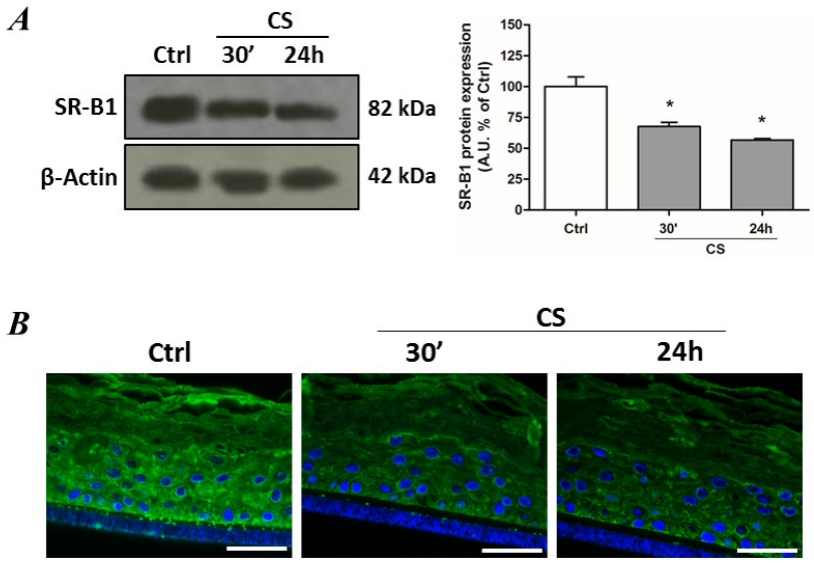

Figure 6.16 - Exposure to CS decreased SR-B1 expression in RHE. RHE were exposed to CS for 30 min and tissues were harvested after 30 min and 24 h. WB shown in the top is representative of three experiments. Quantification of SR-B1 bands is shown in the panel on the right. Data are expressed as arbitrary units (averages of three different experiments, *p<0.05). β-Actin was used as loading control (A). Data were confirmed by IHC for SR-B1; green staining represents SR-B1 and blue staining (DAPI) represents nuclei; scale bar 50 μm (B).

6.17 SR-B1 levels in RHE were reduced upon particles exposure

In addition, since CS-induced decrease of SR-B1 in keratinocytes appeared to be redox-associated, we investigated SR-B1 expression also upon exposure to other stressors known to promote redox imbalance. Therefore, we first exposed human RHE to CAPs (25 μg/ml), $PM_{2.5}$ air particles, for 24 and 48 h. As depicted in Figure 6.17A, SR-B1 protein levels decreased significantly in time-dependent manner. This effect was also confirmed by immunofluorescence (Figure 6.17B).

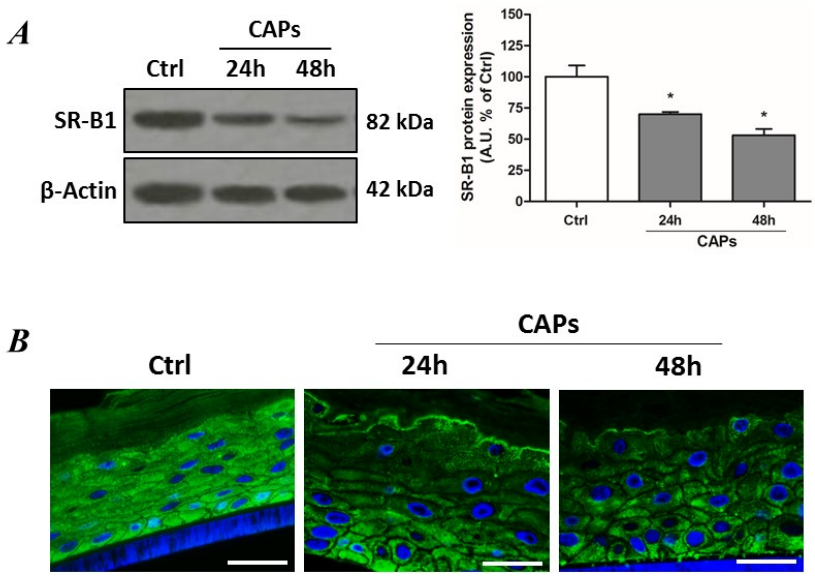

Figure 6.17 - Exposure to CAPs decreased SR-B1 expression in RHE. RHE were exposed to 25 μg/ml CAPs for 24 and 48 h and tissues were harvested forthwith. WB shown in the top is representative of three experiments. Quantification of SR-B1 bands is shown in the panel on the right. Data are expressed as arbitrary units (averages of three different experiments, *p<0.05). β-Actin was used as loading control (A). Data were confirmed by IHC for SR-B1; green staining represents SR-B1 and blue staining (DAPI) represents nuclei; scale bar 25 μm (B).

6.18 Ozone affected SR-B1 epidermal levels

Finally we also exposed RHE to O_3 (dose of 0.8 ppm), a known pro-oxidant environmental gas, for 1 and 4 h and, as shown in Figure 6.18A, O_3 induced a decrease of SR-B1 expression of 40% after 1h and of 50% after 4h of exposure. The WB results were confirmed also by immuno-staining (Figure 6.18B).

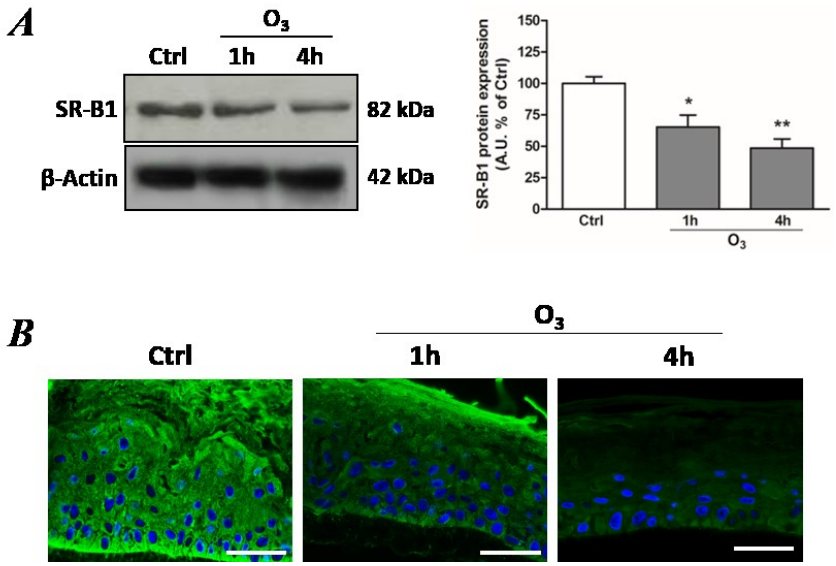

Figure 6.18 - Exposure to O_3 decreased SR-B1 expression in RHE. RHE were exposed to 0.8 ppm O_3 for 1 and 4 h and tissues were harvested forthwith. WB shown in the top is representative of three experiments. Quantification of SR-B1 bands is shown in the panel on the right. Data are expressed as arbitrary units (averages of three different experiments, *p<0.05, **p<0.01). β-Actin was used as loading control (A). Data were confirmed by IHC for SR-B1; green staining represents SR-B1 and blue staining (DAPI) represents nuclei; scale bar 50 μm (B).

6.19 SR-B1 expression was reduced by ozone in human skin

Human skin has a more complex structure and composition compared to RHE, thus we investigated whether SR-B1 was modulated by O_3 in human skin in a similar manner as observed in RHE. For this purpose, the forearm of healthy subjects was exposed to O_3 and SR-B1 expression was evaluated in skin biopsies (see methods for details). As illustrated in Figure 6.19, skin exposed to O_3 presented almost 50% decreased SR-B1 protein levels compared to control condition, a result which was similar to the one obtained in RHE.

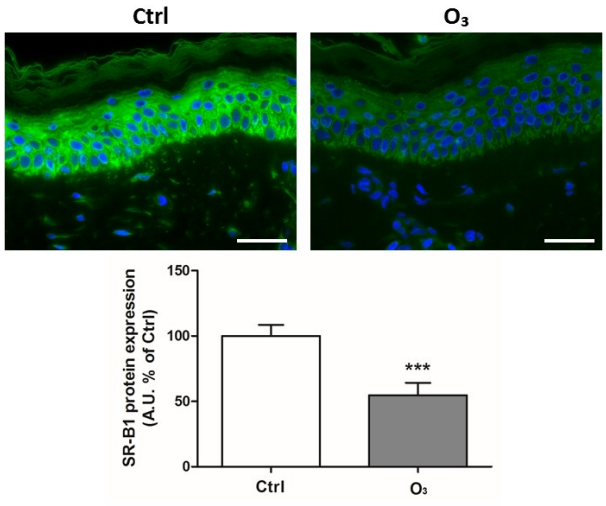

Figure 6.19 - Exposure to O_3 decreased SR-B1 expression in human skin. Biopsies from human skin exposed to O_3 for 3 h/day for five consecutive days were harvested forthwith. The IHC for SR-B1 is representative of 15 subjects; green staining represents SR-B1 and blue staining (DAPI) represents nuclei; scale bar 50 µm. Quantification of SR-B1 expression is shown in the bottom. Data are expressed in arbitrary units (average of 15 independent subjects; ***p<0.001).

6.20 Resveratrol pretreatment antagonized ozone-induced SR-B1 decrease

In order to confirm that SR-B1 loss induced by O_3 was mediated by oxidative damage, we applied resveratrol, a radical quenching compound, on top of RHE and then exposed the tissues to O_3 in the absence or presence of the compound. As shown in Figure 6.20, resveratrol pretreatment had a protective effect on SR-B1 expression; in fact, SR-B1 levels in resveratrol pretreated RHE were significantly higher compared to the not pretreated RHE and similar to the levels of the control condition.

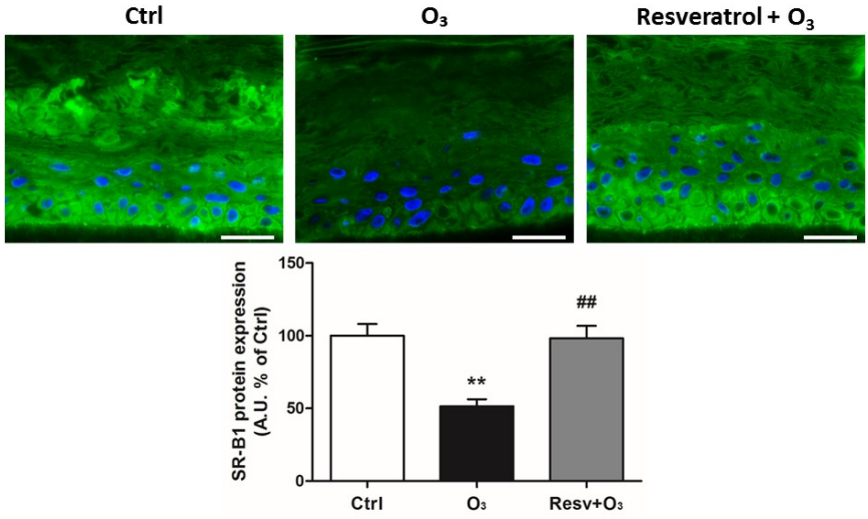

Figure 6.20 - Resveratrol counteracted O_3-induced SR-B1 loss. RHE were treated with resveratrol-containing formulation for 24 h, then RHE were exposed to 0.8 ppm O_3 for 4 h and tissues were harvested forthwith. SR-B1 expression was assessed by IHC; green staining represents SR-B1 and blue staining (DAPI) represents nuclei; scale bar 50 µm. Quantification of SR-B1 expression is shown in the bottom. Data are expressed as arbitrary units (average of three independent experiments; **p<0.01 vs Ctrl; ##p<0.01 vs O_3).

CHAPTER 7

Discussion and conclusions

Scavenger receptor B1 is a membrane receptor implicated in cholesterol uptake from HDL (Acton et al. 1996) and only recently its expression in human epidermis (Sticozzi et al. 2012) has been revealed, althought this finding was kind of surprising since the epidermis is not vascularized, and therefore does not receive direct supply of blood and HDL. Since several studies have demonstrated that SR-B1 is a target of oxidative stress (Sticozzi et al. 2012; Sticozzi et al. 2013) it is possible to assume that its main function in cutaneous tissues is to protect the skin from oxidative damage, although its function is still not clearly defined. Therefore, the purpose of this work was to investigate the role of SR-B1 in the main cutaneous physiological processes, such as proliferation, migration and differentiation. The biological models used were 2- and 3-dimensional cell culture skin models and human skin. All the models analyzed expressed SR-B1, confirming that their use was suitable for our investigation.

The first approach to our study was to assess SR-B1 expression during wound healing, which consists in a series of different cellular processes aimed to restore skin integrity. We performed an *in vitro* scratch healing assay on human keratinocytes, an assay used for the evaluation of both cell migration and proliferation (Latifi-Pupovci et al. 2015). Surprisingly, we observed a significant up-regulation of SR-B1 in cells at the wound edges, directly involved in scratch closure. Such response suggested an active implication of SR-B1 in scratch healing; in fact, transiently knockdown keratinocytes presented reduced ability of wound closure, which could be due to either decreased cellular proliferation or migration. Recent studies have reported the involvement of SR-B1 in cell proliferation. For instance, SR-B1 knockdown in breast cancer cell lines reduced HDL-mediated cell growth (Danilo et al. 2013). Moreover, blockage of the receptor inhibited SAA-induced proliferation in endothelial cells (Hong et al. 2015). Also in our case, we observed a significant decrease in growth capacity of SR-B1 knockdown keratinocytes, which might explain the delay in the scratch wound closure. A major regulator of cell cycle and proliferation is cyclin D1 (Stacey 2003), which, indeed, resulted poorly expressed, upon wounding, in nuclei of keratinocytes silenced for SR-B1. This suggests that the delayed wound closure could be a consequence of an altered cyclin D1 expression dependent on SR-B1 levels.

In parallel, SR-B1 appeared to be implicated also in cell migration and MMPs activation. MMPs (matrix metallo-proteinases) are a family of zinc-dependent endopeptidases capable of degrading different components of the extracellular matrix (ECM) and are essential for the remodeling of pericellular microenvironment required for keratinocytes migration during wound healing (Ravanti & Kähäri 2000). Increasing evidence suggests that MMP9

is essential in keratinocytes re-epithelization (Reiss et al. 2010). SR-B1 knockdown keratinocytes had lower levels of active cellular MMP9 at early time-points upon wounding, pattern that could be explained by the low basal MMP9 expression observed in keratinocytes lacking SR-B1. At late time-points post-wounding, the difference between control and SR-B1 knockdown cells became opposite to the one observed at early time-points. In fact, knockdown keratinocytes expressed more intracellular MMP9 compared to control cells, while secreted MMP9 levels were significantly higher in control compared to SR-B1 knockdown condition, suggesting that MMP secretion could be modulated by SR-B1. Since MMPs are released from cells through vesicles, this could be in line with SR-B1 role in vesicles trafficking (Plebanek et al. 2015). MMP9 modulation led to a defect in knockdown keratinocytes migration, as seen by transwell migration assay. Other studies reported the involvement of SR-B1 in cellular migration. Zhu and colleagues (Zhu et al. 2008) have demonstrated that SR-B1-PDZK1 interaction is required for endothelial cells motility. Reduced migration was observed also in cultured human nasopharyngeal carcinoma cells after SR-B1 knockdown (Zheng et al. 2013). Cell motility not only is induced by MMPs upon matrix degradation, but it is in close relation with cellular cytoskeleton (Small et al. 1998). We evaluated the morphology of wounded keratinocytes by SEM and observed that control cells appeared with migratory flat phenotype, while SR-B1 knockdown cells presented a rounded and bulging aspect, suggesting that SR-B1 might participate to cell cytoskeleton rearrangement. This is also suggested by the work by Holm et al., which highlighted the presence of modified cellular membrane and cytoplasm structures in SR-B1 KO animals (Holm et al. 2002).

Cell proliferation and migration are regulated by different transcription factors, among which NF-kB. In fact, it has been reported that MMP9 promoter presents one binding site for NF-kB (Van den Steen et al. 2002) and cyclin D1 promoter contains two binding sites for this transcription factor (Hinz et al. 1999). Therefore, we evaluated the activation of NF-kB by translocation of p65 subunit into the nuclei and observed that SR-B1 knockdown keratinocytes were not able to activate NF-kB after scratch formation. Previous studies have shown that NF-kB activation is required for SR-B1 down-regulation by LPS in macrophages, but no direct modulation of NF-kB by SR-B1 has been reported yet. It is not clear whether the receptor alone is able to inhibit p65 nuclear translocation, or if such inhibition is mediated by SR-B1 ligands or by intracellular molecules. It has been demonstrated that HDL binding to SR-B1 led to activation of PI3K/Akt pathway (Danilo et al. 2013; Saddar et al. 2010), which is known to stimulate IKK activity and IKB phosphorylation with subsequent p65 nuclear translocation (Bai et al. 2009). This indicates

that SR-B1-induced NF-kB inhibition can be promoted upon ligand binding, although more investigation is needed in order to understand the link between the scavenger receptor and this transcription factor.

Tsuruoka and colleagues have reported the expression of SR-B1 in human skin with higher degree of staining in basal layer and less in upper epidermal layers (Tsuruoka et al. 2002). This could be in line with SR-B1 role in cholesterol uptake since the basal layer is in contact with the vascularized dermis, which can represent a source of HDL. On the other hand, the degree of expression suggests a down-regulation of the receptor induced by epidermal differentiation. In fact, it has been shown that SR-B1 protein levels in cultured keratinocytes are reduced upon calcium-induced differentiation (Tsuruoka et al. 2002). The cultured model gives limited information about the relationship between SR-B1 and epidermal differentiation, since such process involves several signaling pathways along with high calcium concentration (Klein & Andersen 2015). An elegant model for the study of keratinocytes differentiation is represented by three-dimensional organotypic skin equivalent, which allows also the use of genetically modified cells. We created this "home-made" skin equivalents with keratinocytes lacking SR-B1 and observed that SR-B1 knockdown keratinocytes maintained their ability to differentiate, since all four epidermal layers were present, although morphological changed were detected. SR-B1-deficient tissues appeared thinner, with keratinocytes layers less well-organized compared to control conditions. In fact, cornified and granular layers were well defined, while there was no clear separation between basal and spinous layers. Also the number of basal cells appeared reduced compared to control tissues. This may suggest a SR-B1-induced modulation of the initial epidermal proliferation/differentiation process and it could be related to the negative effect of SR-B1 on cellular proliferation, as detected in two-dimensional culture model.

K14 is a keratin expressed in basal layer of the epidermis, therefore associated with the mitotic capacity of basal keratinocytes (Coulombe et al. 1989; Troy & Turksen 1999). Recently, it has been shown a tight correlation between K14 and mechanical skin toughness (Ramms et al. 2013). Skin equivalents created with SR-B1 knockdown keratinocytes contained similar K14 expression as control tissues, indicating that SR-B1 does not affect tissue physical stability. K14 staining revealed a diffused signal of this keratin throughout the entire epidermis and not restricted to basal layer, probably due to limitation of the *in vitro* model, which may lack of certain components present in the *in vivo* human skin. K10 represents a keratin produced by post-mitotic keratinocytes in suprabasal epidermal layers, where together with K1 forms dense bundles in order to ensure mechanical strength to the tissue (Moll et al. 2008). K10 has also been reported as

an inhibitor of cell proliferation (Koch & Roop 2004). SR-B1-deficient skin equivalents presented a slight increase of K10 protein level, but not significant possibly due to limited sample replications. However, K10 up-regulation trend could in part justify tissue's thinning, as anti-proliferative effect. Furthermore, it could indicate an increase in differentiation tendency, supporting the relationship between keratinocytes differentiation and SR-B1 low expression (Tsuruoka et al. 2002). Additional support for differentiation/SR-B1 relationship derives from the up-regulated expression of filaggrin (FLG) encountered in SR-B1-deficient skin equivalents. FLG represents a late differentiation marker; it is expressed mostly in cornified layer as a result of proteolysis of profilaggrin contained in keratohyalin granules (Sandilands et al. 2009). Therefore, higher FLG expression is synonym of increased terminal differentiation induced by SR-B1 deficiency. Epidermal differentiation complex is an ensemble of genes implicated in terminal differentiation, which comprise FLG, but also S100A family of proteins (Marenholz et al. 2001). S100A9 is a calcium sensor protein expressed in upper layers of epidermis. It was reported to be implicated in inflammatory and hyperproliferative cutaneous diseases. Moreover, it forms heterodimers with S100A8 giving life to calprotectin, a known epidermal antimicrobial peptide (Kypriotou et al. 2012). S100A9 expression in SR-B1 knockdown tissues appeared limited to the most superficial epidermal layers compared to control tissues, with decreased overall expression, suggesting furthermore a possible modulation of SR-B1 on cell proliferation. In addition, the reduction of S100A9 implicates a decrease of calprotectin and a probable increased susceptibility for bacterial infections. Moreover, an in vivo study revealed that S100A9 acts as a ligand for RAGE receptor, which is a potent inducer of NF-kB pathway (Gebhardt et al. 2008), putting in relation once more SR-B1 and NF-kB.

Since SR-B1 is implicated in cholesterol uptake, which is essential for barrier function, we evaluated the lipid content in SR-B1 knockdown skin equivalents and observed that such tissues presented extremely low levels of lipids within the epidermis. Lipids were distributed mostly in the upper granular and cornified layers, whereas they were distributed evenly in all layers in control tissues, but no changes in lipid classes were detected. This result clearly underlines the importance of SR-B1 in maintaining lipid homeostasis in the skin. Similar evidence was reported in a previous study, where lipid barrier disruption up-regulated SR-B1 expression in human epidermis (Tsuruoka et al. 2002). SR-B1 knockdown did not suppress cutaneous lipids levels totally, meaning that also other players might influence lipids metabolism in the skin. We found that gene expression of LDLR, a receptor for LDL expressed in human keratinocytes, was down-regulated in SR-B1

deficient skin equivalents. This indicates a possible cross-talk between the two receptors, where LDLR could sense SR-B1 deficiency as a signal for low lipoproteins content, but this theory needs to be proven. Also PPAR-α and PPAR-γ gene expression was significantly lower in SR-B1 knockdown tissues. PPARs are nuclear receptors that regulate lipid homeostasis and improve epidermal barrier function by up-regulation of key enzymes responsible for ceramides synthesis (Chon et al. 2015). It has been shown that PPAR-α and PPAR-γ increase SR-B1 expression (Ahmed et al. 2009; Mashurabad et al. 2016), but no evidence of SR-B1 modulating PPARs has been yet reported. Since PPARs and LDLR resulted down-regulated, a further explanation for the lipid content observed in superficial layers of SR-B1 knockdown epidermis might come from HMG-CoA reductase, an enzyme in charge of cholesterol intracellular synthesis, which is expressed in epidermal layers (Proksch et al. 1991). Cutaneous lipids do not drive exclusively from differentiated keratinocytes, but they are secreted also by sebaceous glands (De Luca & Valacchi 2010). We demonstrated that SR-B1 is highly expressed in human sebaceous glands and knockdown of this receptor in human sebocytes lead to a striking decrease of intracellular content, underlining once more SR-B1 role in cutaneous lipid metabolism (Crivellari et al. 2017).

The above mentioned data demonstrated that SR-B1 deficiency in human skin impaired cellular proliferation, migration, differentiation and epidermal lipid homeostasis, thus the expression of this receptor is essential in cutaneous tissue. Skin is continuously exposed to environmental stressors, which lead to several pathological conditions (Valacchi et al. 2012). A previous study reported that environmental oxidants, such as CS, induced a striking reduction of SR-B1 expression in cultured human keratinocytes due to post-translational modifications induced by lipid peroxidation products (Sticozzi et al. 2012). Cell culture system is more susceptible to CS exposure since it lacks the protective physiological cutaneous structure, therefore we performed CS exposure in a healthy three-dimensional reconstructed human epidermis (RHE), which presents all functional differentiated epidermal layers (Font et al. 1994). CS reduced SR-B1 levels in RHE, suggesting that CS components are able to reach the inner layers of the epidermis and/or trigger a superficial response that influences also the underlying areas, probably leading to post-translational modifications of the scavenger receptor, as demonstrated previously on cultured keratinocytes (Sticozzi et al. 2012). Not only CS, but also particulate matter (PM), another environmental stressor, reduced SR-B1 cutaneous expression. Recently, it has been shown the ability of air particles to penetrate into epidermis, inducing oxidative reactions and lipid peroxidation (Magnani et al. 2016), which might be able to promote SR-B1

degradation. Furthermore, O_3, an important environmental oxidant, revealed its capacity in SR-B1 down-regulation within RHE. Although O_3 does not penetrate the skin, it reacts with the superficial lipid envelope, inducing a cascade of oxidative events which affect deeper cutaneous layers (Valacchi et al. 2016). This might explain the loss of SR-B1 expression also in the inner layers of the epidermis. Exposure of skin to O_3 induces a series of molecular reactions, such as oxidant and inflammatory responses as well as activation of stress proteins. RHE is a good model to represent the skin *in vitro* but has some limitations, therefore, SR-B1 loss upon O_3 could be a consequence of the lower protective capacity of the reconstructed tissue respect to the human skin. For this reason we tested the effect of O_3 also in skin of human subjects exposed to 0.8 ppm of O_3 for 3 h/day per 5 days. Also in this case SR-B1 was significantly down-regulated by O_3 exposure in human skin. To confirm that the effect of O_3 on SR-B1 expression was redox-mediated, we performed a topical application of resveratrol, a natural polyphenol and observed whether this approach was able to prevent O_3 skin damage. Indeed, resveratrol pre-treatment was able to counteract O_3-induced SR-B1 loss in RHE, indicating a redox-dependent down-regulation of receptor's expression (Rodrigo & Bosco 2006).

Altogether, the results presented in this study underline the importance of scavenger receptor B1 in cutaneous physiological processes. It has been shown that SR-B1 reduced significantly keratinocytes proliferation and migration, modulating thus the skin injury repair. The total absence of SR-B1 in epidermal layers induced the formation of a thin epidermis, probably due to the use of more cellular energy in differentiation and less in cell proliferation. SR-B1 down-regulation was associated with a reduction of S100A9 levels, an essential protein for calprotectin expression, therefore it may decrease cutaneous antimicrobial defense. Nevertheless, SR-B1 itself is implicated in bacteria recognition (Baranova et al. 2012). SR-B1 low levels modulate also lipid metabolism both in keratinocytes and sebocytes, compromising cutaneous lipid barrier. Finally, SR-B1 is down-regulated by oxidant environmental stressors in human skin, leading to all above mentioned physiopathological events. Since environmental-induced SR-B1 loss is redox-dependent, the use of radical quenchers as topical products may counteract the harmful effects on skin.

CHAPTER 8

References

Acton, S. et al., 1994. Expression cloning of SR-BI, a CD36-related class B scavenger receptor. *J Biol Chem*, 269(33), pp.21003–21009.

Acton, S. et al., 1996. Identification of Scavenger Receptor SR-BI as a High Density Lipoprotein Receptor. *Science*, 271(5248), pp.518–520.

Ahmed, R. et al., 2009. Human scavenger receptor class b type 1 is regulated by activators of peroxisome proliferators-activated receptor-gamma in hepatocytes. *Endocrine*, 35(2), pp.233–242.

Aliev, G. et al., 2010. Oxidative Stress Induced Mitochondrial Failure and Vascular Hypoperfusion as a Key Initiator for the Development of Alzheimer Disease. *Pharmaceuticals (Basel)*, 3(1), pp.158–187.

Allen, T. & Potten, C., 1974. Fine-structural identification and organization of the epidermal proliferative unit. *J Cell Sci*, 15(2), pp.291–319.

Alonso, L. & Fuchs, E., 2003. Stem cells of the skin epithelium. *Proc Natl Acad Sci U S A*, 100(Suppl 1), pp.11830–11835.

Altmann, S. et al., 2002. The identification of intestinal scavenger receptor class B, type I (SR-BI) by expression cloning and its role in cholesterol absorption. *Biochim Biophys Acta*, 1580(1), pp.77–93.

Angeloni, N. et al., 2016. Pathways for Modulating Exosome Lipids Identified By High-Density Lipoprotein-Like Nanoparticle Binding to Scavenger Receptor Type B-1. *Scientific Reports*, 6(February), p.22915.

Arda, O. et al., 2014. Basic histological structure and functions of facial skin. *Clin Dermatol*, 32(1), pp.3–13.

Armstrong, A. et al., 2011. Smoking and pathogenesis of psoriasis: a review of oxidative, inflammatory and genetic mechanisms. *Br J Dermatol*, 165(6), pp.1162–1168.

Babitt, J. et al., 1997. Murine SR-BI, a high density lipoprotein receptor that mediates selective lipid uptake, is N-glycosylated and fatty acylated and colocalizes with plasma membrane caveolae. *J Biol Chem*, 272(20), pp.13242–13249.

Bai, D. et al., 2009. Akt-mediated regulation of NFkB and the essentialness of NFkB for the oncogenicity of PI3K and Akt. *Int J Cancer*, 125(12), pp.2863–2870.

Baranova, I. et al., 2012. Class B scavenger receptor types I and II and CD36 mediate bacterial recognition and proinflammatory signaling induced by Escherichia coli, lipopolysaccharide, and cytosolic chaperonin 60. *J Immunol*, 188(3), pp.1371–1380.

Barreiro, E. et al., 2010. Cigarette smoke-induced oxidative stress: A role in chronic obstructive pulmonary disease skeletal muscle dysfunction. *Am J Respir Crit Care*

Med, 182(4), pp.477–488.

Bartosch, B. et al., 2005. An interplay between Hypervariable Region 1 of the Hepatitis C Virus E2 glycoprotein, the scaveneger receptor BI, and high-density lipoprotein promotes both enhancement of infection and protection against neutralizing antibodies. *J Virol*, 79(13), pp.8217–8229.

van Bennekum, A. et al., 2005. Class B scavenger receptor-mediated intestinal absorption of dietary beta-carotene and cholesterol. *Biochemistry*, 44(11), pp.4517–4525.

Bi, W. et al., 2015. Scavenger receptor B protects shrimp from bacteria by enhancing phagocytosis and regulating expression of antimicrobial peptides. *Dev Comp Immunol*, 51(1), pp.10–21.

Bocharov, A. et al., 2004. Targeting of scavenger receptor class B type I by synthetic amphipathic α-helical-containing peptides blocks lipopolysaccharide (LPS) uptake and LPS-induced pro-inflammatory cytokine responses in THP-1 monocyte cells. *Journal of Biological Chemistry*, 279(34), pp.36072–36082.

Borel, P. et al., 2007. Human Plasma Levels of Vitamin E and Carotenoids Are Associated with Genetic Polymorphisms in Genes Involved in Lipid Metabolism. *J Nutr*, 137, pp.2653–2659.

Borel, P. et al., 2013. CD36 and SR-BI Are Involved in Cellular Uptake of Provitamin A Carotenoids by Caco-2 and HEK Cells, and Some of Their Genetic Variants Are Associated with Plasma Concentrations of These Micronutrients in Humans. *J Nutr*, 143(4), pp.448–456.

Bove, P. & van der Vliet, A., 2006. Nitric oxide and reactive nitrogen species in airway epithelial signaling and inflammation. *Free Radic Biol Med*, 41(4), pp.515–527.

Braun, A. et al., 2002. Loss of SR-BI expression leads to the early onset of occlusive atherosclerotic coronary artery disease, spontaneous myocardial infarctions, severe cardiac dysfunction, and premature death in apolipoprotein E-deficient mice. *Circ Res*, 90(3), pp.270–276.

Brenner, M. & Hearing, V., 2008. The Protective Role of Melanin Against UV Damage in Human Skin. *Photochem Photobiol*, 84(3), pp.539–549.

Buechler, C. et al., 1999. Lipopolysaccharide inhibits the expression of the scavenger receptor Cla-1 in human monocytes and macrophages. *Biochem Biophys Res Commun*, 262(1), pp.251–254.

Cai, L. et al., 2008. SR-BI protects against endotoxemia in mice through its role in glucocorticoid production and hepatic clearence. *J Clin Invest*, 118(1), pp.364–375.

Calvo, D. & Vega, M., 1993. Identification, primary Structure, and distribution of CLA-1, a novel member of the CD36/LIMPII gene family. *J Biol Chem*, 268(25), pp.18929–18935.

Calvo, D. et al., 1997. CLA-1 is an 85-kD plasma membrane glycoprotein that acts as a high-affinity receptor for both native (HDL, LDL, and VLDL) and modified (OxLDL and AcLDL) lipoproteins. *Arterioscler Thromb Vasc Biol*, 17(11), pp.2341–2349.

Candi, E. et al., 2005. The cornified envelope: a model of cell death in the skin. *Nat Rev Mol Cell Biol*, 6(4), pp.328–340.

Candi, E. et al., 2015. MicroRNAs and p63 in epithelial stemness. *Cell Death Differ*, 22(1), p.12.

Cao, G. et al., 1997. Structure and localization of human gene encoding SR-BI/CLA-1. Evidence for transcriptional control by steroidogenic factor 1. *J Biol Chem*, 272(52), pp.33068–33076.

Cao, W. et al., 2004. Phosphatidylserine receptor cooperates with high-density lipoprotein receptor in recognition of apoptotic cells by thymic nurse cells. *J Mol Endocrinol*, 32(2), pp.497–505.

Carlos, S. et al., 2014. Oxidative damage induced by cigarette smoke exposure in mice: impact on lung tissue and diaphragm muscle. *J Bras Pneumol*, 40(4), pp.411–420.

Catanese, M. et al., 2007. High-avidity monoclonal antibodies against the human scavenger class B type I receptor efficiently block hepatitis C virus infection in the presence of high-density lipoprotein. *J Virol*, 81(15), pp.8063–8071.

Catanese, M. et al., 2010. Role of scavenger receptor class B type I in hepatitis C virus entry: kinetics and molecular determinants. *J Virol*, 84(1), pp.34–43.

Cejka, C. & Cejkova, J., 2015. Oxidative Stress to the Cornea, Changes in Corneal Optical Properties, and Advances in Treatment of Corneal oxidative injuries. *Oxid Med Cell Longev*, 2015, p.591530.

Chon, S. et al., 2015. Keratinocyte differentiation and upregulation of ceramide synthesis induced by an oat lipid extract via the activation of PPAR pathways. *Exp Dermatol*, 24(4), pp.290–295.

Chung, H. & Uitto, J., 2010. Type VII Collagen: The Anchoring Fibril Protein at Fault in Dystrophic Epidermolysis Bullosa. *Dermatol Clin*, 28(1), pp.93–105.

Clayton, E. et al., 2007. A single type of progenitor cell maintains normal epidermis. *Nature*, 446(185–189).

Coulombe, P. et al. 1989. Expression of Keratin K14 in the Epidermis and Hair Follicle:

Insights into Complex Programs of Differentiation. *J Cell Biol*, 109, pp.2295–2312.

Covey, S. et al., 2003. Scavenger receptor class B type I-mediated protection against atherosclerosis in LDL receptor-negative mice involves its expression in bone marrow-derived cells. *Arteriosclerosis, Thrombosis, and Vascular Biology*, 23(9), pp.1589–1594.

Crivellari, I. et al., 2017. SRB1 as a new redox target of cigarette smoke in human sebocytes. *Free Radic Biol Med*, 102, pp.47–56.

Cross, C. et al., 2002. Environmental oxidant pollutant effects on biologic systems: A focus on micronutrient antioxidant-oxidant interactions. *Am J Respir Crit Care Med*, 166(12 Pt 2), pp.S44–S50.

Dai, X. & Segre, J., 2004. Transcription control of epidermal specification and differentiation. *Curr Opin Genet Dev*, 14, pp.485–491.

Danilo, C. et al., 2013. Scavenger receptor class B type I regulates cellular cholesterol metabolism and cell signaling associated with breast cancer development. *Breast Cancer Res*, 15(5), p.R87.

Davies, K., 1995. Oxidative stress: the paradox of aerobic life. *Biochem Soc Symp*, 61, pp.1–31.

De Luca, C. & Valacchi, G., 2010. Surface lipids as multifunctional mediators of skin responses to environmental stimuli. *Mediators Inflamm*, 2010, p.321494.

Delfino, R. et al., 2005. Potential role of ultrafine particles in associations between airborne particle mass and cardiovascular health. *Environ Health Perspect*, 113(8), pp.934–946.

Deochand, C. et al., 2016. Tobacco Smoke Exposure Impairs Brain Insulin/IGF Signaling: Potential Co-Factor Role in Neurodegeneration. *J Alzheimers Dis*, 50(2), pp.373–386.

DiPersio, C. et al., 2016. Integrin-mediated regulation of epidermal wound functions. *Cell Tissues Res*, 365(3), pp.467–482.

Dominici, F. et al., 2006. Fine particulate air pollution and hospital admission for cardiovascular and respiratory diseases. *JAMA*, 295(10), pp.1127–1134.

Duggan, A. et al., 2002. Expression of SR-BI (Scavenger receptor class B type I) in turtle (Chrysemys picta) tissues and other nonmammalian vertebrates. *J Exp Zool*, 292(5), pp.430–434.

During, A. & Harrison, E., 2007. Mechanisms of provitamin A (carotenoid) and vitamin A (retinol) transport into and out of intestinal Caco-2 cells. *J Lipid Res*, 48(10), pp.2283–2294.

Ehmann, L. et al., 2011. Cutaneous side-effects of EGFR inhibitors and their management. *Skin Therapy Lett*, 16(1), pp.1–3.

Fenske, S. et al., 2009. Normal hepatic cell surface localization of the high density lipoprotein receptor, scavenger receptor class B, type I, depends on all four PDZ domains of PDZK1. *J Biol Chem*, 284(9), pp.5797–806.

Filosto, S. et al., 2012. Cigarette smoke induces aberrant EGF receptor activation that mediates lung cancer development and resistance to tyrosine kinase inhibitors. *Mol Cancer Ther*, 11(4), pp.795–804.

Fluiter, K. et al., 1998. In vivo regulation of scavenger receptor BI and the selective uptake of high density lipoprotein cholesteryl esters in rat liver parenchymal and Kupffer cells. *J Biol Chem*, 273(14), pp.8434–8438.

Font, J. et al., 1994. A new three-dimensional culture of human keratinocytes: optimization of differentiation. *Cell Biol Toxicol*, 10(5–6), pp.353–359.

Fuchs, E. & Byrne, C., 1994. The epidermis: rising to the surface. *Curr Opin Genet Dev*, 4(5), pp.752–736.

Fuchs, E. & Raghavan, S., 2002. Getting Under the Skin of Epidermal Morphogenesis. *Nat Rev Genet*, 3(3), pp.199–209.

Fuchs, E., 2008. Skin stem cells: Rising to the surface. *J Cell Biol*, 180(2), pp.273–284.

Fukasawa, M. et al., 1996. SRB1, a class B scavenger receptor, recognizes both negatively charged liposomes and apoptotic cells. *Exp Cell Res*, 222, pp.246–250.

Ganesan, L. et al., 2016. Scavenger receptor B1, the HDL receptor, is expressed abundantly in liver sinusoidal endothelial cells. *Sci Rep*, 6, p.20646.

Gebhardt, C. et al., 2008. RAGE signaling sustains inflammation and promotes tumor development. *J Exp Med*, 205(2), pp.275–285.

Gillotte-Taylor, K. et al., 2001. Scavenger receptor class B type I as a receptor for oxidized low density lipoprotein. *J Lipid Res*, 42, pp.1474–1482.

Godic, A. et al., 2014. The role of antioxidants in skin cancer prevention and treatment. *Oxid Med Cell Longev*, 2014, p.860479.

Goncalves, A. et al., 2014. Intestinal scavenger receptors are involved in vitamin K1 absorption. *J Biol Chem*, 289(44), pp.30743–30752.

Greaves, M., 1976. Physiology of skin. *J Invest Dermatol*, 67(1), pp.66–69.

Gruber, F. et al., 2007. Photooxidation generates biologically active phospholipids that induce heme oxygenase-1 in skin cells. *J Biol Chem*, 282(23), pp.16934–16941.

Gu, X. et al., 1998. The efficient cellular uptake of high density lipoprotein lipids via

scavenger receptor class B type I requires not only receptor-mediated surface binding but also receptor-specific lipid transfer mediated by its extracellular domain. *J Biol Chem*, 273(41), pp.26338–26348.

Gu, X. et al., 2000. Dissociation of the high density lipoprotein and low density lipoprotein binding activities of murine scavenger receptor class B type I (mSR-BI) using retrovirus library-based activity dissection. *J Biol Chem*, 275(13), pp.9120–9130.

Gu, X. et al., 2000. Scavenger receptor class B, type I-mediated [3H]cholesterol efflux to high density and low density lipoproteins is dependent on lipoprotein binding to the receptor. *J Biol Chem*, 275(39), pp.29993–30001.

Hamilton, R.J. et al., 1998. Potential involvement of 4-hydroxynonenal in the response of human lung cells to ozone. *Am J Physiol*, 274(1 Pt 1), pp.L8–L16.

Hatzopoulos, A. et al., 1998. Temporal and spatial pattern of expression of the HDL receptor SR-BI during murine embryogenesis. *J Lipid Res*, 39, pp.495–508.

Henchcliffe, C. & Beal, M., 2008. Mitochondrial biology and oxidative stress in Parkinson disease pathogenesis. *Nat Clin Pract Neurol*, 4(11), pp.600–609.

Hinz, M. et al., 1999. NF-κB Function in Growth Control: Regulation of Cyclin D1 Expression and G0/G1-to-S-Phase Transition. *Mol Cell Biol*, 19(4), pp.2690–2698.

Holloway, S. & Jones, V., 2005. The importance of skin care and assessment. *Br J Nurs*, 14(22), pp.1172–1176.

Holm, T. et al., 2002. Failure of red blood cell maturation in mice with defects in the high-density lipoprotein receptor SR-BI Failure of red blood cell maturation in mice with defects in the high-density lipoprotein receptor SR-BI. *Blood*, 99(5), pp.1817–1824.

Hong, C. et al., 2015. An involvement of SR-B1 mediated p38 MAPK signaling pathway in serum amyloid A-induced angiogenesis in rheumatoid arthritis. *Mol Immunol*, 66(2), pp.340–345.

Hopkinson, S. et al., 2014. Focal Contact and Hemidesmosomal Proteins in Keratinocyte Migration and Wound Repair. *Adv Wound Care (New Rochelle)*, 3(3), pp.247–263.

Husemann, J. et al., 2001. Scavenger receptor class B type I (SR-BI) mediates adhesion of neonatal murine microglia to fibrillar beta-amyloid. *J Neuroimmunol*, 114(1–2), pp.142–150.

Ikemoto, M. et al., 2000. Identification of a PDZ-domain-containing protein that interacts with the scavenger receptor class B type I. *Proc Natl Acad Sci U S A*, 97(12), pp.6538–6543.

Imachi, H. et al., 1999. Evidence for a potential role for HDL as an important source of

cholesterol in human adrenocortical tumors via the CLA-1 pathway. *Endocr J.*, 46(1), pp.27–34.

Imachi, H. et al., 2000. Human scavenger receptor B1 is involved in recognition of apoptotic thymocytes by thymic nurse cells. *Lab Invest*, 80(2), pp.263–270.

Iram, T. et al., 2016. Astrocytes from old Alzheimer's disease mice are impaired in Aβ uptake and in neuroprotection. *Neurobiol Dis*, 96, pp.84–94.

Ishikawa, Y. et al., 2009. Distribution of smooth muscle cells and macrophages expressing scavenger receptor BI/II in atherosclerosis. *J.Atheroscler.Thromb.*, 16(6), pp.829–839.

Ji, Y. et al., 1997. Scavenger receptor BI promotes high density lipoprotein-mediated cellular cholesterol efflux. *J Biol Chem*, 272(34), pp.20982–20985.

Jiang, T. et al., 2016. Oxidative stress: A major pathogenesis and potential therapeutic target of antioxidative agents in Parkinson's disease and Alzheimer's disease. *Prog Neurobiol*, 147, pp.1–19.

Jiménez, L. et al., 2010. Scavenger receptor-B1 and luteal function in mice. *J Lipid Res*, 51(8), pp.2362–2371.

Johnson, A. et al., 2003. Experimental glomerulopathy alters renal cortical cholesterol, SR-B1, ABCA1, and HMG CoA reductase expression. *Am J Pathol*, 162(1), pp.283–291.

Jones, P. et al., 1995. Stem cell patterning and fate in human epidermis. *Cell*, 80, pp.83–93.

Karin, M. & Shaulian, E., 2001. AP-1: linking hydrogen peroxide and oxidative stress to the control of cell proliferation and death. *IUBMB Life*, 52(1–2), pp.17–24.

Kim, G. et al., 2015. The Role of Oxidative Stress in Neurodegenerative Diseases. *Exp Neurobiol*, 24(4), pp.325–340.

Kim, K. et al., 2015. A review on the human health impact of airborne particulate matter. *Environ Int*, 74, pp.136–143.

Kim, K. et al., 2016. Air pollution and skin diseases: Adverse effects of airborne particulate matter on various skin diseases. *Life Sci*, 152, pp.126–134.

Klein, R. & Andersen, B., 2015. Dynamic networking for epidermal differentiation. *Developmental Cell*, 32(6), pp.661–662.

Kleveland, E. et al., 2006. Characterization of scavenger receptor class B, type I in Atlantic salmon (Salmo salar L.). *Lipids*, 41(11), pp.1017–1027.

Koch, P. & Roop, D., 2004. The role of keratins in epidermal development and homeostasis--going beyond the obvious. *J Invest Dermatol*, 123(5), pp.x–xi.

Kocher, O. et al., 2003. Targeted disruption of the PDZK1 gene in mice causes tissue-

specific depletion of the high density lipoprotein receptor scavenger receptor class B type I and altered lipoprotein metabolism. *J Biol Chem*, 278(52), pp.52820–52825.

Kolarsick, P. et al., 2009. Anatomy and physiology of the skin. In P. Muehlbauer & C. McGowan, eds. *Site-specific cancer series: Skin cancer*. Pittsburgh: Oncology Nursing Society, pp. 1–12.

Kolleck, I. et al., 1999. HDL is the major source of vitamin E for type II pneumocytes. *Free Radic Biol Med*, 27(7–8), pp.882–890.

Kolmakova, A. et al., 2010. Deficiency of scavenger receptor class B type I negatively affects progesterone secretion in human granulosa cells. *Endocrinology*, 151(11), pp.5519–5527.

Kozarsky, K. et al., 1997. Overexpression of the HDL receptor SR-BI alters plasma HDL and bile cholesterol levels. *Nature*, 387(6631), pp.414–417.

Krieger, M., 2001. Scavenger receptor class B type I is a multiligand HDL receptor that influences diverse physiologic systems. *J Clin Invest*, 108(6), pp.793–797.

Kryston, T. et al., 2011. Role of oxidative stress and DNA damage in human carcinogenesis. *Mutat Res*, 711(1–2), pp.193–201.

Kypriotou, M. et al., 2012. The human epidermal differentiation complex: Cornified envelope precursors, S100 proteins and the “fused genes” family. *Exp Dermatol*, 21(9), pp.643–649.

Lai-Cheong, J. & McGrath, J., 2013. Structure and function of skin, hair and nails. *Medicine*, 41(6), pp.317–320.

Landschulz, K. et al., 1996. Regulation of scavenger receptor, class B, type I, a high density lipoprotein receptor, in liver and steroidogenic tissues of the rat. *J Clin Invest*, 98(4), pp.984–995.

Lanuti, E. & Kirsner, R., 2010. Effects of pollution on skin aging. *J Invest Dermatol*, 130(12), p.2696.

Latifi-Pupovci, H. et al., 2015. In vitro migration and proliferation (“wound healing”) potential of mesenchymal stromal cells generated from human CD271+ bone marrow mononuclear cells. *J Transl Med*, 13(1), p.315.

Laverdet, B. et al., 2015. Skin innervation: important roles during normal and pathological cutaneous repair. *Histol Histopathol*, 30(8), pp.875–892.

Lavie, M. et al., 2014. Identification of Conserved Residues in Hepatitis C Virus Envelope Glycoprotein E2 That Modulate Virus Dependence on CD81 and SRB1 Entry Factors. *J Virol*, 88(18), pp.10584–10597.

Li, J. et al., 2016. Up-regulation expression of scavenger receptor class B type 1 (SR-B1) is associated with malignant behaviors and poor prognosis of breast cancer. *Pathol Res Pract*, 212(6), pp.555–559.

Li, N. et al., 2009. The adjuvant effect of ambient particulate matter is closely reflected by the particulate oxidant potential. *Environ Health Perspect*, 117(7), pp.1116–1123.

Li, X. et al., 1998. In situ hybridization of high density lipoprotein (scavenger, type 1) receptor messenger ribonucleic acid (mRNA) during folliculogenesis and luteinization: evidence for mRNA expression and induction by human chorionic gonadotropin specifically in cell typ. *Endocrinology*, 139(7), pp.3043–3049.

Li, X. et al., 2006. Scavenger receptor BI prevents nitric oxide-induced cytotoxicity and endotoxin-induced death. *Circ Res*, 98(7), pp.e60-65.

Liadaki, K. et al., 2000. Binding of high density lipoprotein (HDL) and discoidal reconstructed HDL to the HDL receptor scavenger receptor class B type I. *J Biol Chem*, 275(28), pp.21262–21271.

Liu, F. et al., 2015. Macrophages treated with particulate matter PM2.5 induce selective neurotoxicity through glutaminase-mediated glutamate generation. *J Neurochem*, 134(2), pp.315–326.

Lopez, D. & McLean, M., 1999. Sterol regulatory element-binding protein-1a binds to cis elements in the promoter of the rat high density lipoprotein receptor SR-BI gene. *Endocrinology*, 140(12), pp.5669–5681.

Magnani, N. et al., 2016. Skin damage mechanisms related to airborne particulate matter exposure. *Toxicol Sci*, 149(1), pp.227–236.

Maillard, P. et al., 2006. The interaction of natural hepatitis C virus with human scavenger receptor SR-BI/Cla1 is mediated by ApoB-containing lipoproteins. *FASEB J*, 20(6), pp.735–737.

Malerod, L. et al., 2002. Oxysterol-activated LXRalpha/RXR induces hSR-BI-promoter activity in hepatoma cells and preadipocytes. *Biochem Biophys Res Commun*, 299(5), pp.916–923.

Manohar, A. et al., 2004. Alpha 3 beta 1 integrin promotes keratinocyte cell survival through activation of a MEK/ERK signaling pathway. *J Cell Sci*, 117(Pt 18), pp.4043–4054.

Marchini, T. et al., 2014. Time course of systemic oxidative stress and inflammatory response induced by an acute exposure to residual oil fly ash. *Toxicol Appl Pharmacol*, 274(2), pp.274–282.

Mardones, P. et al., 2002. Alpha-tocopherol metabolism is abnormal in scavenger receptor class B type I (SR-BI)-deficient mice. *J Nutr*, 132(3), pp.443–449.

Marenholz, I. et al., 2001. Identification of human epidermal differentiation complex (EDC)-encoded genes by subtractive hybridization of entire YACs to a gridded Keratinocyte cDNA library. *Genome Res*, 11(3), pp.341–355.

Martins-Green, M. et al., 2014. Cigarette smoke toxins deposited on surfaces: Implications for human health. *PLoS ONE*, 9(1), pp.1–12.

Mashurabad, P. et al., 2016. Eicosapentaenoic acid inhibits intestinal β-carotene absorption by downregulation of lipid transporter expression via PPAR-α dependent mechanism. *Arch Biochem Biophys*, 590, pp.118–124.

Michopoulou, A. & Rousselle, P., 2015. How do epidermal matrix metalloproteinases support re-epithelialization during skin healing? *Eur J Dermatol*, 25 Suppl 1, pp.33–42.

Mildner, M. et al., 2010. Knockdown of filaggrin impairs diffusion barrier function and increases UV sensitivity in a human skin model. *J Invest Dermatol*, 130(9), pp.2286–2294.

Minciacchi, V. et al., 2015. Extracellular vesicles in cancer: exosomes, microvesicles and the emerging role of large oncosomes. *Semin Cell Dev Biol*, 40, pp.41–51.

Mizutani, T. et al., 1997. Cloning, characterization, and cellular distribution of rat scavenger receptor calss B type I (SRBI) in the ovary. *Biochem Biophys Res Commun*, 234(2), pp.499–505.

Model, D., 1985. Smoker's face: an underrated clinical sign? *Br Med J (Clin Red Ed)*, 291(6511), pp.1760–1762.

Moll, R. et al., 2008. The human keratins: Biology and pathology. *Histochem Cell Biol*, 129(6), pp.705–733.

Moussa, M. et al., 2008. Lycopene absorption in human intestinal cells and in mice involves scavenger receptor class B type I but not Niemann-Pick C1-like 1. *J Nutr*, 138(8), pp.1432–6.

Murao, K. et al., 1997. Characterization of CLA-1, a Human Homologue of Rodent Scavenger Receptor BI, as a Receptor for High Density Lipoprotein and Apoptotic Thymocytes. *J Biol Chem*, 272(28), pp.17551–17557.

Muresan, X. et al., 2015. The loss of cellular junctions in epithelial lung cells induced by cigarette smoke is attenuated by corilagin. *Oxid Med Cell Longev*, 2015, p.631758.

Mutlu, G. et al., 2007. Ambient particulate matter accelerates coagulation via an IL-6

dependent pathway. *J Clin Invest*, 117(10), pp.2952–2961.

Naldo, L., Peli, L. & Parazzini, F., 1999. Association of early-stage psoriasis with smoking and male alcohol consumption: evidence from an Italian case-control study. *Arch Dermatol*, 135(12), pp.1479–1484.

Nel, A., 2005. Atmosphere. Air pollution-related illness: effects of particles. *Science*, 308(5723), pp.804–806.

Nieland, T. et al., 2002. Discovery of chemical inhibitors of the selective transfer of lipids mediated by the HDL receptor SCARB1. *Proc Natl Acad Sci U S A*, 99(24), pp.15422–15427.

Niki, E., 2014. Role of vitamin E as a lipid-soluble peroxyl radical scavenger: in vitro and in vivo evidence. *Free Radic Biol Med*, 66, pp.3–12.

Niki, E., 2015. Lipid oxidation in the skin. *Free Radic Res*, 49(7), pp.827–834.

Ortiz, A. & Grando, S., 2012. Smoking and the skin. *Int J Dermatol*, 51(3), pp.250–262.

Osada, Y. et al., 2009. Signalling pathway involving GULP, MAPK and Rac1 for SR-BI-induced phagocytosis of apoptotic cells. *J Biochem*, 145(3), pp.387–394.

Patel, R. et al., 2008. Cigarette smoking and diffuse lunf disease. *Drugs*, 68(11), pp.1511–1527.

Pattinson, D. et al., 2012. Photo-oxidation of proteins. *Photochem Photobiol*, 132, pp.976–984.

Perricone, C. et al., 2016. Smoke and autoimmunity: The fire behind the disease. *Autoimmun Rev*, 15(4), pp.354–374.

Philips, J. et al., 2005. Drosophila RNAi Screen Reveals CD36 Family Member Required for Mycobacterial Infection. *Science*, 309(5738), pp.1251–1253.

Di Pietro, N. et al., 2016. Physiology and pathophysiology of oxLDL uptake by vascular wall cells in atherosclerosis. *Vascul Pharmacol*, 84, pp.1–7.

Plebanek, M. et al., 2015. Nanoparticle Targeting and Cholesterol Flux Through Scavenger Receptor Type B-1 Inhibits Cellular Exosome Uptake. *Scientific Reports*, 5(October), p.15724.

Powell, J. & Soon, C., 2002. Physiology of the skin. *Surgery*, 20(6), pp.ii–vi.

Proksch, E. et al., 1991. Localization and regulation of epidermal 3-hydroxy-3-methylglutaryl-coenzyme A reductase activity by barrier requirements. *Biochim Biophys Acta*, 1083(1), pp.71–79.

Proksch, E. et al., 2008. The skin: an indispensable barrier. *Exp Dermatol*, 17(12), pp.1063–1072.

Pryor, W., 1999. Mechanisms of radical formation from reactions of ozone with target molecules in the lung. *Free Radic Biol Med*, 17(5), pp.451–465.

Rahman, I., 2006. Antioxidant therapies in COPD. *Int J Chron Obstruct Pulmon Dis*, 1(1), pp.15–29.

Rajapaksha, W. et al., 1997. Sequence of the bovine HDL-receptor (SR-BI) cDNA and changes in receptor mRNA expression during granulosa cell luteinization in vivo and in vitro. *Mol Cell Endocrinol*, 134(1), pp.59–67.

Ramms, L. et al., 2013. Keratins as the main component for the mechanical integrity of keratinocytes. *Proc Natl Acad Sci U S A*, 110(46), pp.18513–18518.

Ravanti, L. & Kähäri, V., 2000. Matrix metalloproteinases in wound repair (review). *Int J Mol Med*, 6(4), pp.391–407.

Ray, P. et al., 2012. Reactive oxygen species (ROS) homeostasis and redox regulation in cellular signaling. *Cell Signal*, 24(5), pp.981–990.

Reboul, E. et al., 2005. Lutein transport by Caco-2 TC-7 cells occurs partly by a facilitated process involving the scavenger receptor class B type I (SR-BI). *Biochem J*, 387(2), pp.455–461.

Reboul, E. et al., 2006. Scavenger receptor class B type I (SR-BI) is involved in vitamin E transport across the enterocyte. *J Biol Chem*, 281(8), pp.4739–4745.

Reinke, J. & Sorg, H., 2012. Wound repair and regeneration. *Eur Surg Res*, 49(1), pp.35–43.

Reiss, M. et al., 2010. Matrix metalloproteinase-9 delays wound healing in a murine wound model. *Surgery*, 147(2), pp.295–302.

Rhainds, D. & Brissette, L., 2004. The role of scavenger receptor class B type I (SR-BI) in lipid trafficking Defining the rules for lipid traders. *Int J Biochem Cell Biol*, 36, pp.39–77.

Rigotti, A. et al., 1996. Regulation by adrenocorticotropic hormone of the in vivo expression of scavenger receptor class B type I (SR-BI), a high density lipoprotein receptor, in steroidogenic cells of the murine adrenal gland. *J Biol Chem*, 271(52), pp.33545–33549.

Rigotti, A. et al., 1997. A targeted mutation in the murine gene encoding the high density lipoprotein (HDL) receptor scavenger receptor class B type I reveals its key role in HDL metabolism. *Proc Natl Acad Sci USA*, 94(23), pp.12610–12615.

Rigotti, A. et al., 2003. The role of the high density lipoprotein receptor SR-BI in the lipid metabolism of endocrine and other tissues. *Endocr Rev*, 24(3), pp.357–387.

Risom, L. et al., 2005. Oxidative stress-induced DNA damage by particulate air pollution. *Mutat Res*, 592(1–2), pp.119–137.

Rodrigo, R. & Bosco, C., 2006. Oxidative stress and protective effects of polyphenols: comparative studies in human and rodent kidney. A review. *Comp Biochem Physiol C Toxicol Pharmacol*, 142(3–4), pp.317–327.

Romanovsky, A., 2014. Skin temperature: its role in thermoregulation. *Acta Physiol (Oxf)*, 210(3), pp.498–507.

Saddar, S. et al., 2010. Signaling by the High-Affinity HDL Receptor Scavenger Receptor B Type I. *Arterioscler Thromb Vasc Biol*, 30, pp.144–150.

Sandilands, A. et al., 2009. Filaggrin in the frontline: role in skin barrier function and disease. *J Cell Sci*, 122(Pt 9), pp.1285–1294.

Scarselli, E. et al., 2002. The human scavenger receptor class B type I is a novel candidate receptor for the hepatitis C virus. *Embo J*, 21(19), pp.5017–5025.

Schäfer, G. et al., 2009. The role of scavenger receptor B1 in infection with Mycobacterium tuberculosis in a murine model. *PLoS ONE*, 4(12), p.e8448.

Schäfer, M. & Werner, S., 2008. Cancer as an overhealing wound: an old hypothesis revisited. *Nat Rev Mol Cell Biol*, 9, pp.628–638.

Shen, W. et al., 2014. Scavenger Receptor class B type I (SR-BI): A versatile receptor with multiple functions and actions. *Metabolism*, 63(7), pp.875–886.

Shiratsuchi, A. et al., 1999. Role of class B scavenger receptor type I in phagocytosis of apoptotic cells. *J Biol Chem*, 274(9), pp.5901–5908.

Siasos, G. et al., 2014. Smoking and atherosclerosis: mechanisms of disease and new therapeutic approaches. *Curr Med Chem*, 21(34), pp.3936–3948.

Sies, H. & de Groot, H., 1992. Role od reactive oxygen species in cell toxicity. *Toxicol Lett*, 64–64, pp.547–551.

Sies, H., 1997. Oxidative stress: oxidants and antioxidants. *Exp Physiol*, 82(2), pp.291–295.

Small, J. et al., 1998. Assembling an actin cytoskeleton for cell attachment and movement. *Biochim Biophys Acta*, 1404(3), pp.271–281.

Smith, C. & Fischer, T., 2001. Particulate and vapor phase constituents of cigarette mainstream smoke and risk of myocardial infarction. *Atherosclerosis*, 158(2), pp.257–267.

Srivastava, R., 2003. Scavenger rceptor class B type I expression in murine brain and regulation by estrogen and dietary cholesterol. *J Neurol Sci*, 210(1–2), pp.11–18.

Stacey, D., 2003. Cyclin D1 serves as a cell cycle regulatory switch in actively proliferating cells. *Curr Opin Cell Biol*, 15(2), pp.158–163.

Van den Steen, P. et al., 2002. Biochemistry and molecular biology of gelatinase B or matrix metalloproteinase-9 (MMP-9). *Crit Rev Biochem Mol Biol*, 37(6), pp.375–536.

Sticozzi, C. et al., 2012. Cigarette smoke affects keratinocytes SRB1 expression and localization via H2O2 production and HNE protein adducts formation. *PLoS ONE*, 7(3), pp.1–14.

Sticozzi, C. et al., 2013. Scavenger receptor B1 post-translational modifications in Rett syndrome. *FEBS LEtt*, 587(14), pp.2199–2204.

Sun, B. et al., 2007. Distinct mechanisms for OxLDL uptake and cellular trafficking by class B scavenger receptors CD36 and SR-BI. *J Lipid Res*, 48(12), pp.2560–2570.

Sun, Y. et al., 1999. Regulation of adrenal scavenger receptor-BI expression by ACTH and cellular cholesterol pools. *J Lipid Res*, 40(10), pp.1799–805.

Svensson, K. et al., 2013. Exosome uptake depends on ERK1/2-Heat Shock Protein 27 signaling and lipid raft-mediated endocytosis negatively regulated by Caveolin-1. *J Biol Chem*, 288(24), pp.17713–17724.

Tanaka, H. et al., 2008. A genome-wide analysis of genes and gene families involved in innate immunity of Bombyx mori. *Insect Biochem Mol Biol*, 38(12), pp.1087–1110.

Thiele, J. et al., 1997. Tropospheric ozone: an emerging environmental stressor to skin. *Biol Chem*, 378, pp.1299–1305.

Trigatti, B. et al., 1999. Influence of the high density lipoprotein receptor SR-BI on reproductive and cardiovascular pathophysiology. *Proc Natl Acad Sci USA*, 96(16), pp.9322–9327.

Trigatti, B. et al., 2003. Influence of the HDL receptor SR-BI on lipoprotein metabolism and atherosclerosis. *Arterioscler Thromb Vasc Biol*, 23(10), pp.1732–1738.

Trigatti, B. et al., 2004. Scavenger receptor class B type I in high-density lipoprotein metabolism, atherosclerosis and heart disease: lessons from gene-targeted mice. *Biochem Soc Trans*, 32(Pt 1), pp.116–120.

Troy, T. & Turksen, K., 1999. In vitro characteristics of early epidermal progenitors isolated from keratin 14 (K14)-deficient mice: Insights into the role of keratin 17 in mouse keratinocytes. *J Cell Physiol*, 180(3), pp.409–421.

Tsukamoto, K. et al., 2013. Noncanonical role of the PDZ4 domain of the adaptor protein PDZK1 in the regulation of the hepatic high density lipoprotein receptor scavenger receptor class B, type I (SR-BI). *J Biol Chem*, 288(27), pp.19845–19860.

Tsuruoka, H. et al., 2002. Scavenger receptor class B type I is expressed in cultured keratinocytes and epidermis. Regulation in response to changes in cholesterol homeostasis and barrier requirements. *J Biol Chem*, 277(4), pp.2916–2922.

Valacchi, G. et al., 2002. Ozone exposure activates oxidative stress responses in murine skin. *Toxicology*, 179(1–2), pp.163–170.

Valacchi, G. et al., 2004. In vivo ozone exposure induces antioxidant/stress-related responses in murine lung and skin. *Free Radic Biol Med*, 36(5), pp.673–681.

Valacchi, G. et al., 2011. Cigarette smoke exposure causes changes in Scavenger Receptor B1 level and distribution in lung cells. *Int J Biochem Cell Biol*, 43(7), pp.1065–1070.

Valacchi, G. et al., 2011. Scavenger receptor class B type I: a multifunctional receptor. *Ann N Y Acad Sci*, 1229, pp.1–7.

Valacchi, G. et al., 2012. Cutaneous responses to environmental stressors. *Ann N Y Acad Sci*, 1271, pp.75–81.

Valacchi, G. et al., 2014. Scavenger Receptor B1 oxidative post-translational modifications are responsible for its loss in Rett syndrome. *Free Radic Biol Med*, 75(Suppl 1), pp.S10–S11.

Valacchi, G. et al., 2015. Ambient Ozone and Bacterium Streptococcus: a Link Between Cellulitis and Pharyngitis. *Int J Occup Med Environ Health*, 28(4), pp.771–774.

Valacchi, G. et al., 2015. Exploring the link between scavenger receptor B1 expression and chronic obstructive pulmonary disease pathogenesis. *Ann N Y Acad Sci*, 1340(1), pp.47–54.

Valacchi, G. et al., 2016. Ozone-induced damage in 3D-Skin Model is prevented by topical vitamin C and vitamin E compound mixtures application. *J Dermatol Sci*, 82(3), pp.209–212.

Van Eck, M. et al., 2003. Differential effects of scavenger receptor BI deficiency on lipid metabolism in cells of the arterial wall and in the liver. *J Biol Chem*, 278(26), pp.23699–23705.

Vasques, M. et al., 2016. Interferon alpha bioactivity critically depends on Scavenger receptor class B type I function. *Oncoimmunology*, 5(8), p.e1196309.

Venus, M. et al., 2011. Basic physiology of the skin. *Surgery*, 29(10), pp.471–474.

Vernier, T. et al., 2004. Nanoelectropulse-induced phosphatidylserine translocation. *Biophys J*, 86(6), pp.4040–4048.

Vierkötter, A. et al., 2010. Airborne particle exposure and extrinsic skin aging. *J Invest Dermatol*, 130(12), pp.2719–2726.

Viñals, M. et al., 2003. Identification of the N-linked glycosylation sites on the high density lipoprotein (HLD) receptor SR-BI and assessment of their effects on HDL binding and selective lipid uptake. *J Biol Chem*, 278(7), pp.5325–5332.

Vishnyakova, T. et al., 2003. Binding and internalization of lipopolysaccharide by Cla-1, a human orthologue of rodent scavenger receptor B1. *J Biol Chem*, 278(25), pp.22771–22780.

Vishnyakova, T. et al., 2006. CLA-1 and its splicing variant CLA-2 mediate bacterial adhesion and cytosolic bacterial invasion in mammalian cells. *Proc Natl Acad Sci U S A*, 103(45), pp.16888–93.

Wacker, M. & Holick, M., 2013. Sunlight and Vitamin D: A global perspective for health. *Dermatoendocrinol*, 5(1), pp.51–108.

Wang, H. & Morrison, G., 2010. Ozone-surface reactions in five homes: surface reaction probabilities, aldehyde yields, and trends. *Indoor Air*, 20(3), pp.224–234.

Watt, F. & Hogan, B., 2000. Out of Eden: stem cells and their niches. *Science*, 287, pp.1427–1430.

Webb, N. et al., 1997. Alternative forms of the scavenger receptor BI (SR-BI). *J Lipid Res*, 38(7), pp.1490–1495.

Webb, N. et al., 1998. SR-BII, an isoform of the scavenger receptor BI containing an alternate cytoplasmic tail, mediates lipid transfer between high density lipoprotein and cells. *J Biol Chem*, 273(24), pp.15241–15248.

Weber, S. et al., 2001. Ozone: an emerging oxidative stressor to skin. *Curr Probl Dermatol*, 29, pp.52–61.

Werder, M. et al., 2001. Role of scavenger receptors SR-BI and CD36 in selective sterol uptake in the small intestine. *Biochemistry*, 40(38), pp.11643–11650.

Werner, S. & Grose, R., 2003. Regulation of wound healing by growth factors and cytokines. *Physiol Rev*, 83(3), pp.835–870.

Wikramanayake, T. et al., 2014. Epidermal Differentiation in Barrier Maintenance and Wound Healing. *Adv Wound Care (New Rochelle)*, 3(3), pp.272–280.

Xu, F. et al., 2011. Ambient ozone pollution as a risk factor for skin disorders. *Br J Dermatol*, 165(1), pp.224–225.

Yamasaki, K. et al., 2003. Keratinocyte growth inhibition by high-dose epidermal growth factor is mediated by transforming growth factor beta autoinduction: a negative feedback mechanism for keratinocyte growth. *J Invest Dermatol*, 120(6), pp.1030–1037.

Yancey, P. et al., 2000. High density lipoprotein phospholipid composition is a major determinant of the bi-directional flux and net movement of cellular free cholesterol mediated by scavenger receptor BI. *J Biol Chem*, 275, p.47.

Yates, M. et al., 2011. Clinical impact of scavenger receptor class B type I gene polymorphisms on human female fertility. *Hum Reprod*, 26(7), pp.1910–1916.

Yeh, Y. et al., 2002. Identification and expression of scavenger receptor SR-BI in endothelial cells and smooth muscle cells of rat aorta in vitro and in vivo. *Atherosclerosis*, 161(1), pp.95–103.

Yesilaltay, A. et al., 2006. PDZK1 is required for maintaining hepatic scavenger receptor, class B, type I (SR-BI) steady state levels but not its surface localization or function. *J Biol Chem*, 281(39), pp.28975–28980.

Zhang, W. et al., 2003. Inactivation of macrophage scavenger receptor class B type I promotes atherosclerotic lesion development in apolipoprotein E-deficient mice. *Circulation*, 108(18), pp.2258–2263.

Zheng, Y. et al., 2013. Scavenger receptor B1 is a potential biomarker of human nasopharyngeal carcinoma and its growth is inhibited by HDL-mimetic nanoparticles. *Theranostics*, 3(7), pp.477–486.

Zhu, P. et al., 2012. Involvement of RAGE, MAPK and NF-κB pathways in AGEs-induced MMP-9 activation in HaCaT keratinocytes. *Exp Dermatol*, 21(2), pp.123–129.

Zhu, W. et al., 2008. The scavenger receptor class B type I adaptor protein PDZK1 maintains endothelial monolayer integrity. *Circ Res*, 102(4), pp.480–487.

Zouboulis, C., 2004. Acne: Sebaceous gland action. *Clin Dermatol*, 22, pp.360–366.